International Seminar Series
SUSTAIN 2026
Scholar's Institute of Technology and Management, Guwahati

Geocell-Reinforced Slopes and Walls

Laboratory Assessment: Commercial and 3D-Printed Geocells

Forensic Investigation: Failure of a Hillslope Reclamation Project

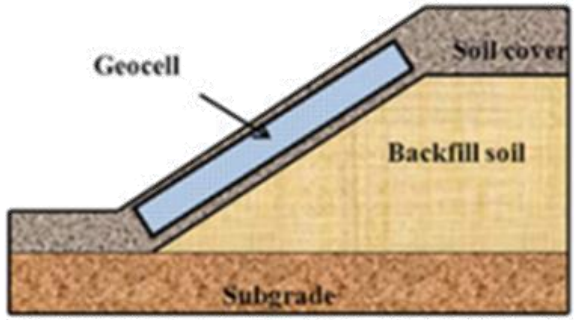

Dr. Arindam Dey
Associate Professor
Geotechnical Engineering Division
Department of Civil Engineering
Center for Disaster Management and Research (CDMR)
IIT Guwahati

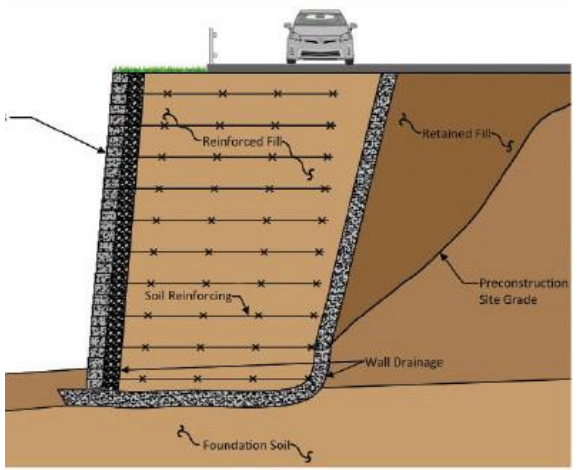

Slope Failures

Slope failure from 2011 Sikkim EQ **(Singh and Som, 2016)**

Slope failure from 2015 Nepal earthquake
(Collins and Jibson, 2015)

Different Slope Stabilization Techniques

Slope Regrading and Benching

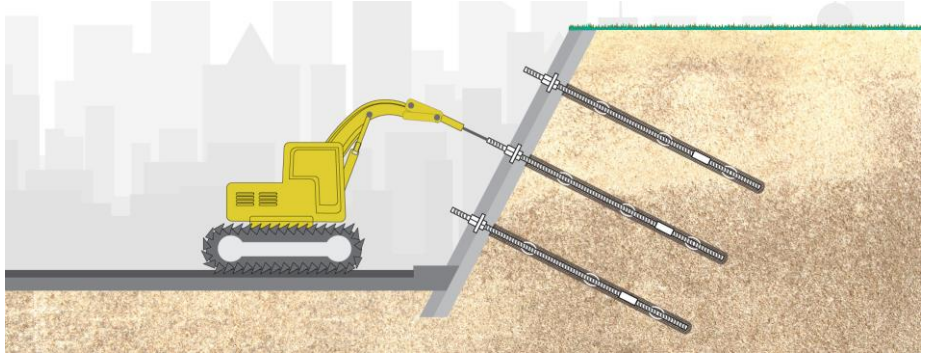

Soil Nailing

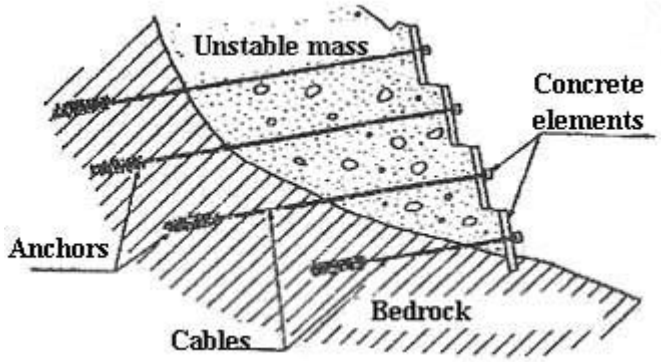

Soil Anchoring

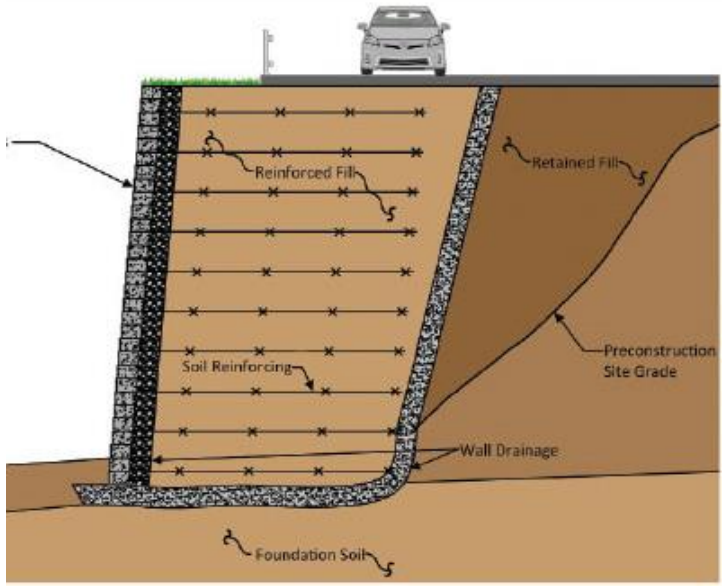

Reinforced earth structures

Stabilization using Geosynthetics

Geosynthetic Products as Sustainable Materials

Geotextiles

Woven

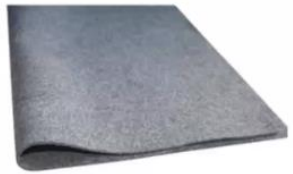

Nonwoven

Geogrids

Uniaxial

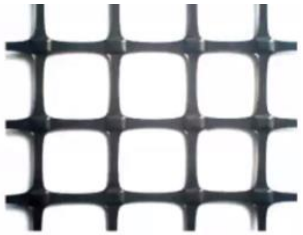

Biaxial

Geonets

Geomembranes

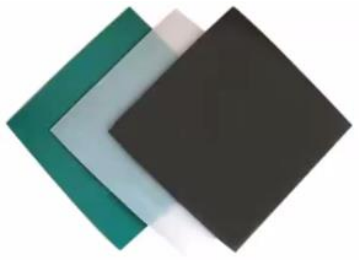

Geocomposites

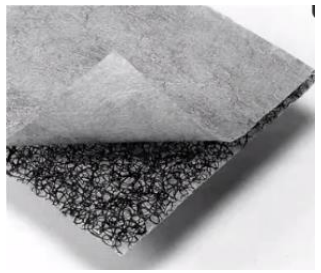

Geocells

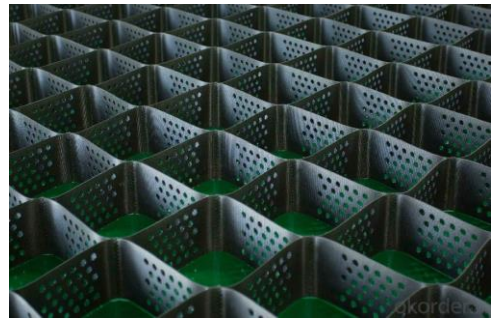

- 3D cellular confinement system
- Honeycomb shaped
- Made of High Density Polyethylene (HDPE)

Reinforcement function

Geotextiles - friction

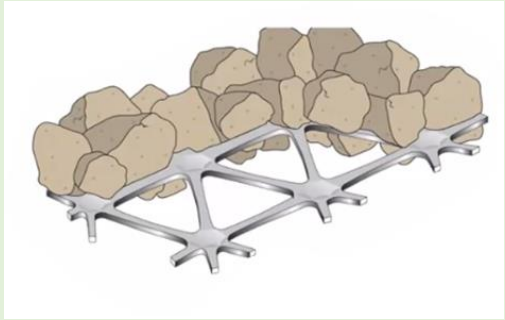

Geogrids – friction and interlocking

Geocells – friction, interlocking, membrane effect, lateral and vertical confinement effect

GEOCELLS

Reinforcement Mechanisms

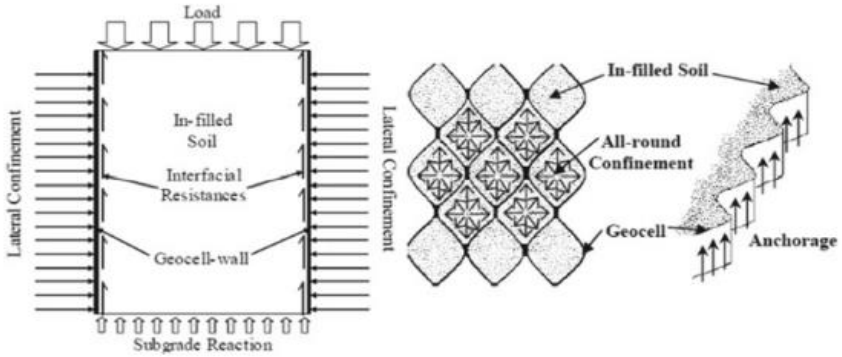

Confinement mechanism **(Biswas & Krishna, 2017)**

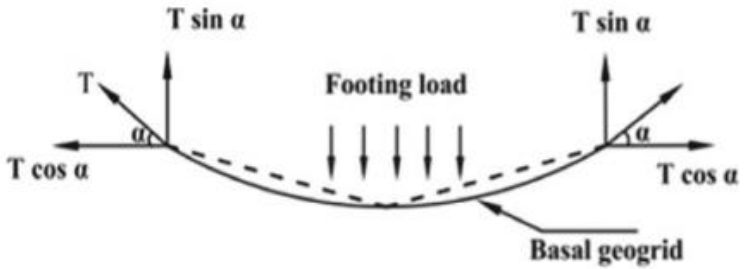

Membrane mechanism **(Sitharam & Hegde, 2013)**

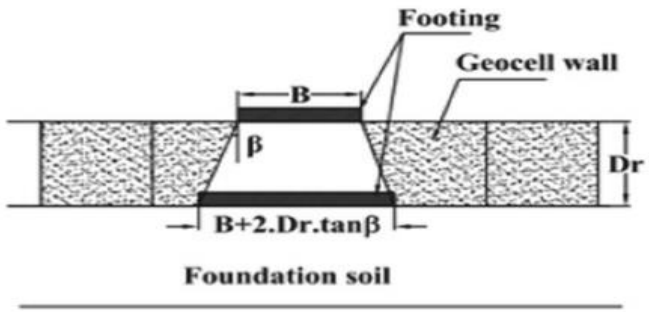

Vertical stress dispersion effect
(Sitharam & Hegde, 2013)

Applications of Geocells

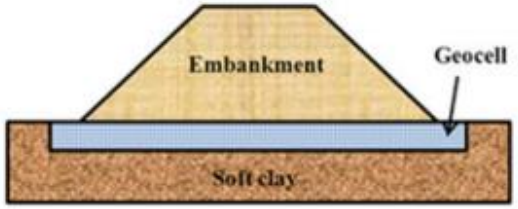

(a) Embankment foundation

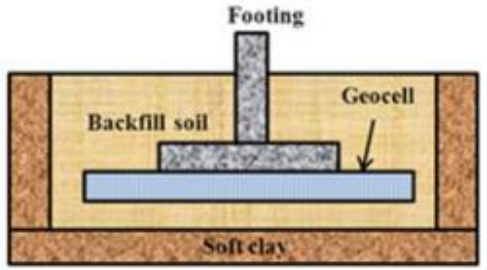

(b) Footing foundation

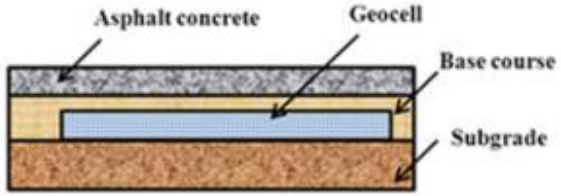

(c) Paved road

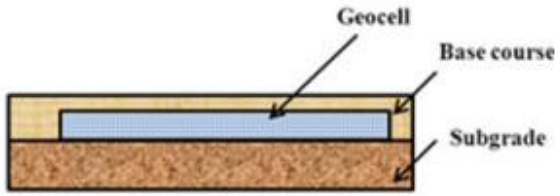

(d) Unpaved road

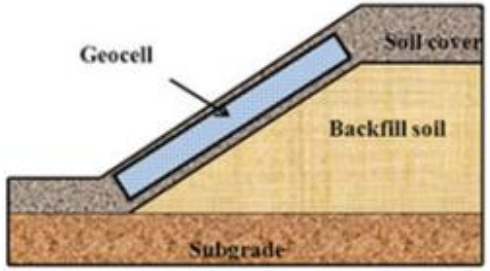

(e) Slopes

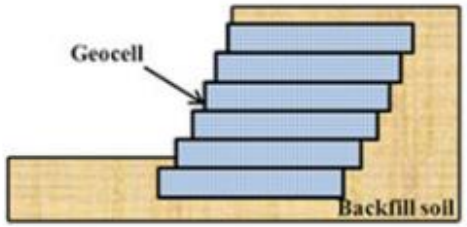

(f) Earth retaining wall

RESEARCH GAPS

- Seismic slope stabilization using geocells through experimental (laboratory or field) and numerical (both 2D and 3D) studies have not been very thoroughly investigated
- Relationship between tensile force in the geocell reinforcement with input maximum ground acceleration and shaking frequency does not exist
- Failure mode and seismic response of geocell reinforced slopes under seismic loading is not vividly identified
- Recommendations for the application of geocells in preventing earthquake-induced landslides is not available

OBJECTIVES

Obj. 1: Characterization of geomaterials and geocells to be implemented in shake table testing

Obj. 2: Assessment of seismic behaviour of laboratory scale geocell-reinforced slopes comprising commercial and 3D printed geocells

Obj. 3: Identifying the best feasible geocell arrangement to attain greater stability in geocell-reinforced slopes

Obj. 4: Seismic response analysis of field-scale geocell-reinforced slopes

S C O P E

Obj. 1: Characterization of geomaterials and geocells to be implemented in shake table testing

- Elemental characterization of geomaterial and Commercial geocells
- Design and methodology of 3D printing
- Elemental characterization of scaled 3D printed geocells

Obj. 2: Assessment of seismic behaviour of laboratory scale geocell-reinforced slopes comprising commercial and 3D printed geocells

- Procurement and Calibration of instrumentations for Shake table testing
- Preliminary numerical analyses for lab-scale models (Instrumentation purpose)
- **Shake table testing** (Scaled and Commercial geocells)
- **Behavioral change in geocells** (Pre-shaking and Post-shaking)

Obj. 3: Seismic response analysis of field-scale geocell-reinforced slopes

- **Frequency response analysis**
- **Seismic response analysis**
- **Case study**

Obj. 4: Identifying the best feasible geocell arrangement to attain greater stability in geocell-reinforced slopes

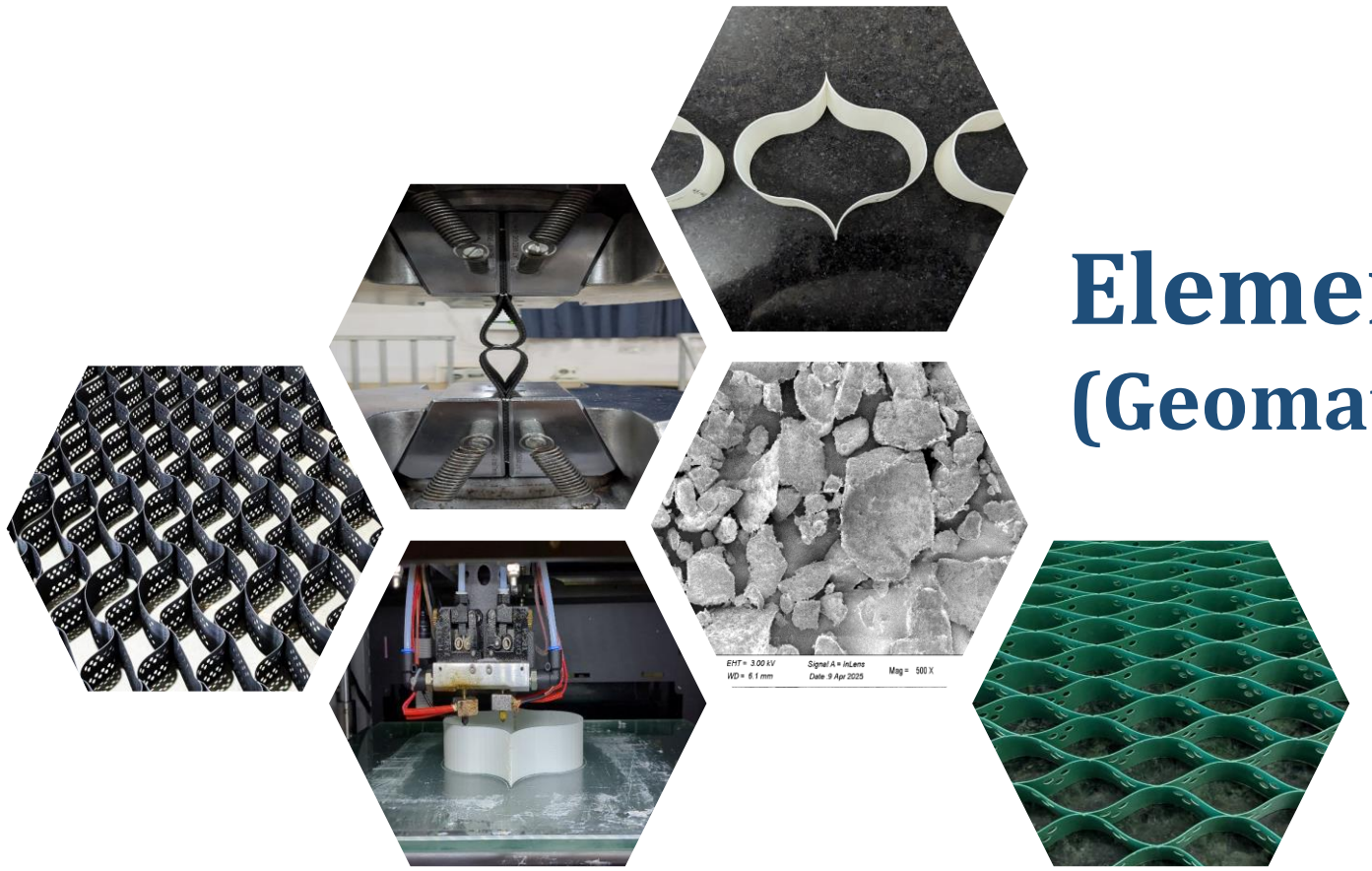

Elemental characterization
(Geomaterial and Geocells)

Geocell faced retaining walls

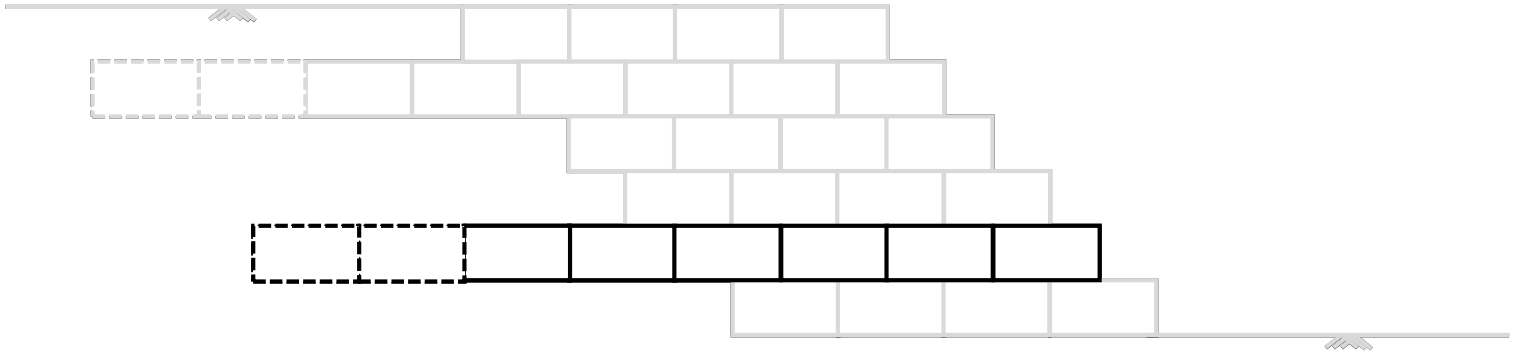

Cross-sectional layout of geocell reinforced slope

Required elemental tests

- Geomaterial characteristics
- Tensile strength
- Interface characteristics
- Unit cell behavior

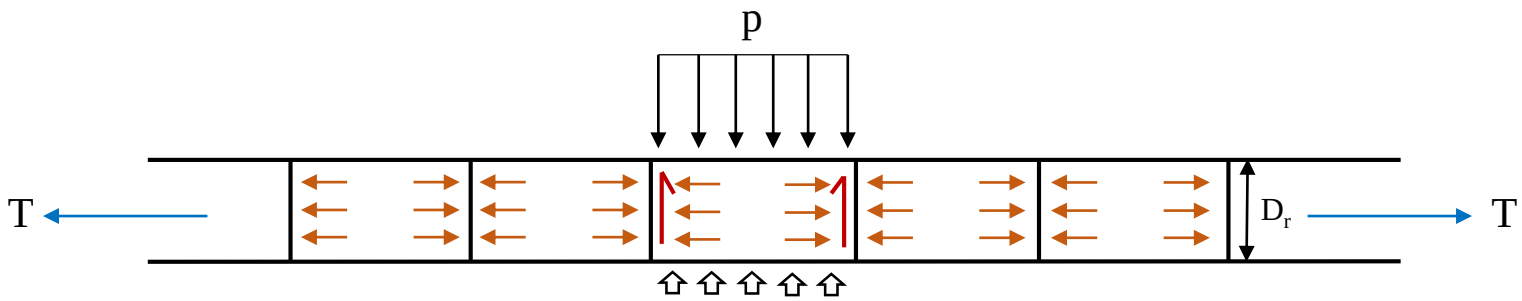

Geomaterial (Infill and Backfill)

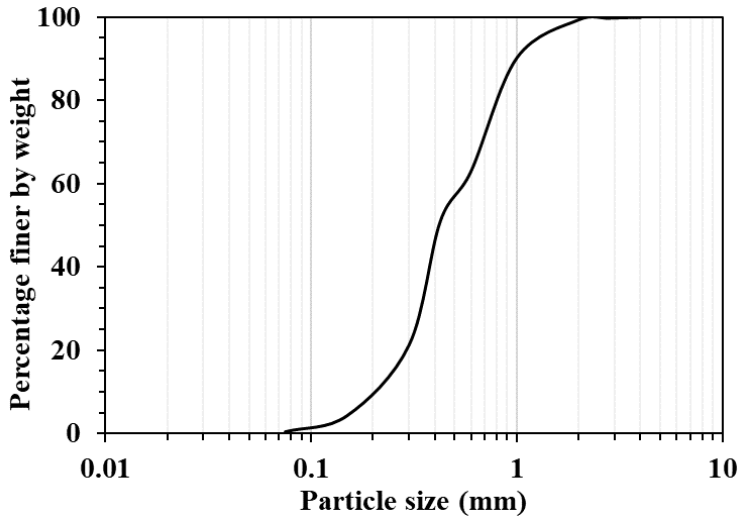

Poorly graded sand (SP)

Parameters	Values
Specific gravity	2.64
Minimum dry unit weight, $\gamma_{d(min)}$ (kN/m^3)	14.4
Maximum dry unit weight, $\gamma_{d(max)}$ (kN/m^3)	16.4
Maximum void ratio, e_{max}	0.81
Minimum void ratio, e_{min}	0.59
Angle of internal friction, φ (°)	46.8

Unit weight calibration

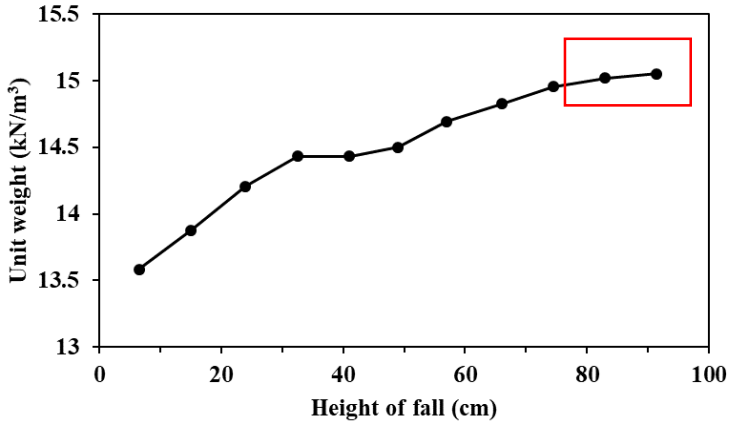

Height of fall maintained above **80 cm** to attain a unit weight of **15 kN/m^3**

Tensile Strength

Type-I geocells

Tension

Peeling

Tensile shear

Splitting

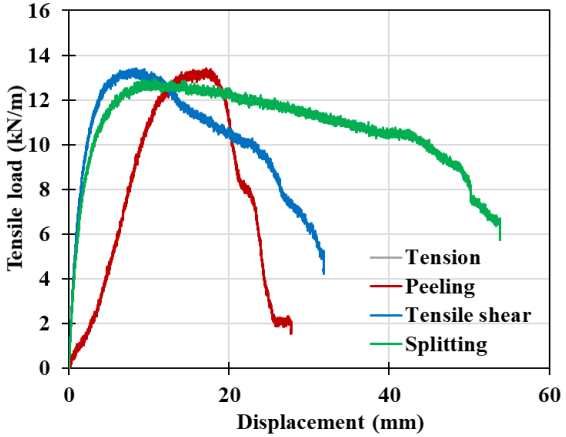

Type-II geocells

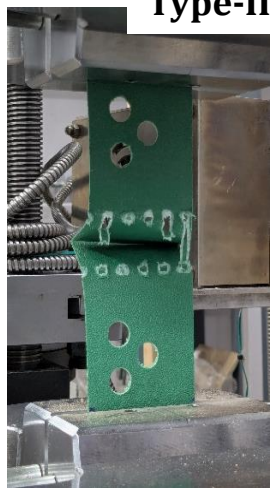

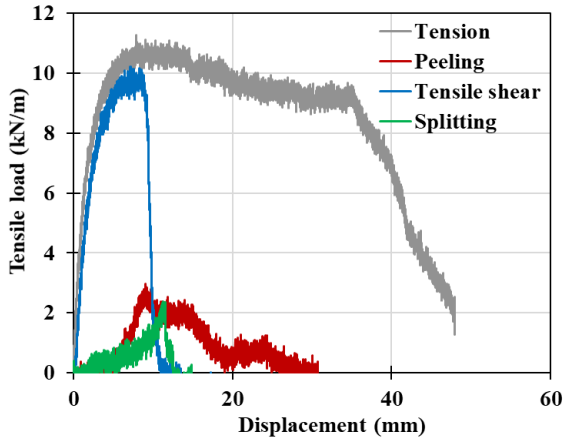

Specifications of Commercial geocells

Properties	Type-I geocells	Type-II geocells
Material	HDPE	HDPE
Strip thickness (mm)	1.65	0.75
Texture	Rhomboidal indentations	-
Weld spacing (mm)	330	145
Cell depth, *H* (mm)	100	50
Equivalent cell diameter, *d* (mm)	192	73
Expanded cell length (mm)	224	70
Expanded cell width (mm)	259	119
Aspect ratio (*H/d*)	0.5	0.7
Tensile strength (kN/m)	12.93	10.5
Average junction peel strength (kN/m)	13.43	2.4
Average junction shear strength (kN/m)	13.41	9.7
Junction split strength (kN/m)	12.93	2

Strips - ASTM D882-18
Junction - ISO-13426-1:2019

Interface Characteristics

Infill soil-Geocell wall interface strength

Interface friction, δ_{sg} = 27° - 38°
Friction angle of sand, φ = 47°

$$\delta_{sg} = \frac{1}{2}\varphi \text{ to } \frac{4}{5}\varphi$$

Average of δ_{sg} matches with wall friction ($\frac{2}{3}\varphi$)

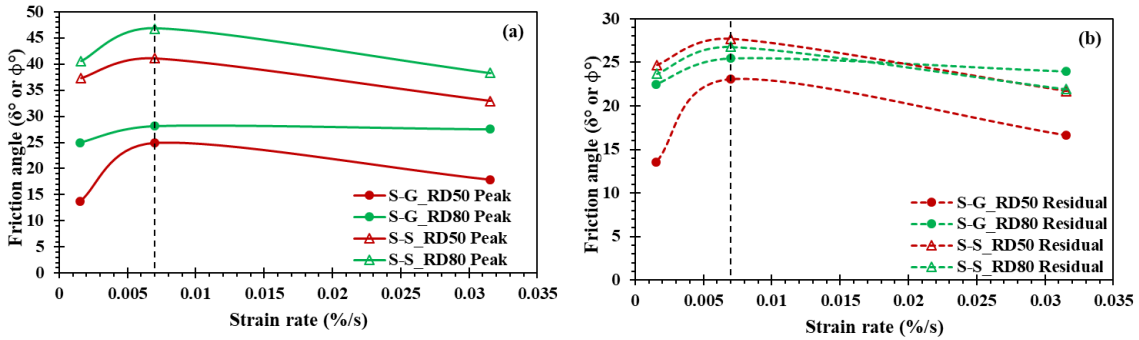

Strain rate variation on S-S and S-G interfaces

Strain rate increase - peak strength of S-S interface decreases
S-G interface is unaffected (due to surface texture)

**S-S = Sand-Sand
S-G = Sand-Geocell

Interlayer interface strength

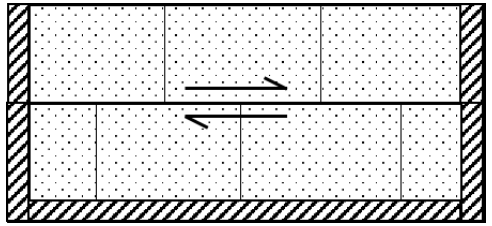

$$\delta_{inter} = \varphi$$

Strength of interface between reinforced layers depends on the internal friction angle of infill sand

Unit Geocell Testing

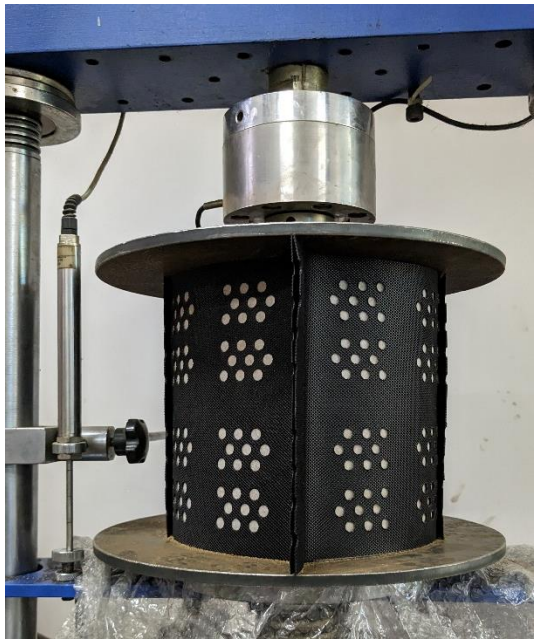

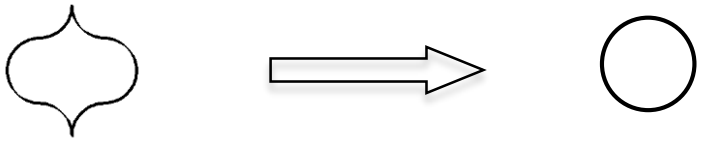

Geocells and soil undergo stiffness degradation in discrete; while, as a composite, an overall improved stiffness is exhibited

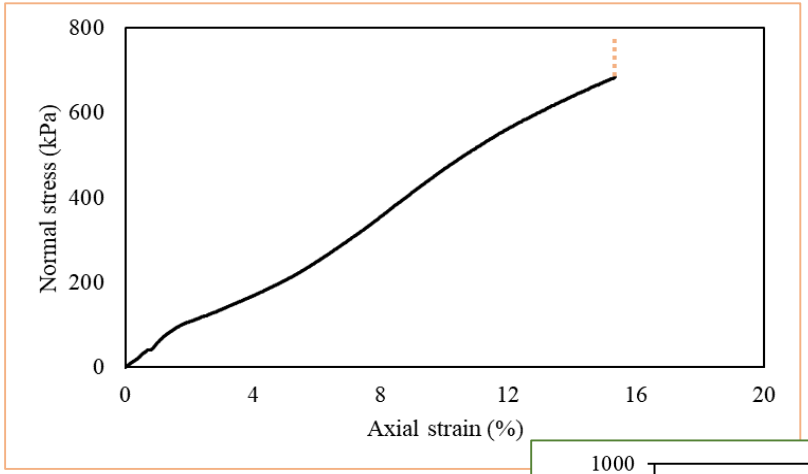

Infilled geocell
Monotonic compression

Infilled geocell
Slow-cyclic compression

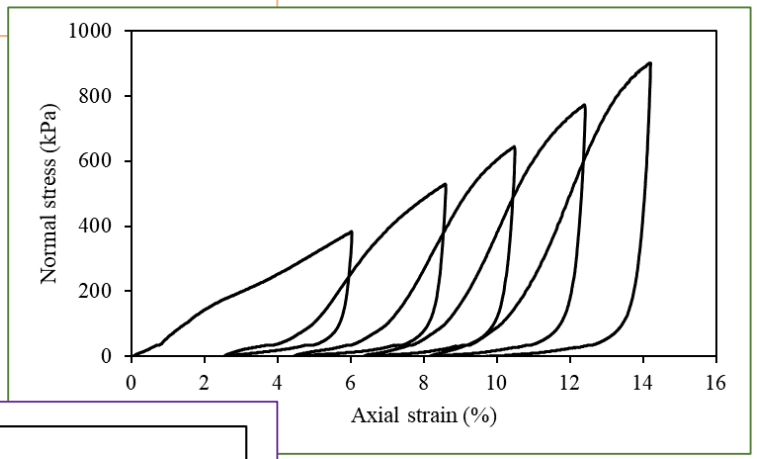

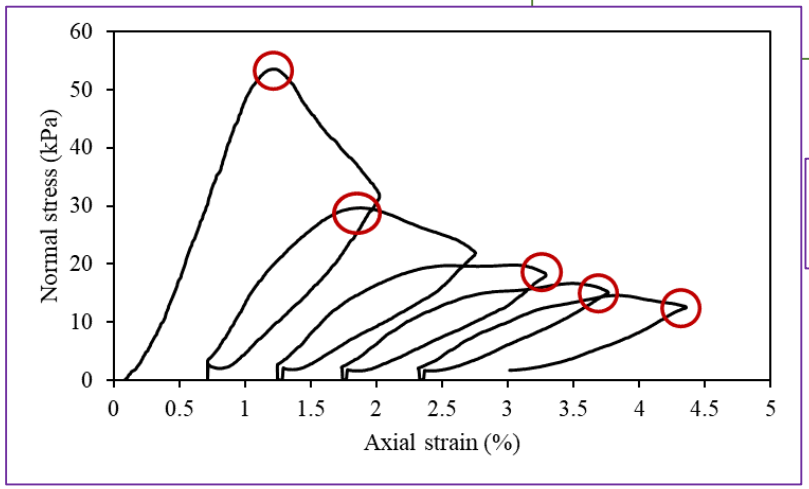

Empty geocell
Slow-cyclic compression

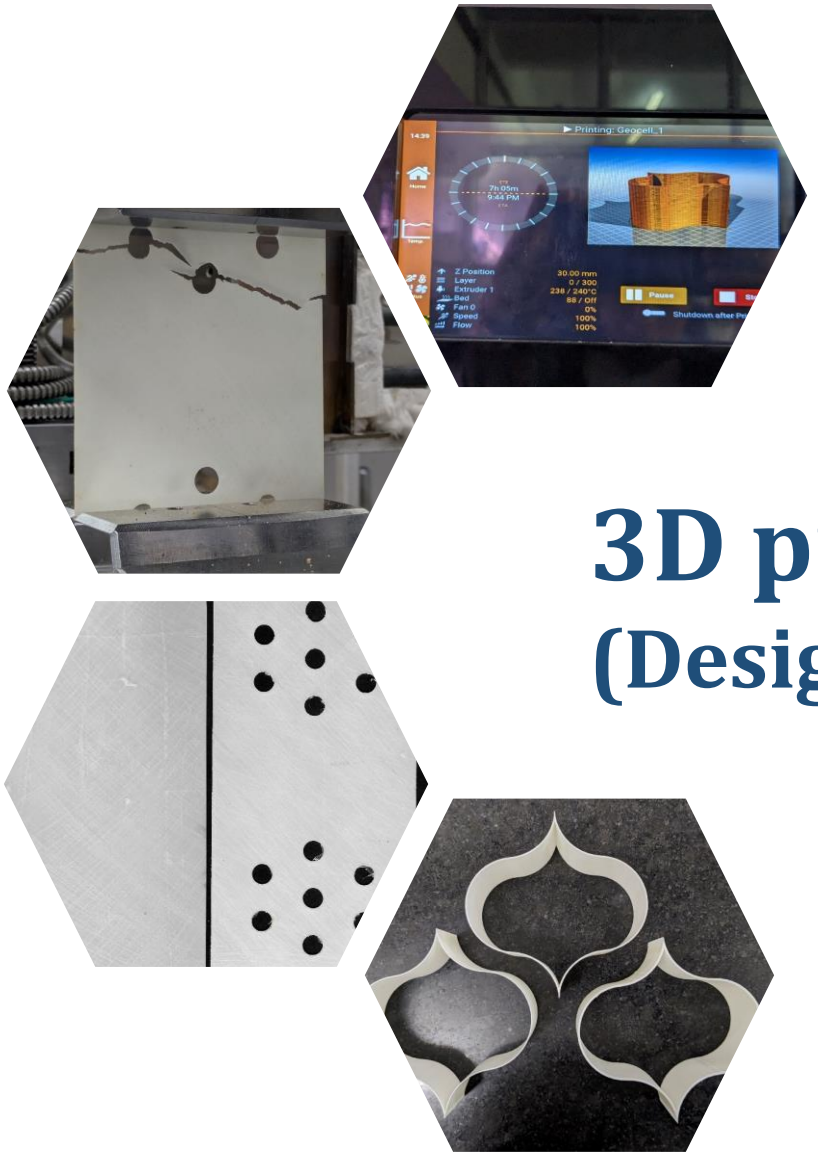

3D printing of Geocells
(Design and Methodology)

Honeycombed Geocell Units

3D-Printer Specifications

- AEQON 400 V3 (make of DIVIDE BY ZERO)
- Fused Deposition Modelling (FDM) technique
- Acrylonitrile Butadiene Styrene (ABS) polymer
  - 1.75 mm diameter filaments
- 0.6 mm diameter nozzle
- Printing domain – 250 mm x 250 mm x 250 mm

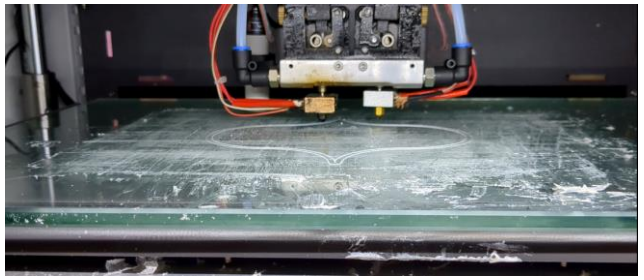

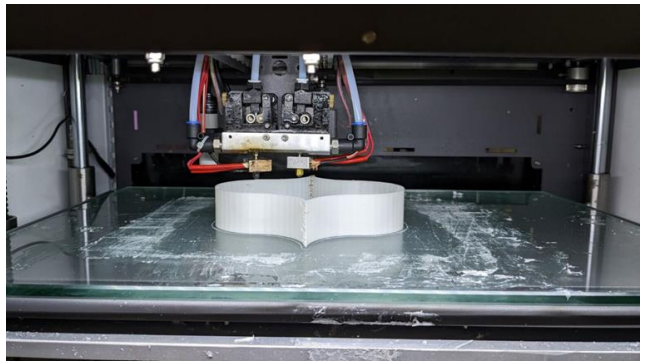

Honeycomb geocell during printing

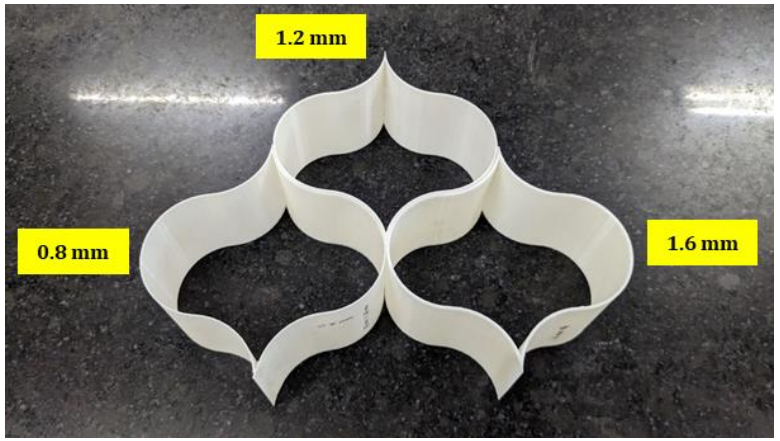

Honeycomb geocell units of varing thickness

Honeycomb geocell under monotonic loading

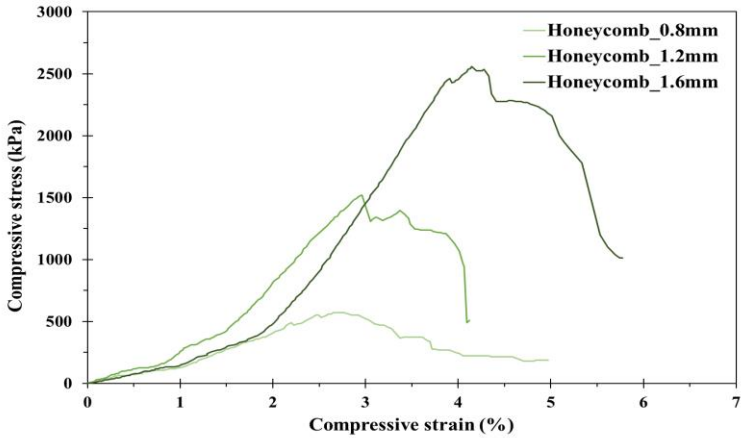

Behaviour of Honeycomb geocell

- Sudden failure; not progressive
- Weak bond between layers
- **Failure propagated from cell wall to the junction**
- Brittle behavior
- No hoop tension development in the cell walls

High stiffness
Very less flexible

Geocell Strips

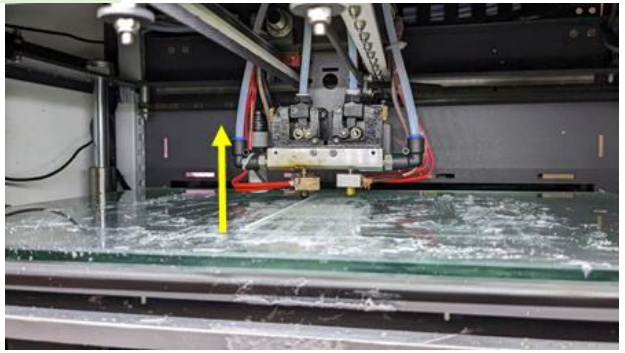

Unidirectional fibre orientation
Printing perpendicular to the bed plane

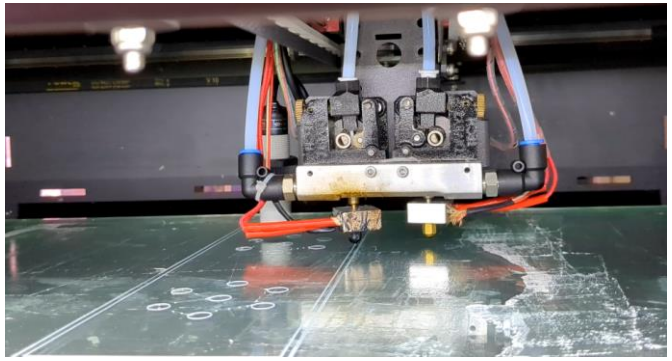

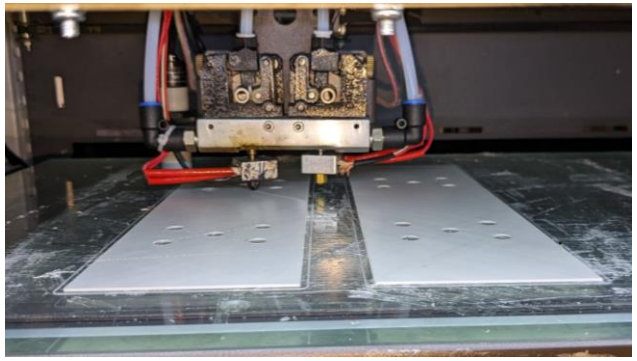

45° fibre orientation
Printing along the bed plane

Bending of strips and Printing failure due to temperature gradient

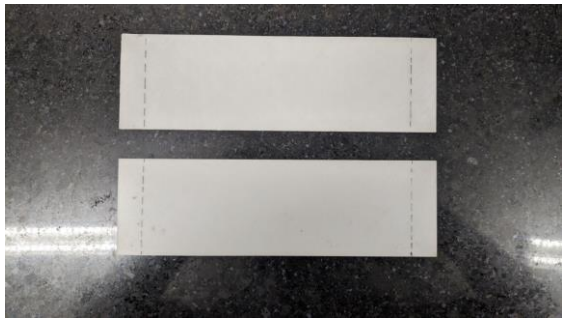

Strips attached using adhesive

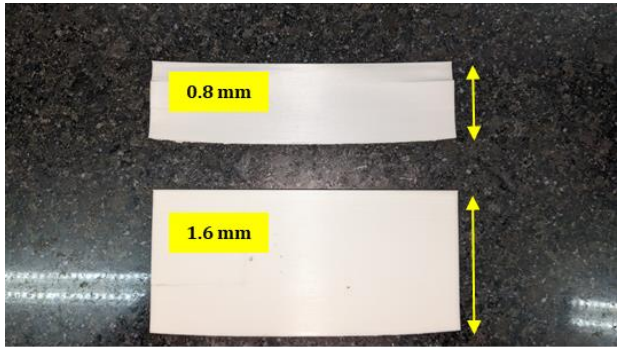

Limited height achieved

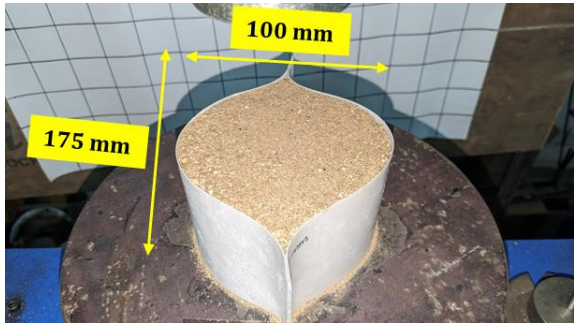

Geocell unit of desire height

Failure Pattern of Commercial and 3D Printed Geocells

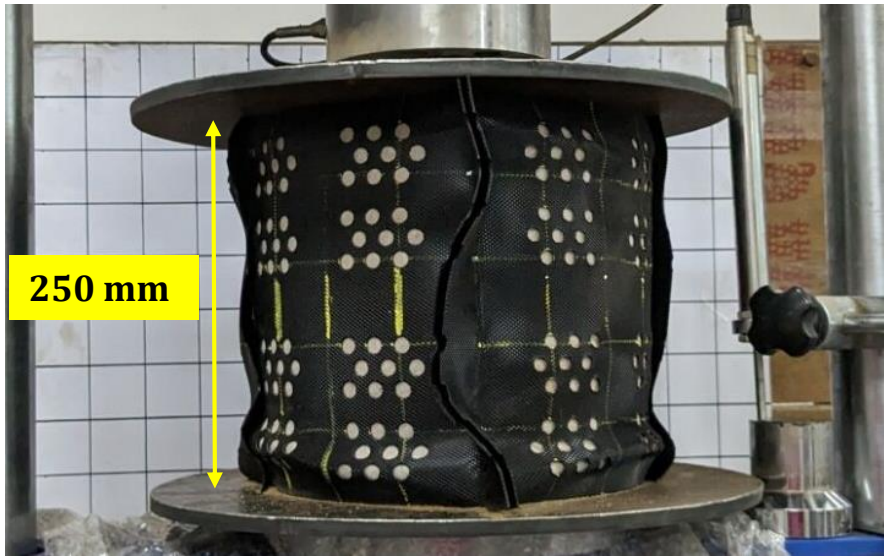

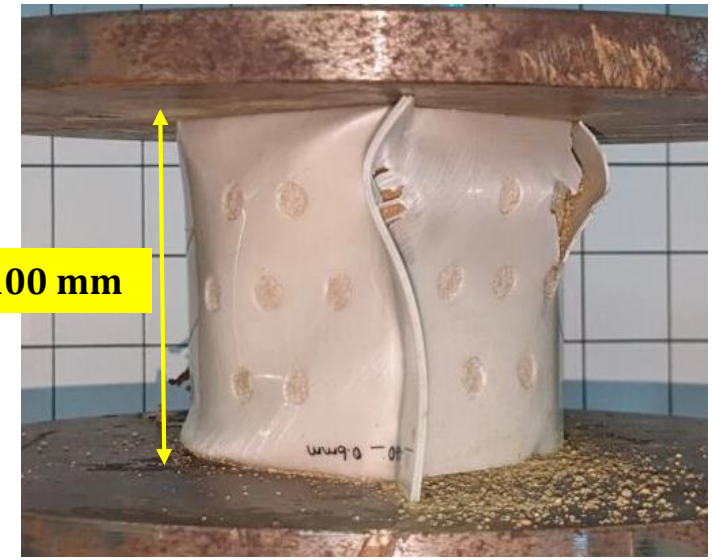

- Failure pattern similar to commercial geocells
- Progressive failure is noted
- Junction failure followed by wall failure

3D printing specifications

Parameters	Values
No. of layers	4
Layer thickness (mm)	0.15
Extrusion width (mm)	0.4
Bed temperature	90°C
Extruder temperature	240 - 270°C
Speed of printing	30 mm/sec

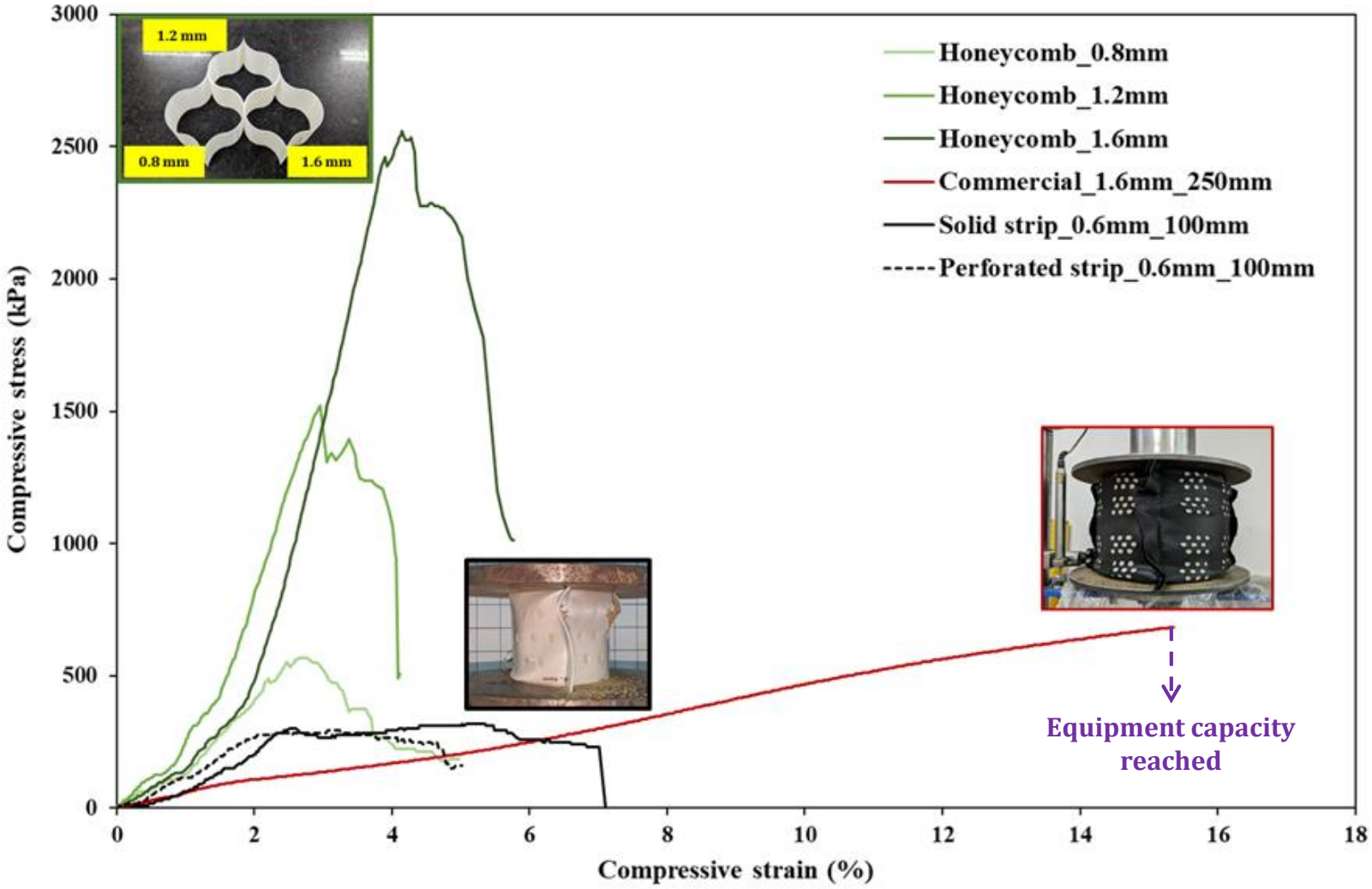

Stress-strain response of commercial and 3D printed geocell units

Material scaling

Scaling between ultimate strengths of commercial and 3D printed geocell units achieved

Characterization of 3D-printed Geocells

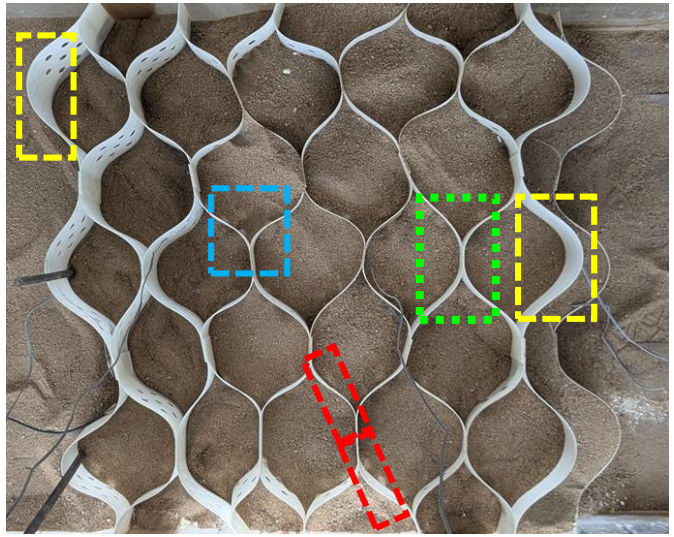

Properties of 3D printed geocells

Properties	Type-III geocells
Material	ABS
Strip thickness (mm)	0.6
Texture	45° fibre orientation
Weld spacing (mm)	210
Cell depth, *H* (mm)	100
Equivalent cell diameter, *d* (mm)	100
Expanded cell length (mm)	100
Expanded cell width (mm)	158
Aspect ratio (*H/d*)	1
Tensile strength (kN/m)	16.3 (Solid) 12.6 (Perforated)
Average junction peel strength (kN/m)	1
Average junction shear strength (kN/m)	17.6
Junction split strength (kN/m)	2.44

Tension tests

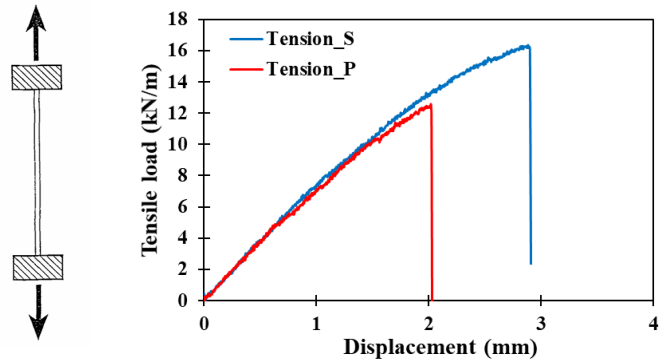

Peeling tests

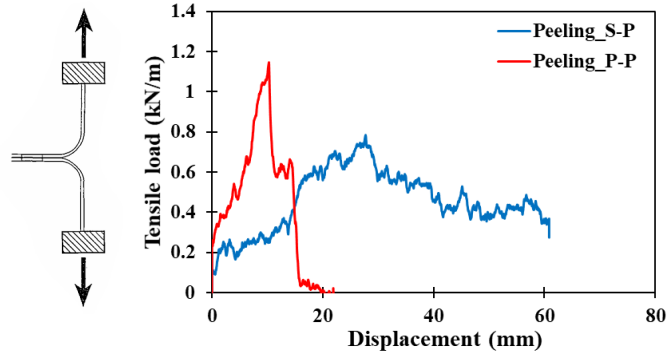

Tensile shear tests

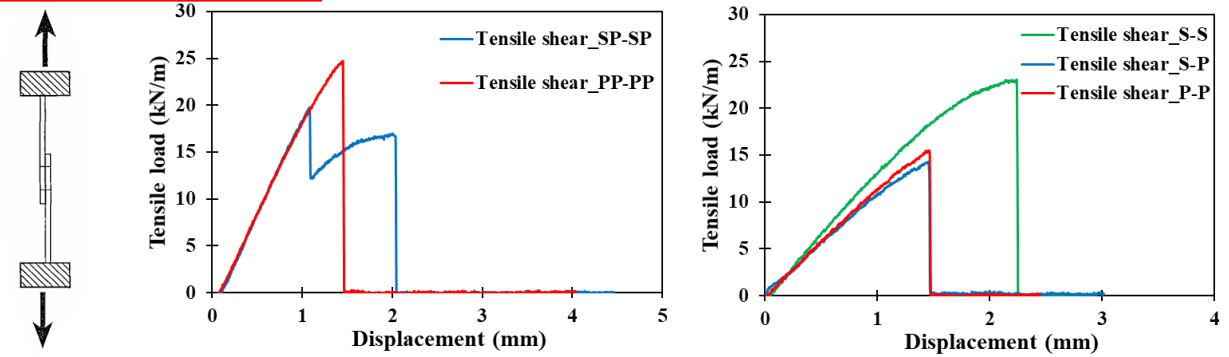

Splitting tests

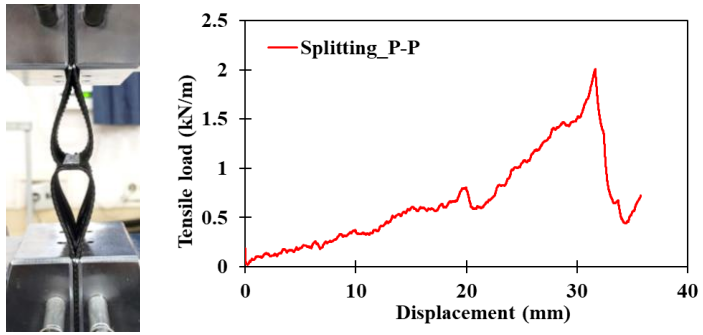

Infill soil-Geocell wall (3D Printed) interface strength

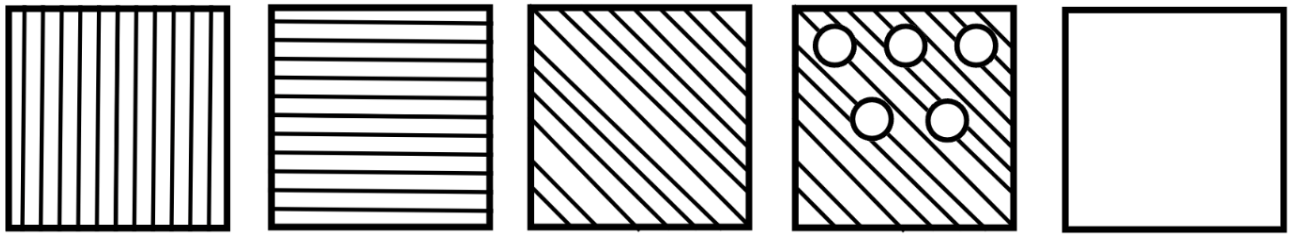

90˚ 0˚ 45˚ solid 45˚ perforated Smooth

Different fibre orientations

Shear behavior of sand-ABS strip interface
(D_r = 80% and surcharge = 150 kPa)

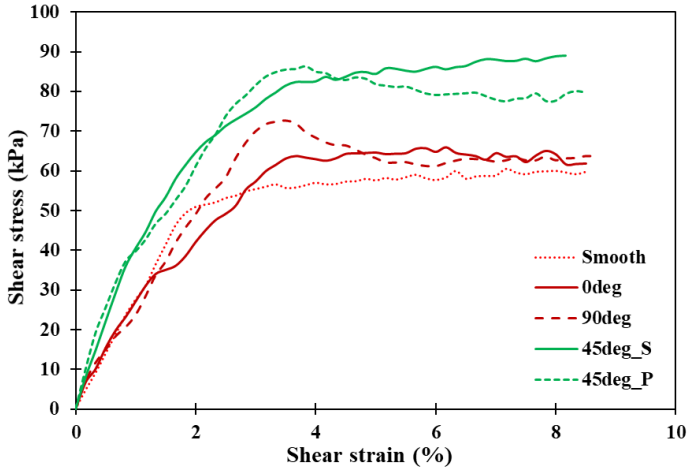

Interface type	δ/φ
Smooth	0.38
0°	0.44
90°	0.54
45°_S	**0.62**
45°_P	**0.58**

Smooth

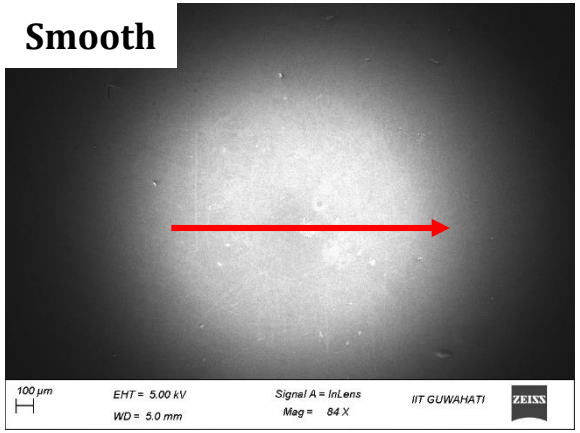

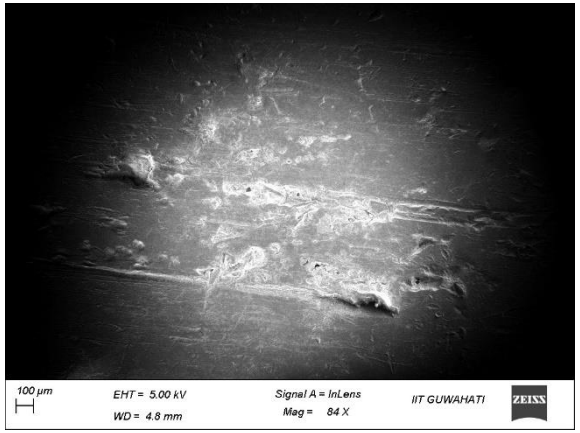

0° and 90°

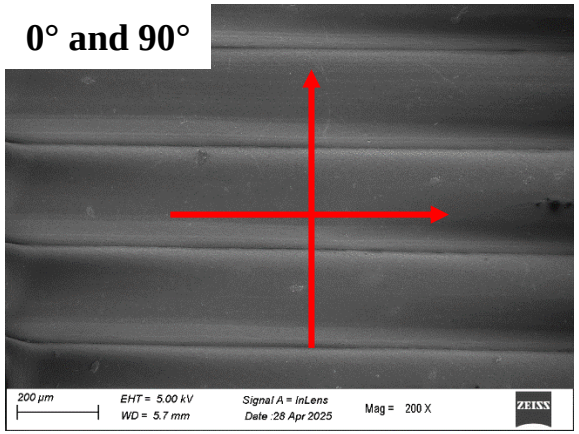

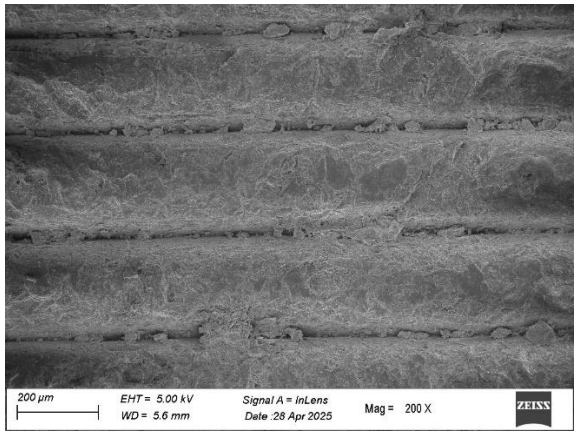

45°

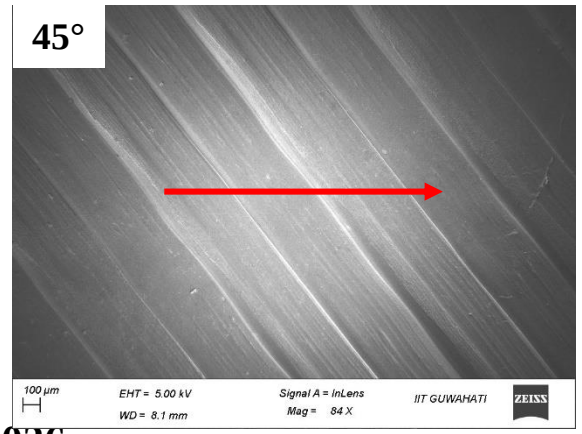

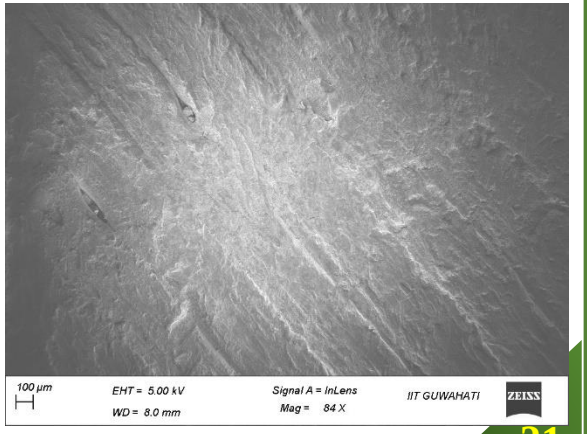

Shake table testing
(Laboratory-scale investigation)

1-g Shake table facility

Shake table specifications

- Loading platform – 2.5 m x 2.5 m
- Payload capacity – 5 ton
- Stroke limit - ± 500 mm
- Acceleration range - ± 2g
- Frequency range – 0.5 Hz to 10 Hz

Perspex tank specifications

- Size – 1200 x 600 x 1000 mm
- Rear wall – Styrofoam sheet;
  Front wall – open
- Tank base – sand paper
- Side wall – marked with 5 cm mesh

Instrumentations

Accelerometer

Laser-type displacement transducer

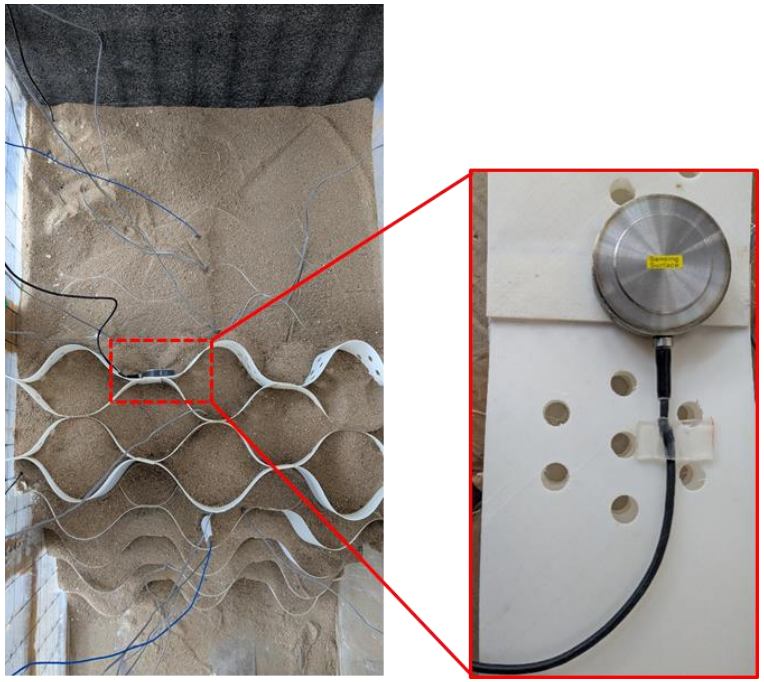

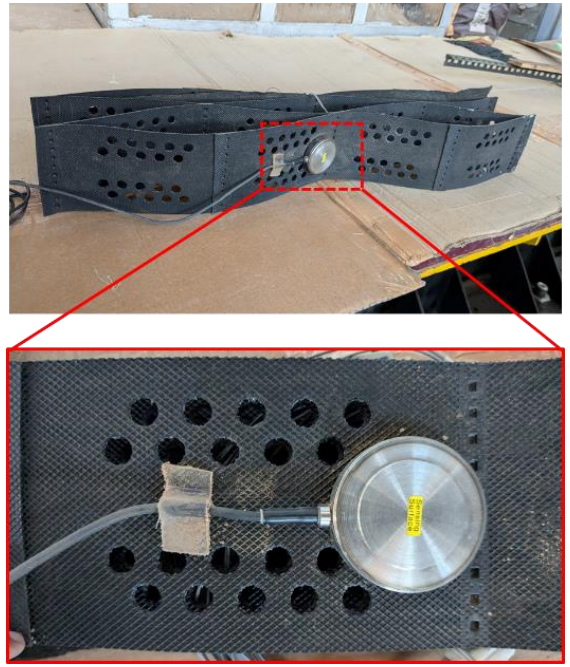

Earth pressure transducers

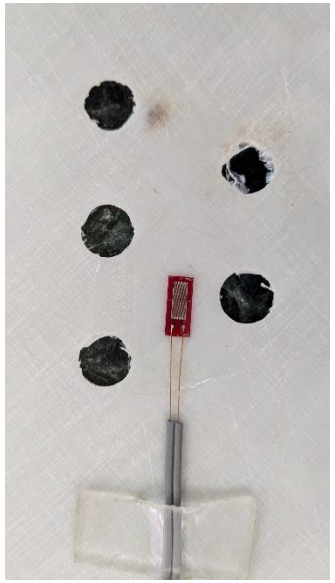

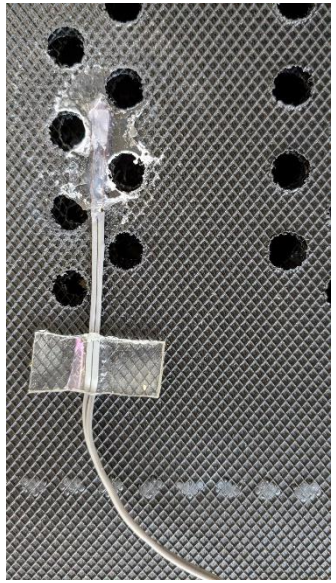

Strain gauges

Data acquisition systems (Current-based and Voltage-based)

Input motions (Table-recorded)

Displacement time histories

Acceleration time histories

1995 Indo-Burma EQ

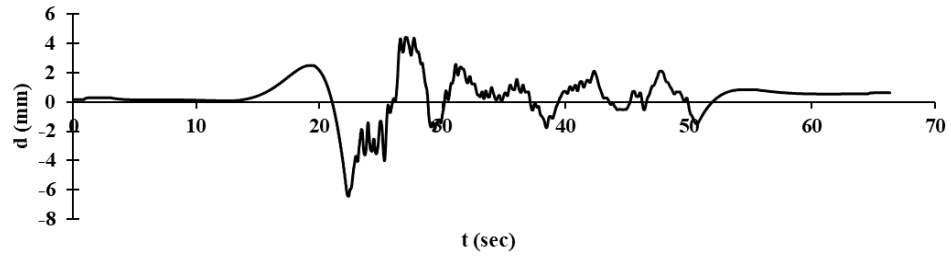

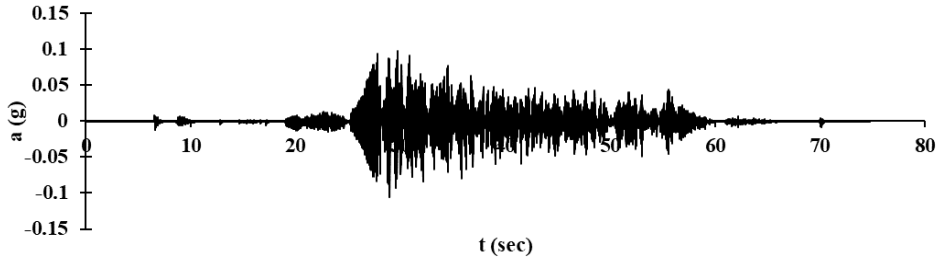

2016 Imphal EQ

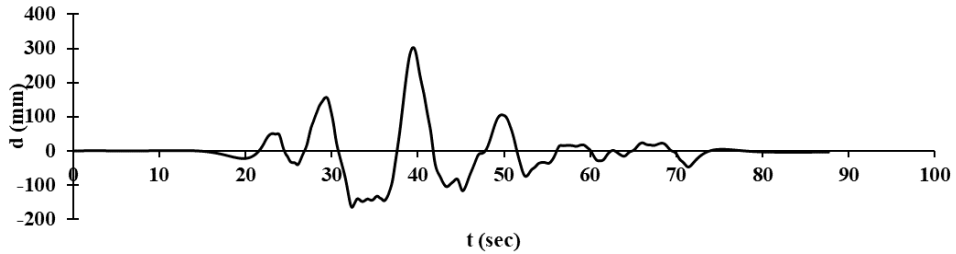

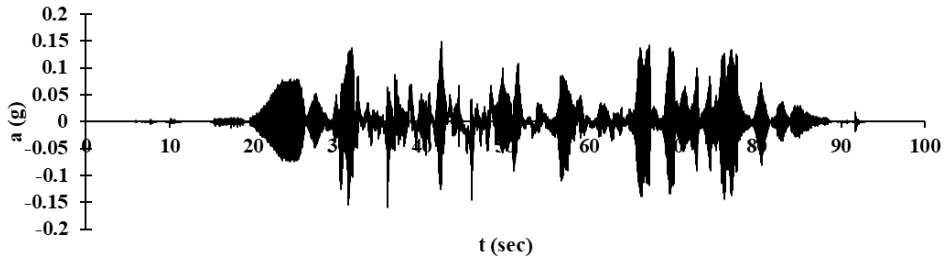

1995 Kobe EQ

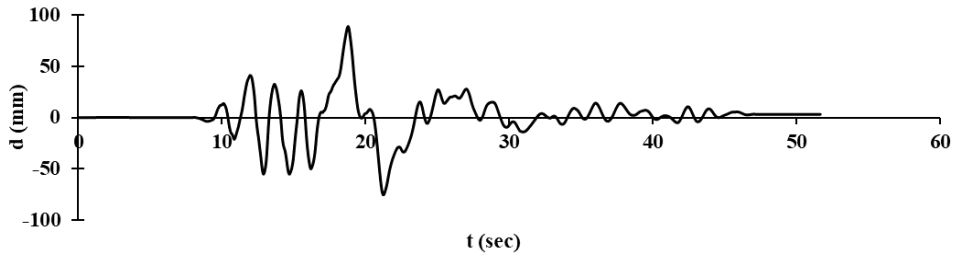

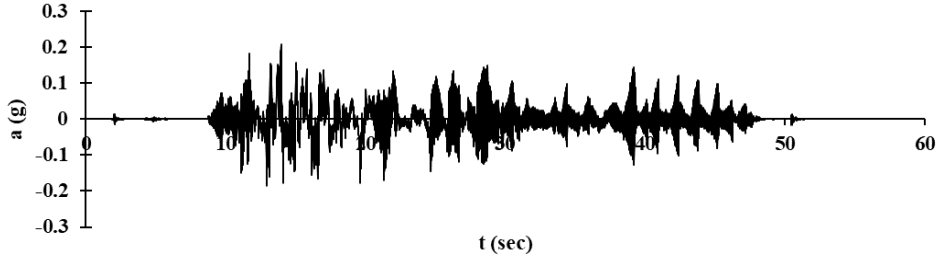

1994 Northridge EQ

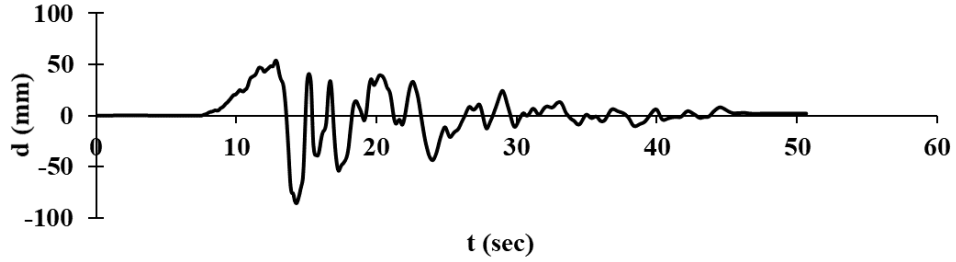

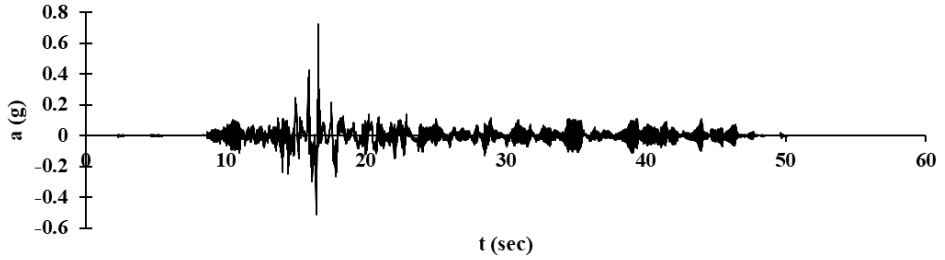

Input motion types

Original

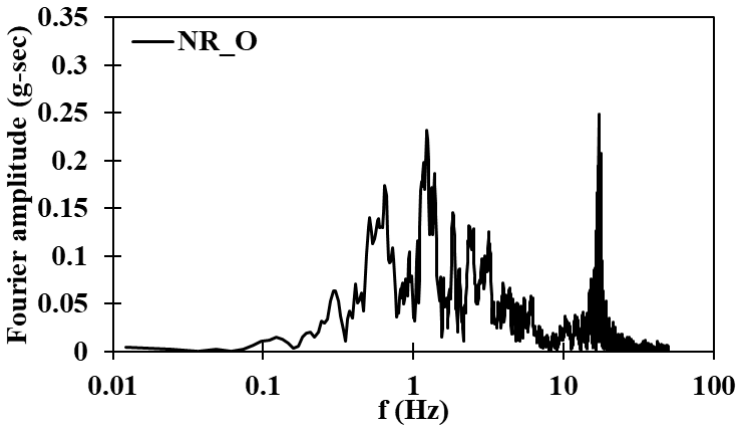

Spectrum-compatible
(Design spectra – Zone V; Site class B)

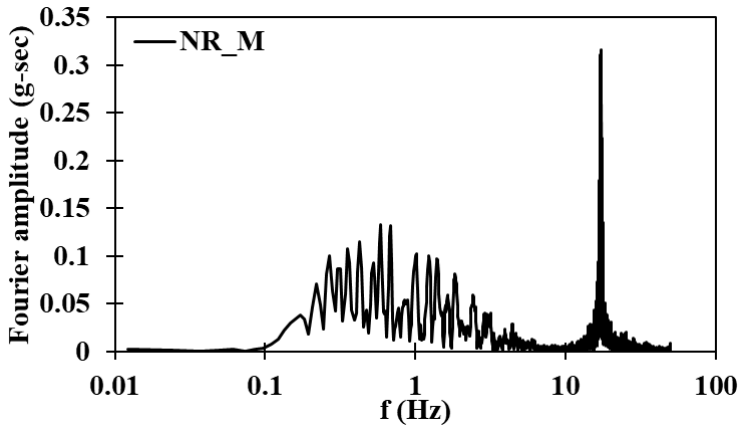

Scaled

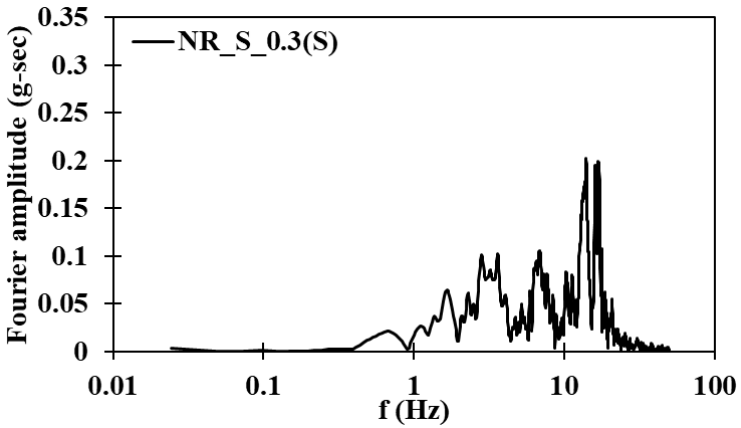

Sinusoidal

0.2Hz_3mm_30
1Hz_0.6mm_30
1Hz_3mm_50
5Hz_3mm_100
5Hz_5mm_150

Motions are sequenced according to the increasing order of energy

Ground motion scaling

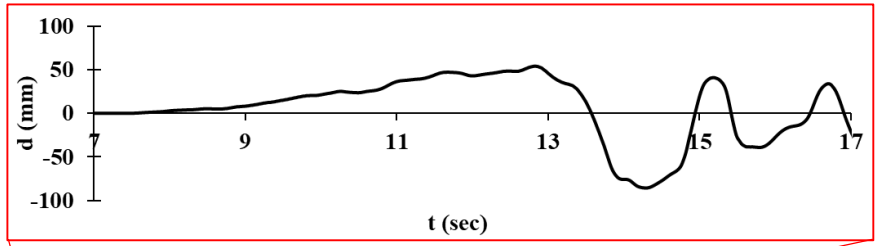

Original motion

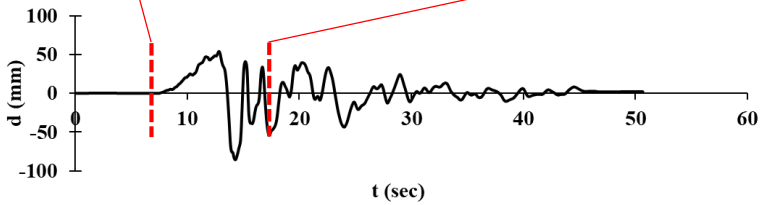

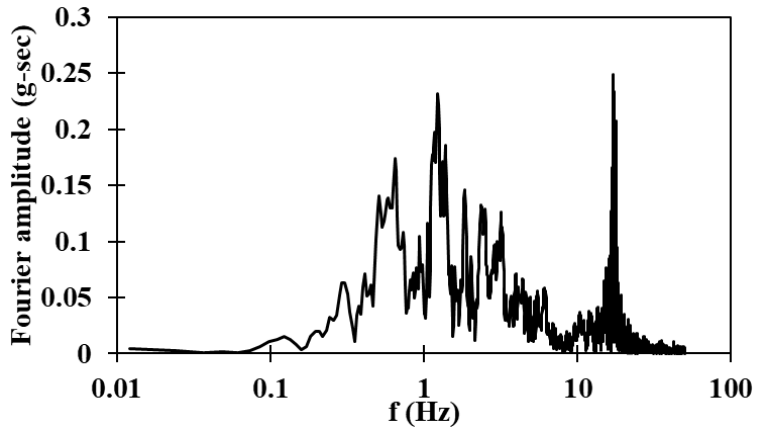

Time-scaled (Δt/5.6)

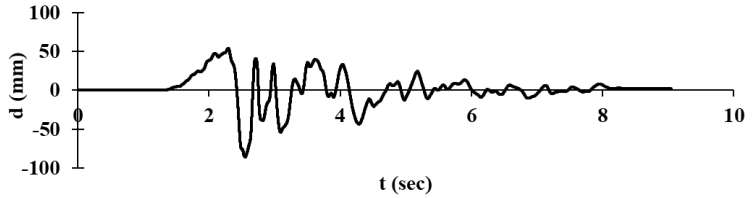

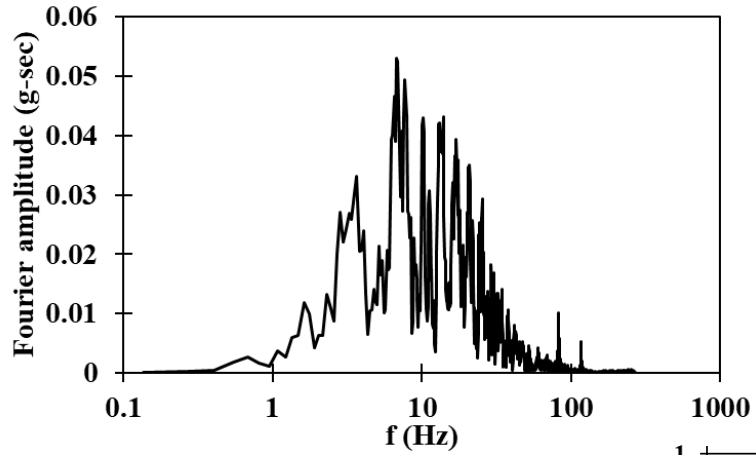

[Scaling due to resource constraint]

Time and amplitude-scaled

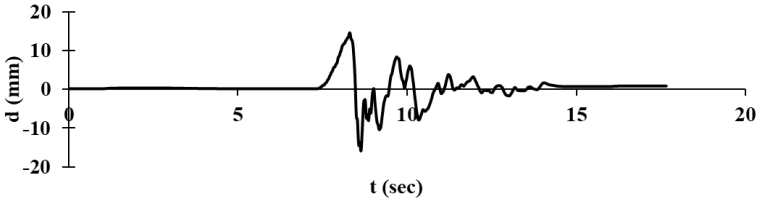

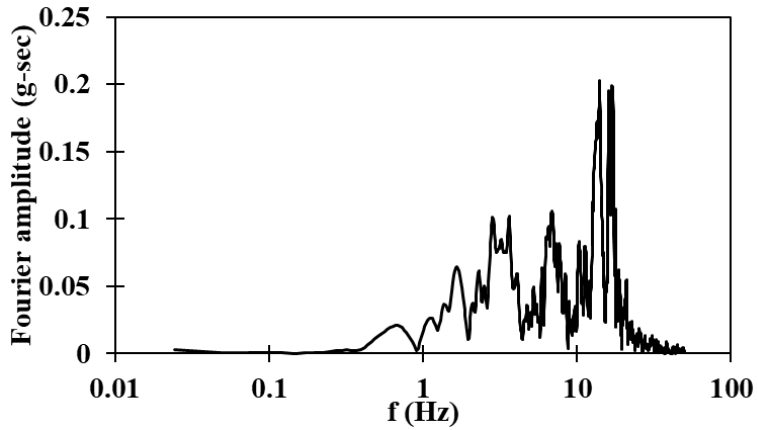

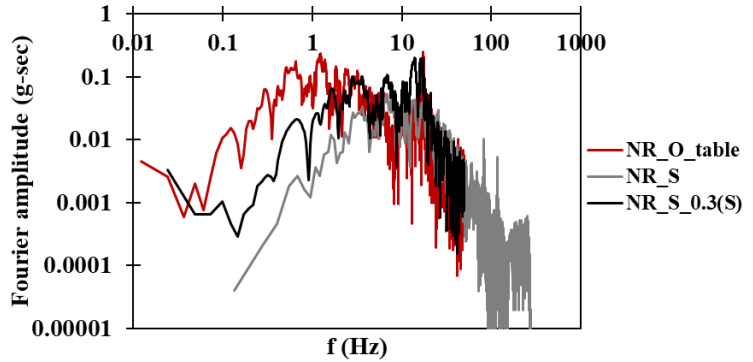

Slope profile evolution of sand slopes (30°)

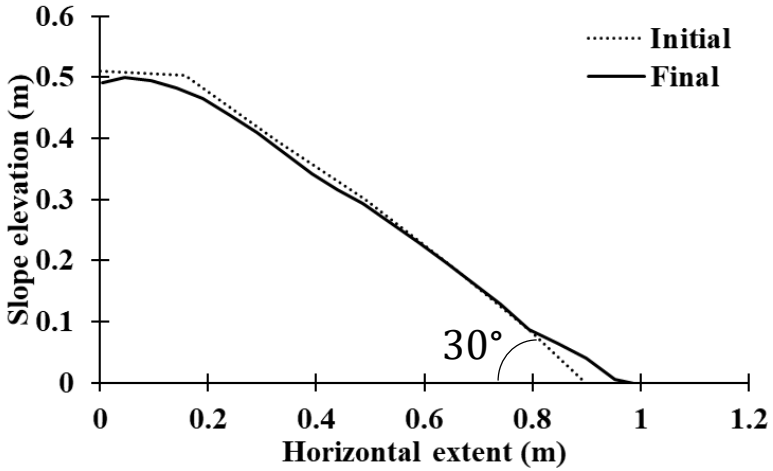

Original motions

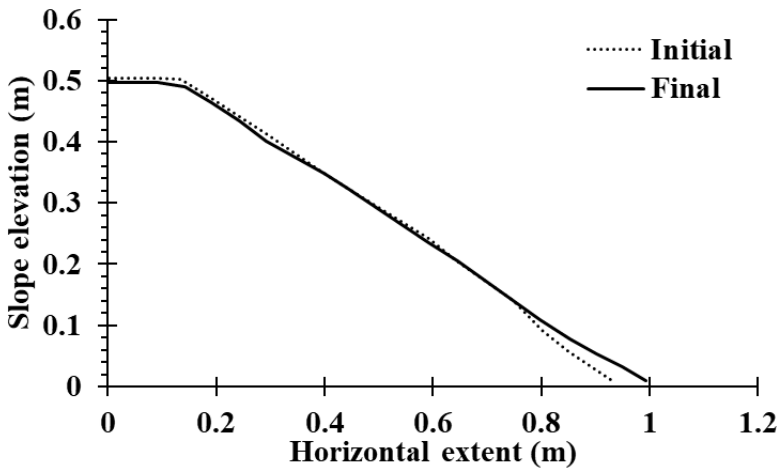

Spectrum-compatible motions

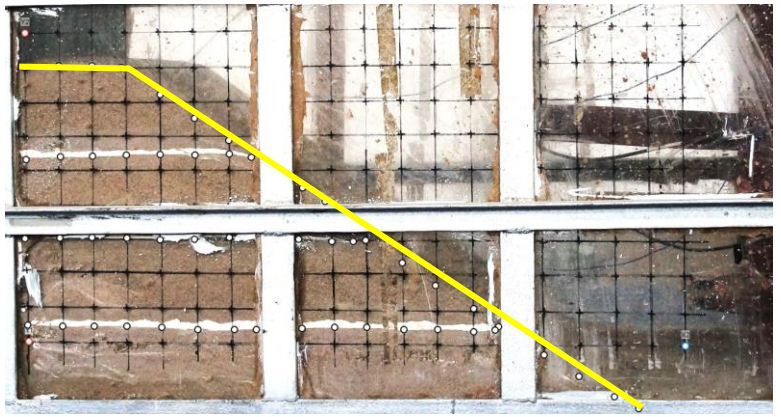

Significant changes in the slope profile evolution is noticed only in scaled and high frequency sinusoidal motions

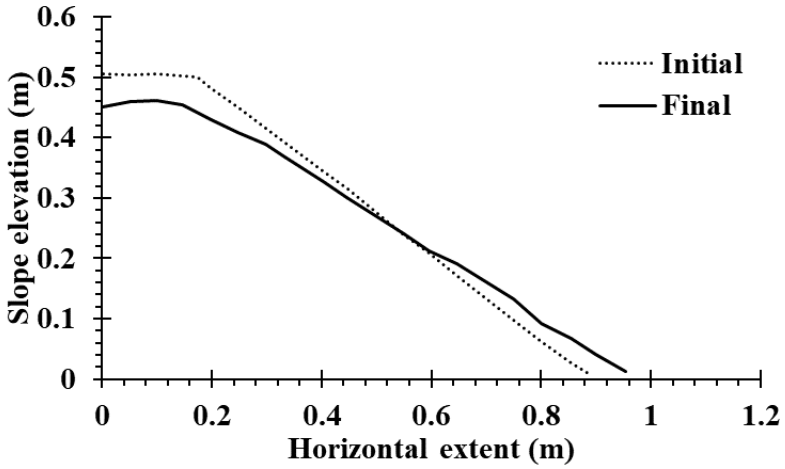

Scaled motions

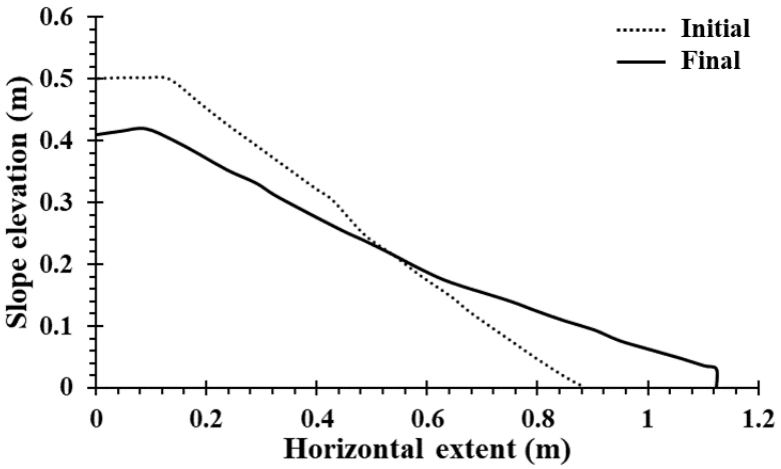

Sinusoidal motions

Experimental model layouts

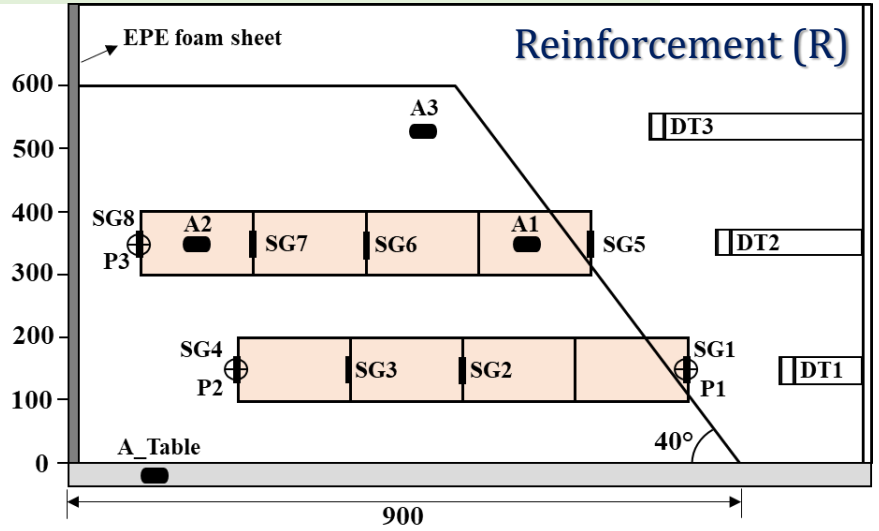

* all dimensions are in mm

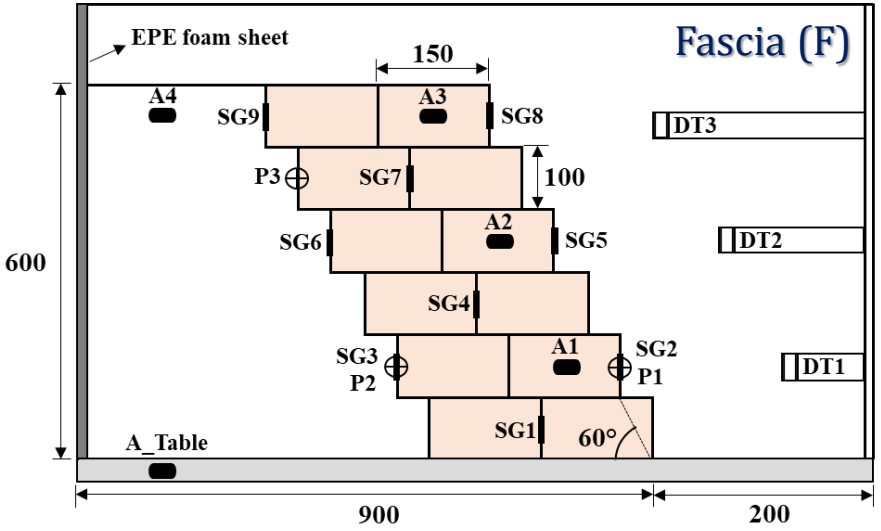

* all dimensions are in mm

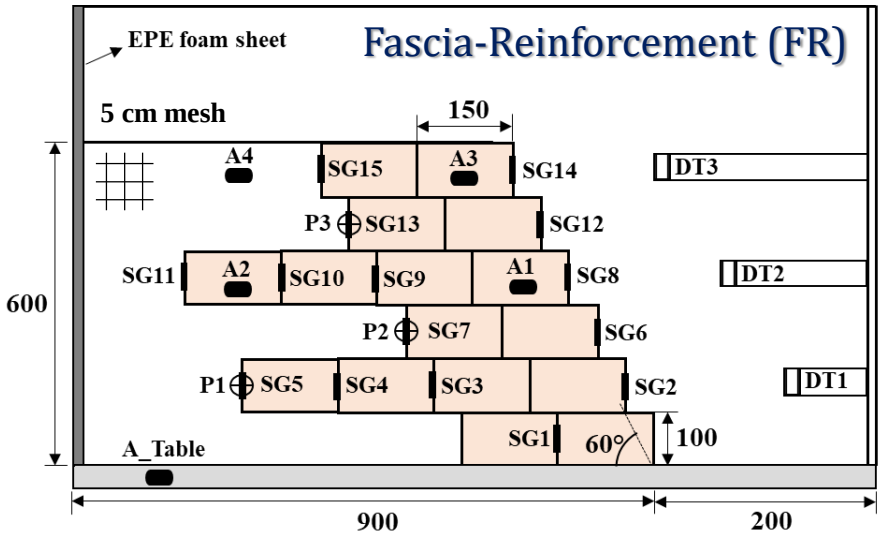

* all dimensions are in mm

Accelerometer (A)

Non-contact displacement transducer (DT)

Pressure transducer (P)

Strain gauge (SG)

Type-I geocells:
- F100
- R100
- F100+R100

Type-II geocells:
- R50
- F50+R50

Type-III geocells (3D printed ones)
- F100
- R100
- F100+R100

Combination of geocells used:
- F100_Type-I and R50_Type-II
- F100_Type-III and R50_Type-II

F – Fascia; **R** – Reinforcement
100 & **50** – geocell heights

Type-I

Type-II

Type-III

Variation in the number of geocell pockets along the length and width of the geocell layer

During model construction

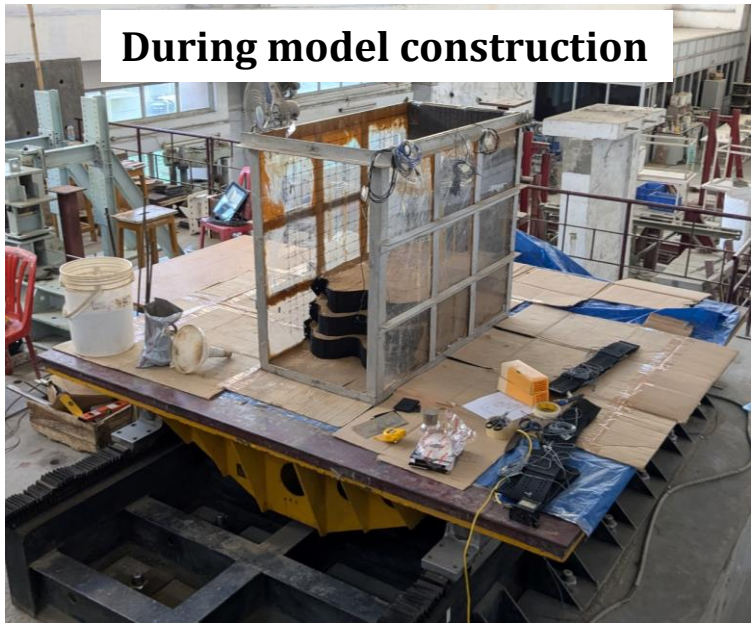

Post-shaking

Unit geocell

Geocell lattice

Constructed model

Damping characteristics

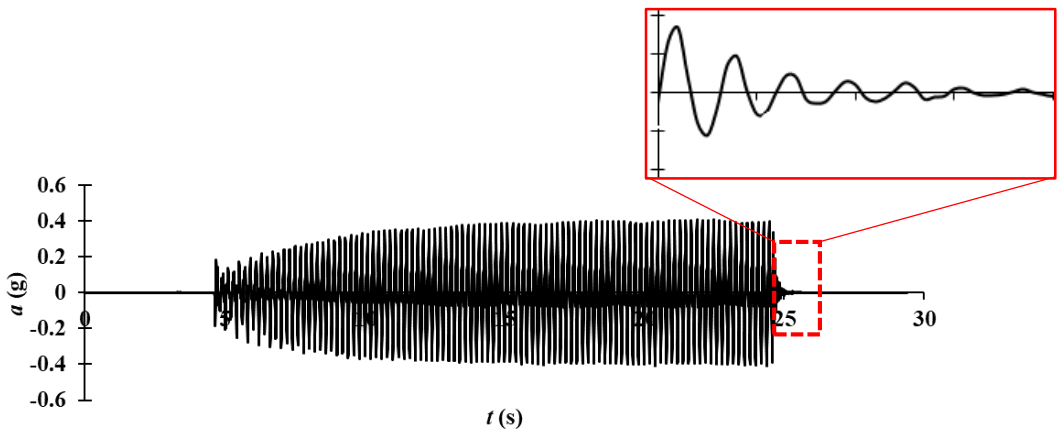

Acceleration response during sinusoidal shaking

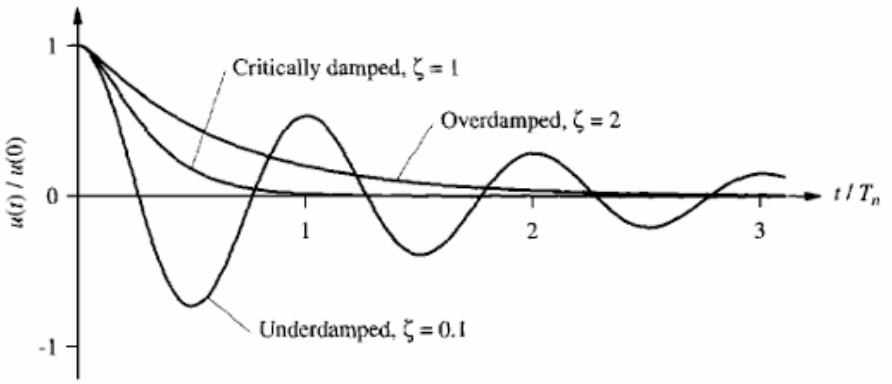

Free vibration of viscous systems

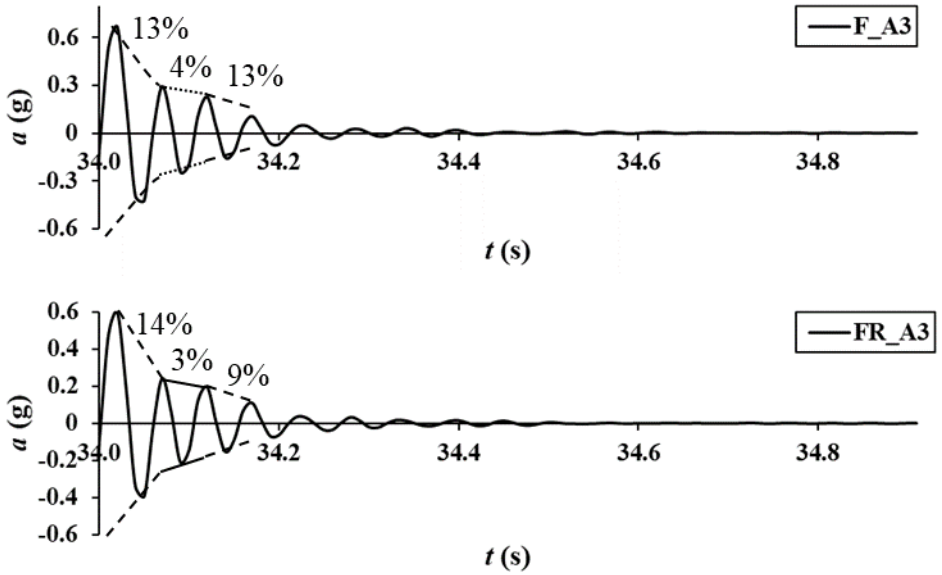

Free vibration response of crest in F and FR

- Higher damping ratio magnitude of 9-11% is noted in F and FR configurations than the standard design values of 2-5%
  - Akbulut and Pamukcu (2010) noted damping increment upon introducing geosynthetic sheets into clay specimens
- F and FR exhibited resemblance in damping
- Soil densification observed after relatively stronger shaking caused reduction in damping
- Similar damping behavior in unreinforced and R configuration models

Failure mode of geocell-reinforced slopes

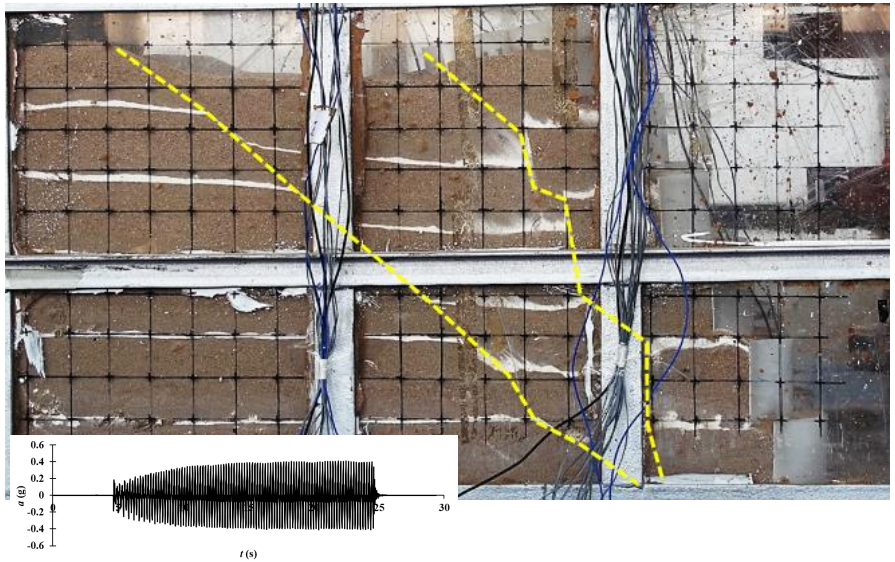

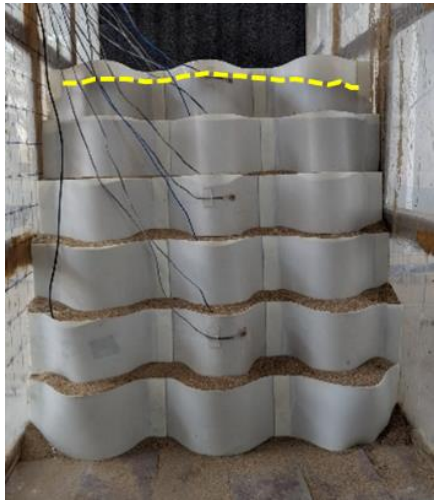

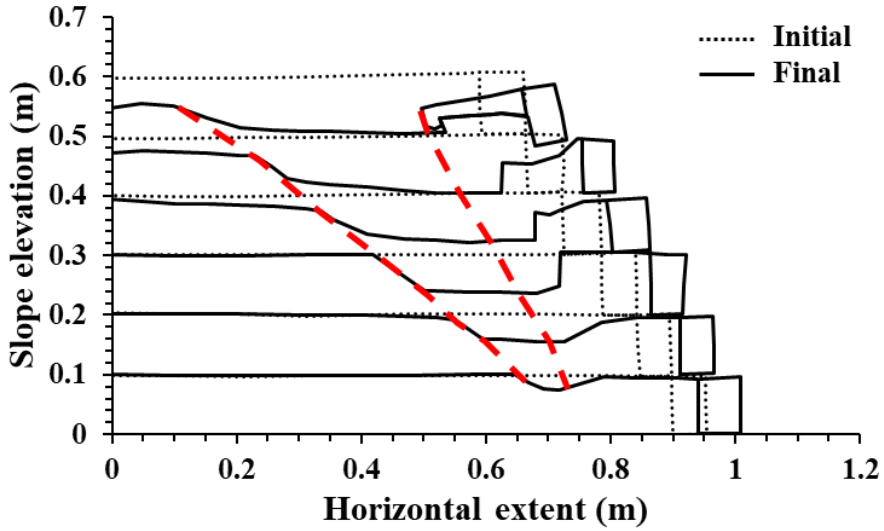

- Failure surface development noticed in F model after a sinusoidal shaking of 5Hz_5mm applied for 150 cycles (PGA = 0.6g)
- Sliding of toe ➔ Settlement of backfil ➔ Overturning of crest fascia
- Wedge-type failure with two slip surfaces: one behind the fascia (64.92°) and the other within the backfill (40.64°)
- Such distinct failure surfaces were observed in
  - Centrifuge model tests conducted under elevated gravity (N-g) conditions (Song et al., 2017, 2018)
  - Large-scale physical models that closely replicate field geometry (Leshchinsky et al., 2009),
  - Monotonic loading experiments with supplemental surcharge to modify structural response (Chen and Chiu, 2008),
  - Numerical analyses of full-scale configurations (Zeng et al., 2024)

F configuration

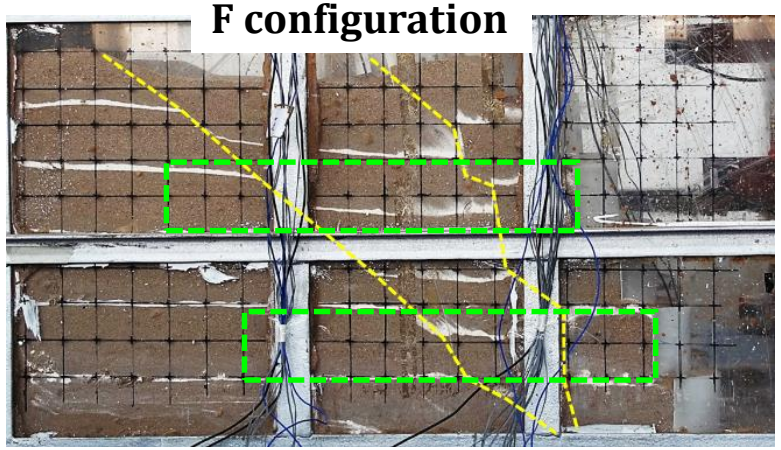

FR configuration

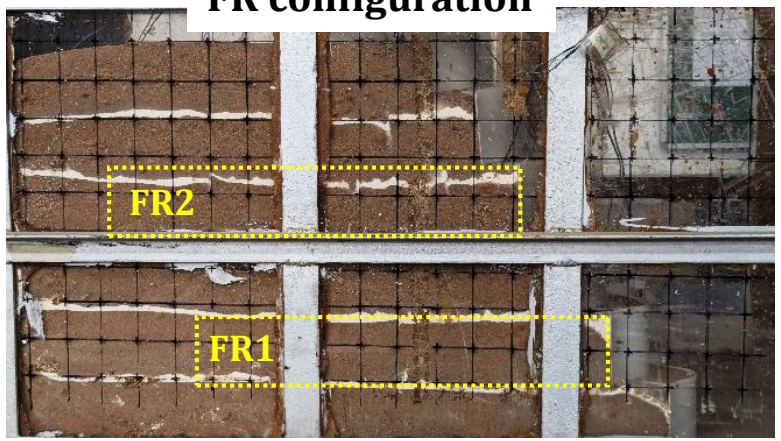

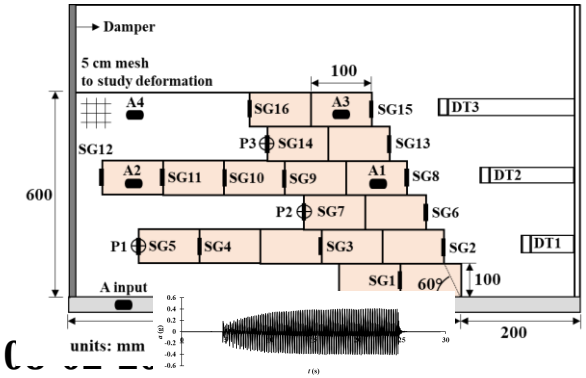

Tensile strain in geocells

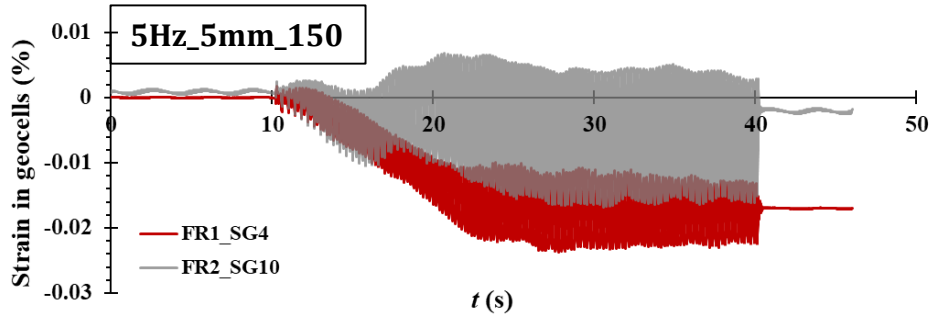

- Wider strain bandwidth in the upper reinforcement layer (lesser confinement)
- Strain mobilization in the bottom reinforcement layer arresting the slip surface

Dynamic lateral earth pressure

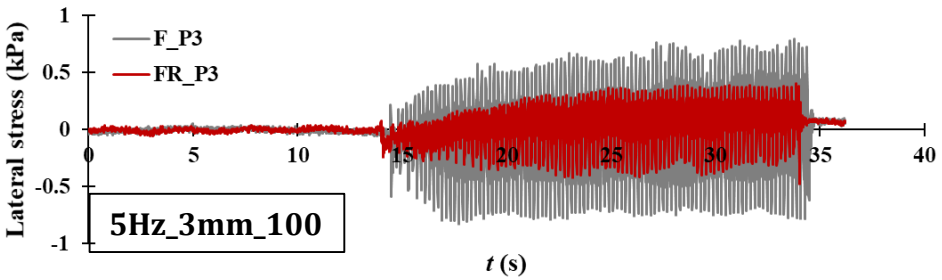

- Peak stresses and the range of cyclic stress reversals decreased by about 50% in FR

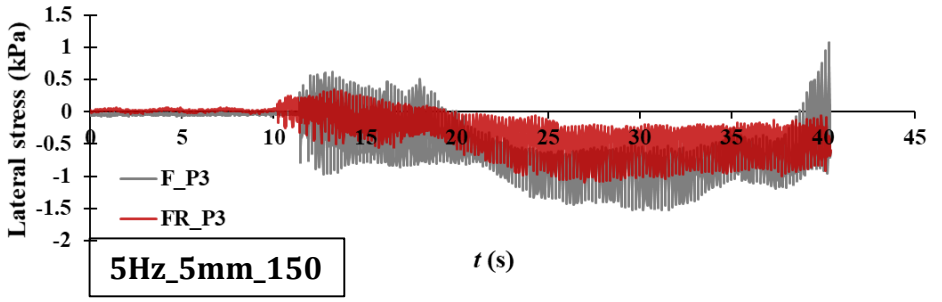

- Dip down in lateral stresses indicate settlement of backfill leading to failure surface development

Amplification Factor (AF)

Commercial geocells (Type I & II)

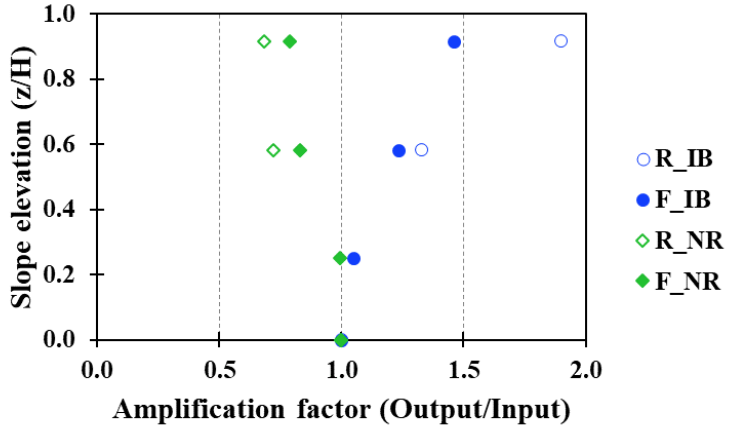

- 'R' models forms the extremes; Fascia components increased the stiffness and reduced the amplification-deamplification bandwidth
- Applicable for scaled geocell models and for different motion types

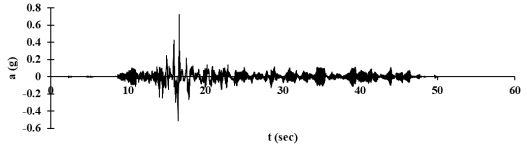

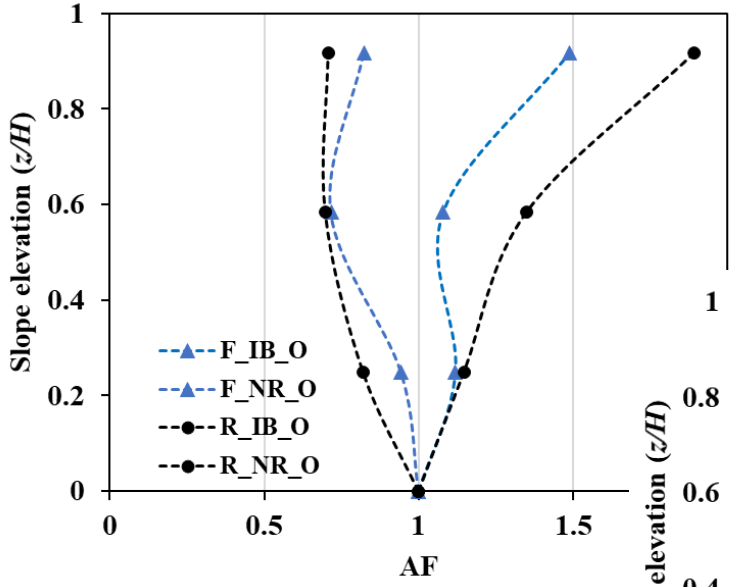

3D printed geocells (Type III)

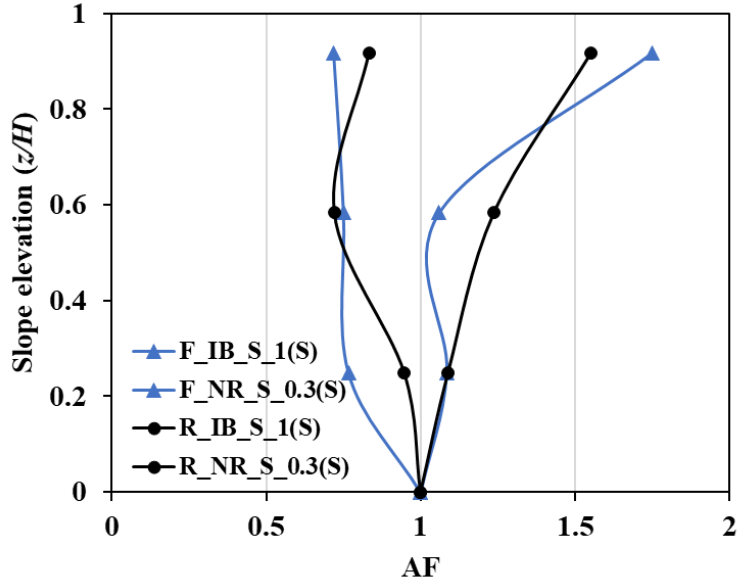

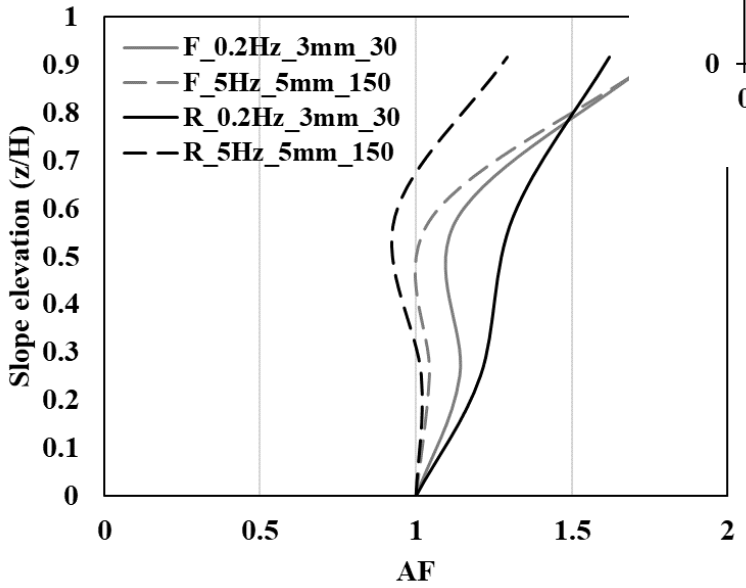

Peak tensile forces

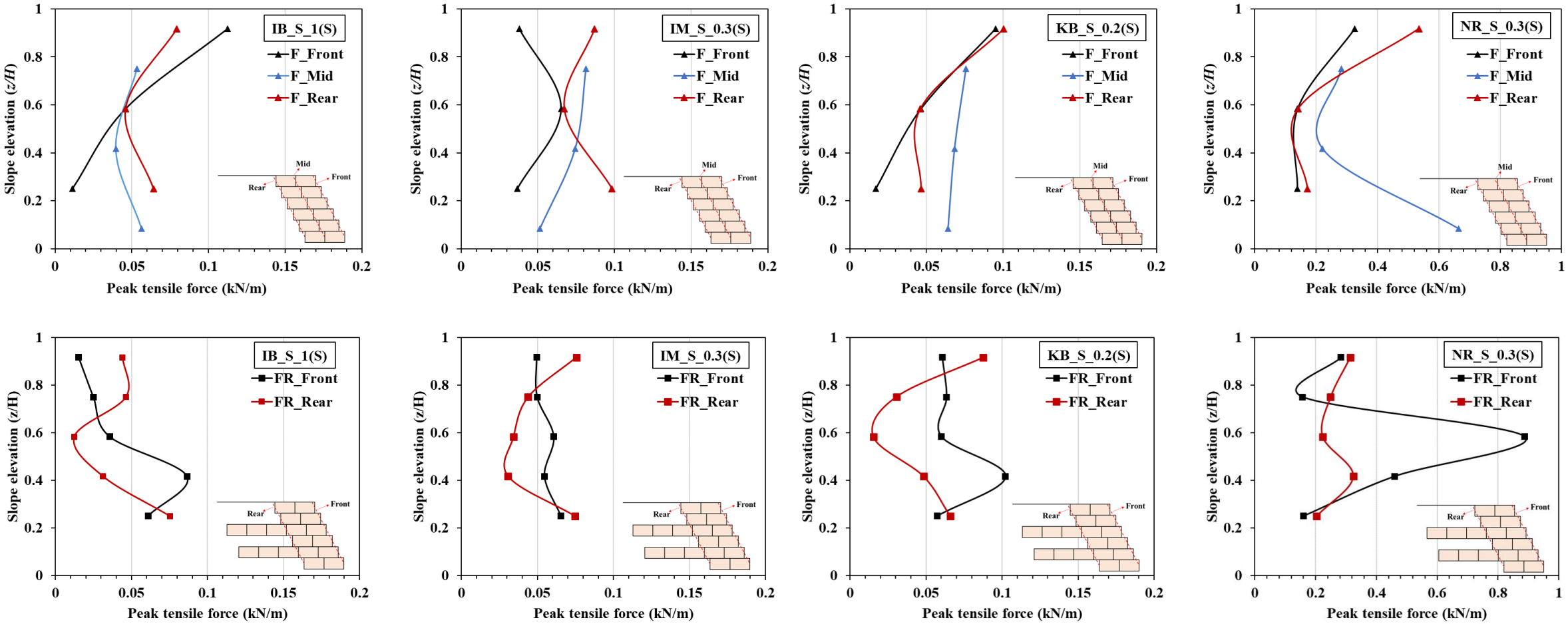

Peak tensile forces along the slope elevation of F and FR model configurations

Predominant section for peak tensile forces

F configuration - rear face of fascia

FR configuration – frontal face (partially taken over)

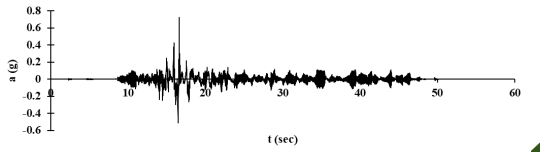

Failure of 3D printed geocell layers

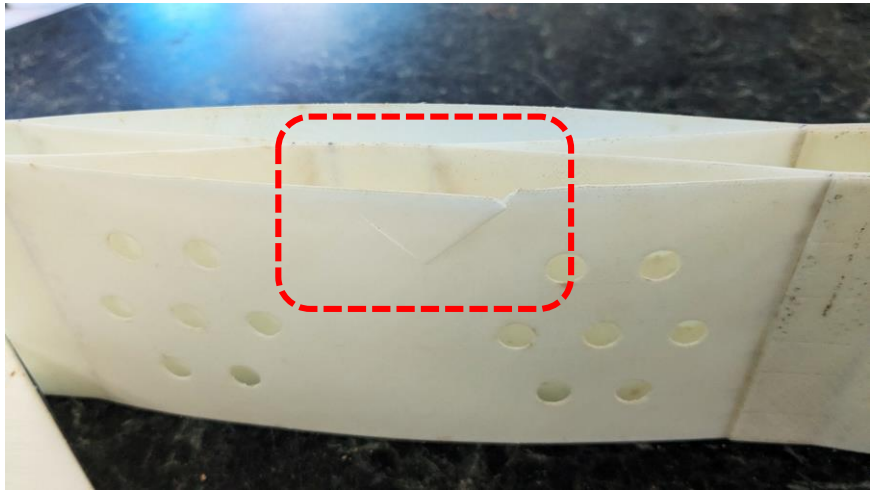

Breaking of strips

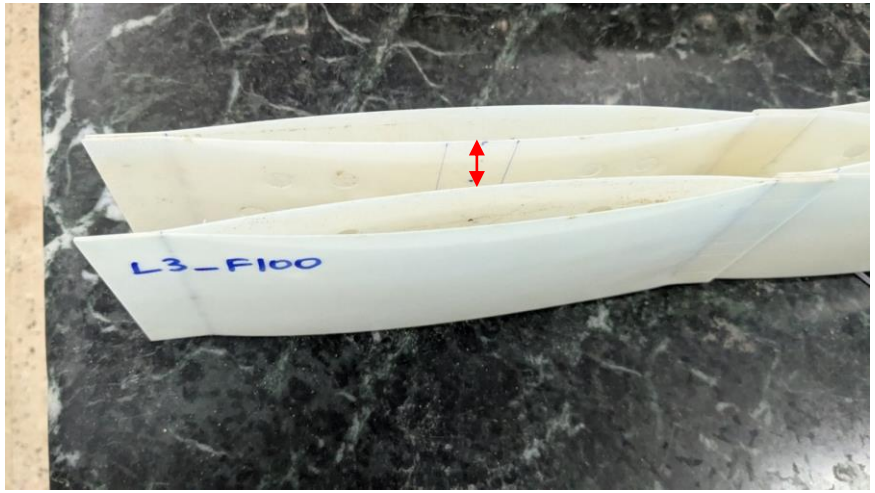

Detachment of geocells (splitting failure)

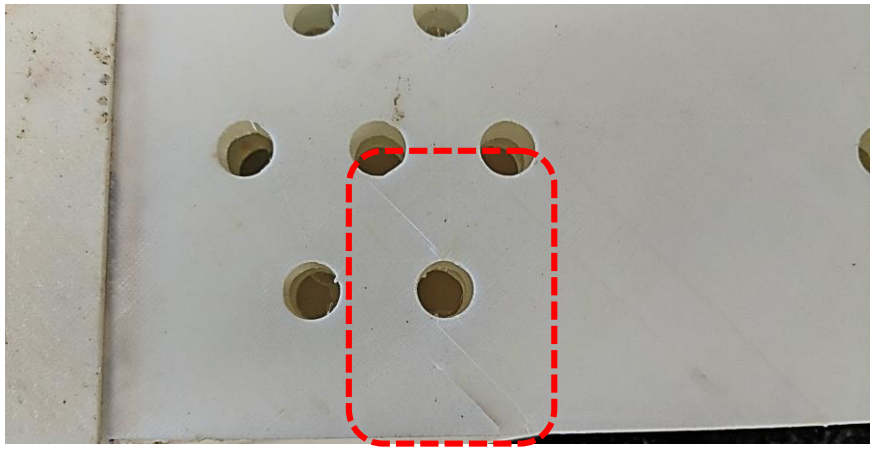

Crack propagation

Pre-shaking and Post-shaking tensile behaviour (Type-I)

Tension tests

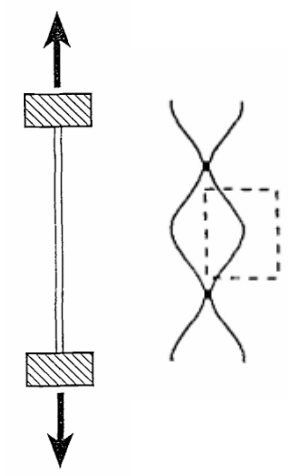

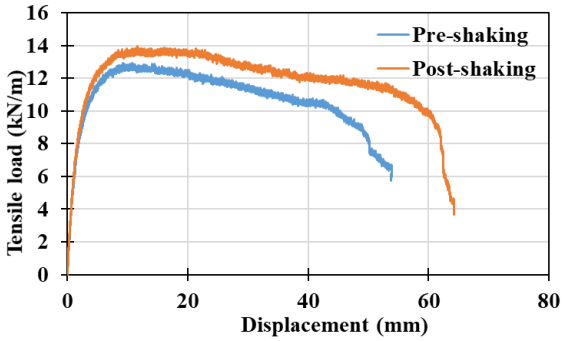

The post-shaking specimens possess increased tensile deformation capacity than the pre-shaking ones

Peeling tests

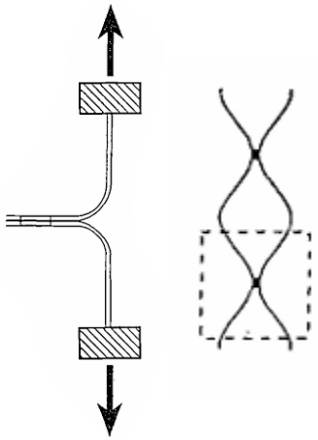

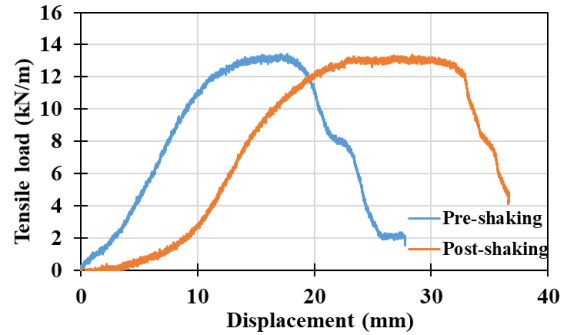

The tensile load acts upon the strips only after crossing the interval of mobilised deformation

The trend is same for the pre-shaking and post-shaking specimens

Tensile shear tests

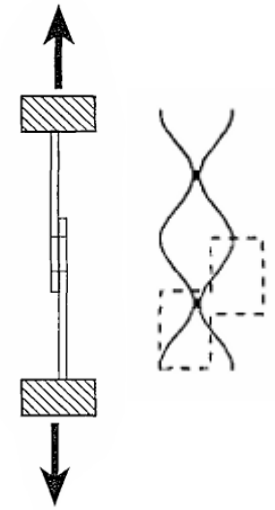

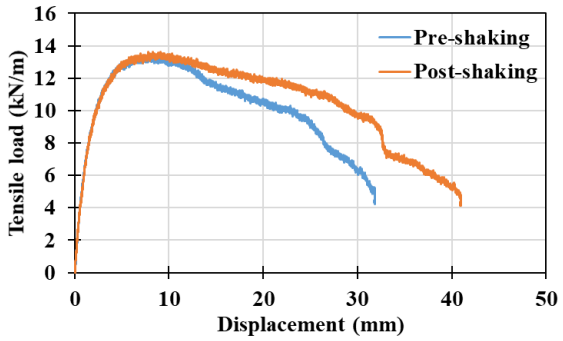

Splitting tests

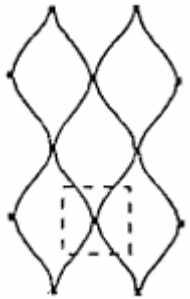

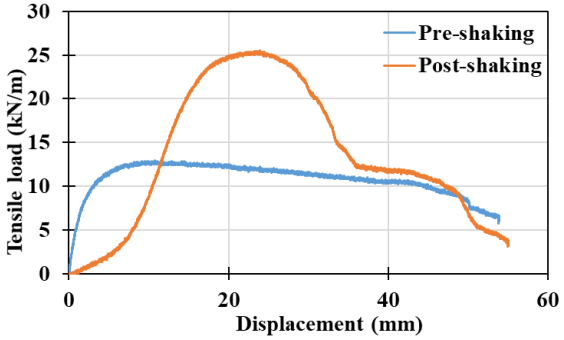

Tensile deformation in post-shaking specimen induced junction failure in one of the upper legs and a tensile strip failure in the other

Pre-shaking and Post-shaking tensile behaviour (Type-III)

Tension tests

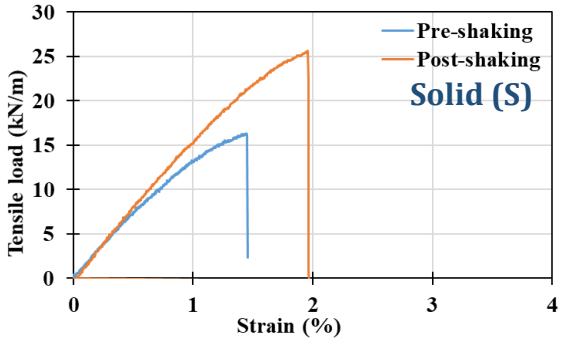

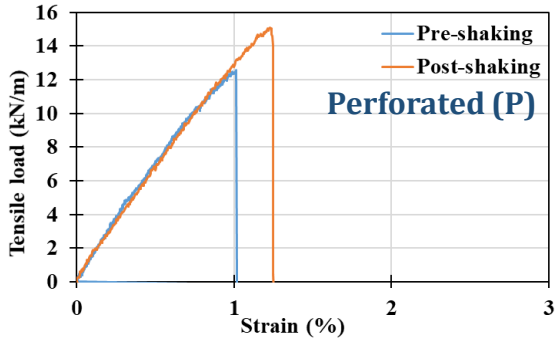

Peeling tests

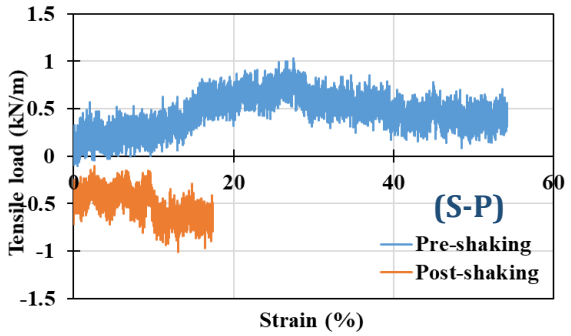

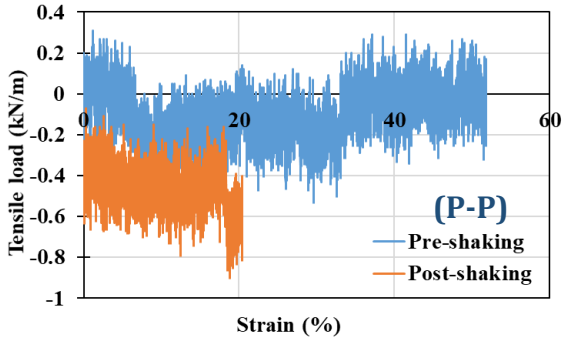

Tensile shear tests

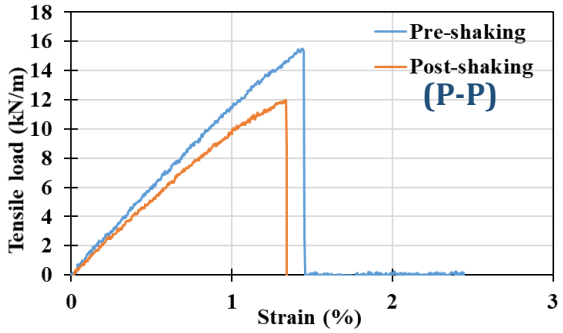

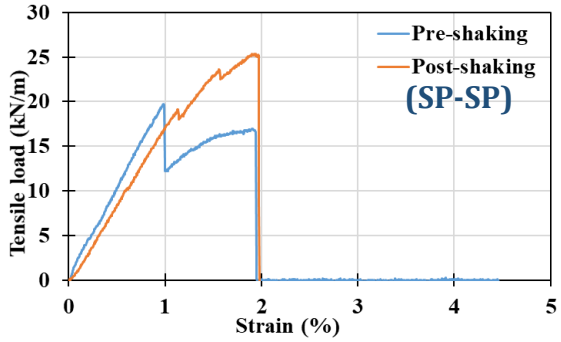

Splitting tests

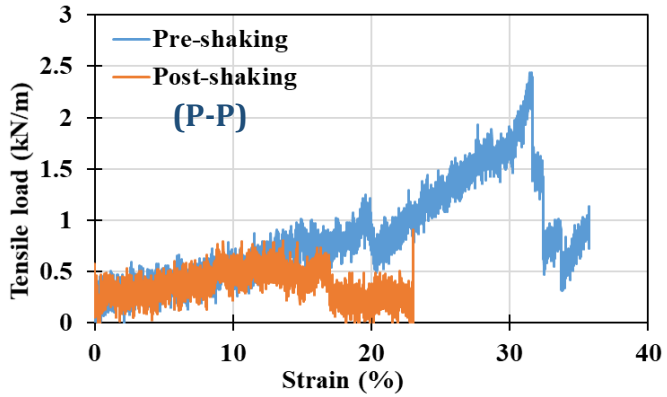

- Junction strengths are completely mobilized
- Tensile load capacity of strips have increased

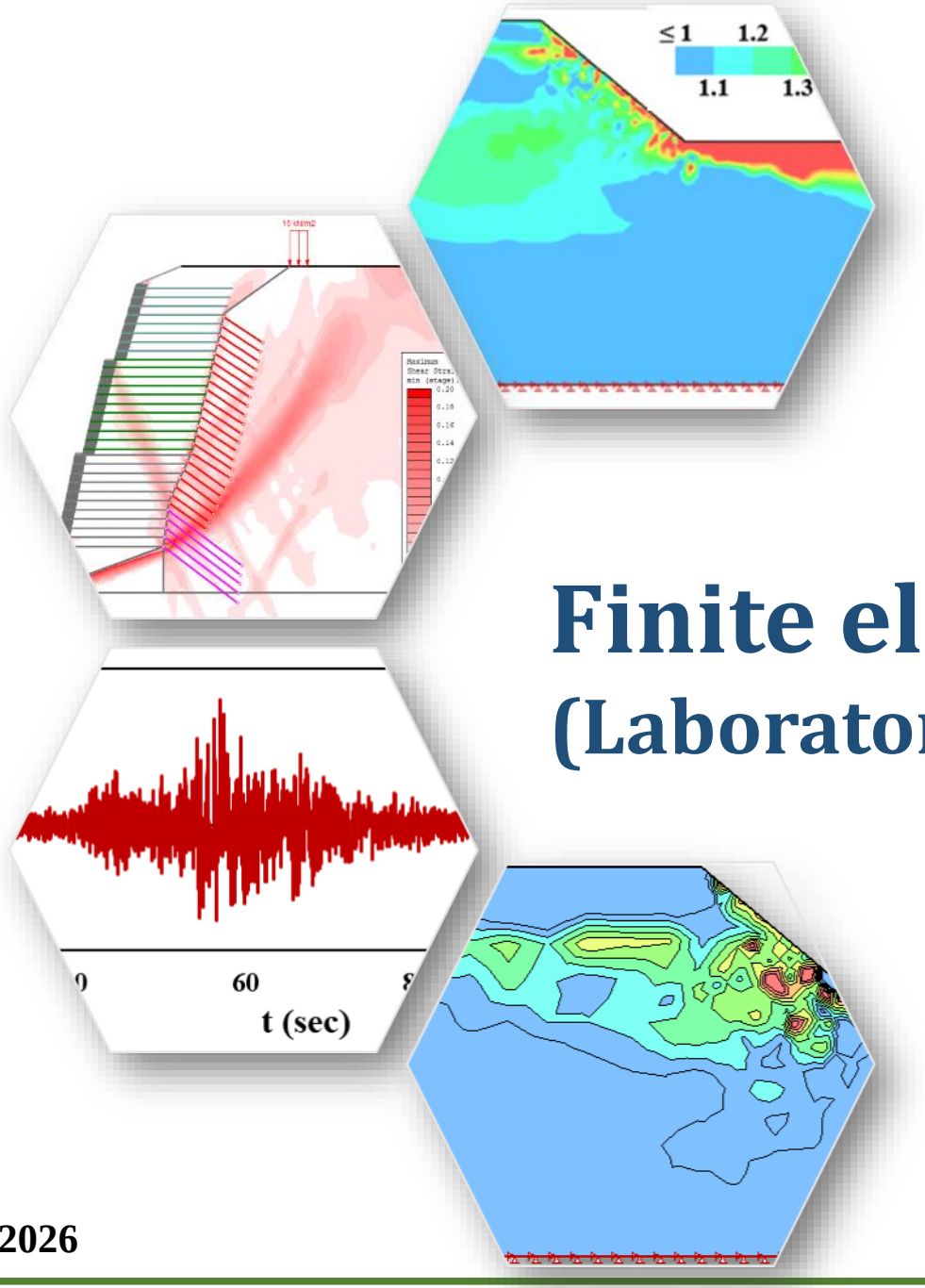

Finite element modelling
(Laboratory-scale and field-scale)

Methodology

Model domain

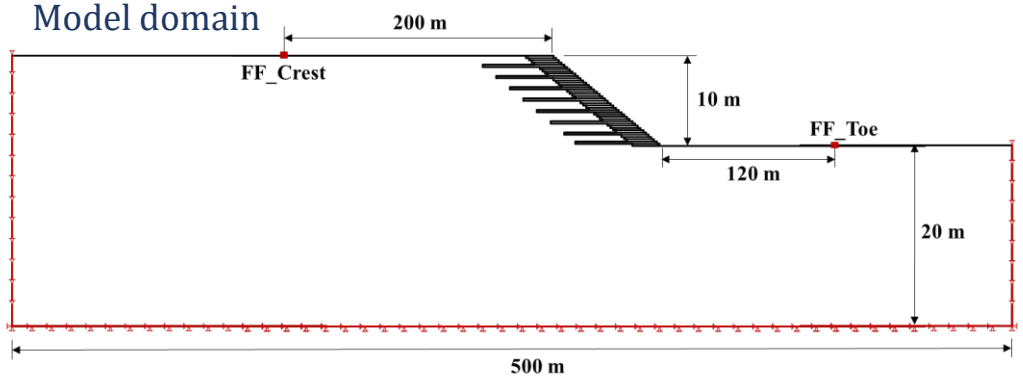

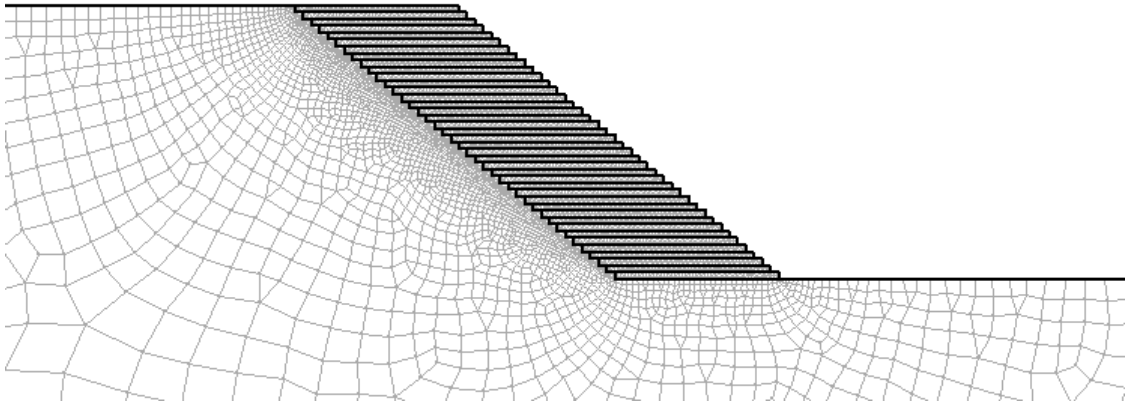

R-configuration

F-configuration

FR-configura

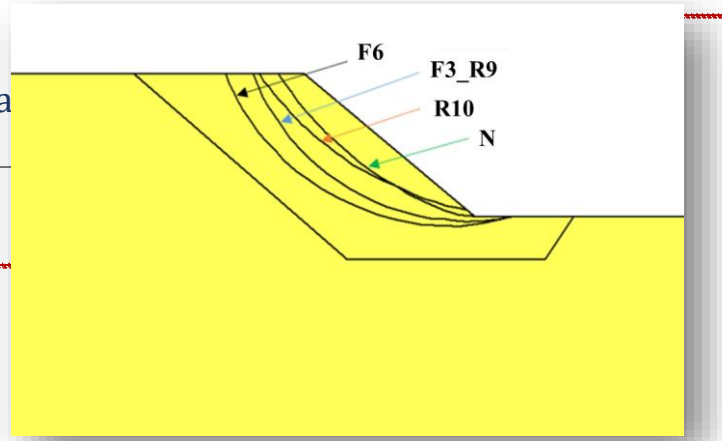

- Geocell layers – 0.25 m thick
- Static and pseudostatic analyses – SLOPE/W; Dynamic analyses – QUAKE/W (GeoStudio v2024)
- Mesh elements – Quadrilaterals and Triangles
- Soil-infilled geocells - Equivalent Composite Approach (ECA)

Material properties (Ujjawal and Hegde, 2020)

Parameters	Backfill Soil (Unreinforced parameters)	Composite Soil (ECA parameters)
Unit weight, γ (kN/m^3)	20	20
Cohesion, c (kPa)	5	33
Internal friction angle, ϕ (˚)	32	32
Shear Modulus, G (MPa)	7.28	15.95
Damping ratio, ξ (%)	2.06	5.45
Poisson's ratio, ν	0.33	0.33

$$C_r = \frac{\Delta\sigma_3}{2}\sqrt{K_p} \qquad \Delta\sigma_3 = \frac{2M}{d_0}\left[\frac{1-\sqrt{1-\varepsilon_a}}{1-\varepsilon_a}\right]$$

Validation

Srilatha et al., 2017

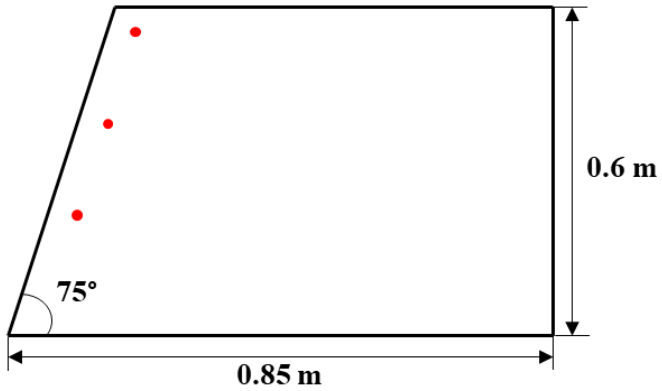

$\gamma = 15$ kN/m^3
$c = 33$ kPa
$\varphi = 33°$
$G_{max} = 0.2$ MPa
$\xi = 0.5$ %

Shake table model

Sinusoidal excitation – 0.1 g; 2 Hz

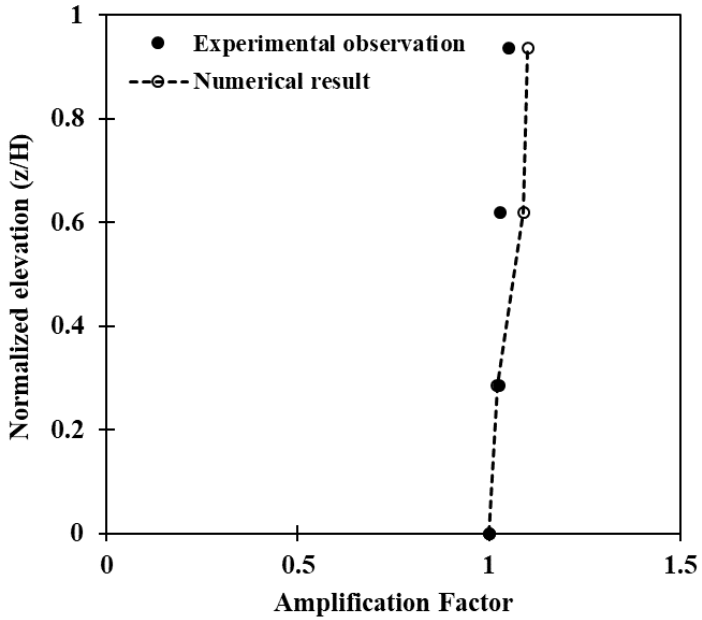

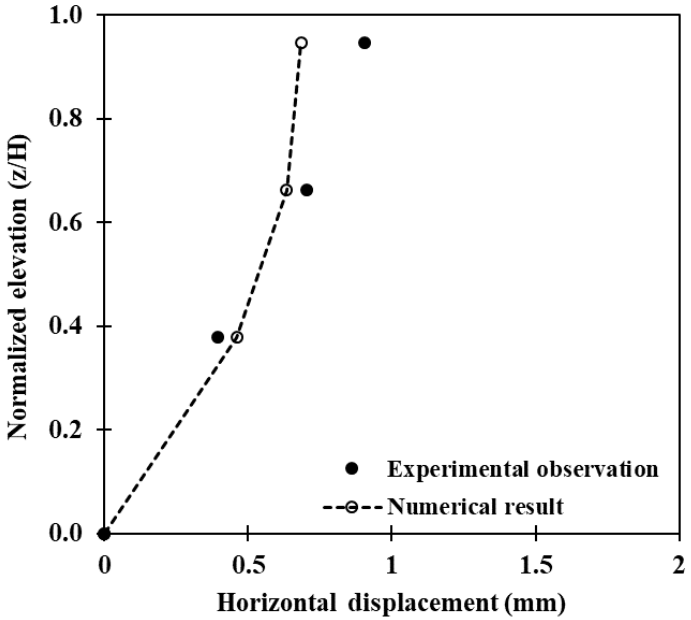

- Amplification factor – close to unity
- Maximum deviation in horizontal displacement is at the crest
  - Displacement difference of 0.2 mm
  - (0.03% with respect to wall height)

Laboratory-scale geocell-reinforced slopes

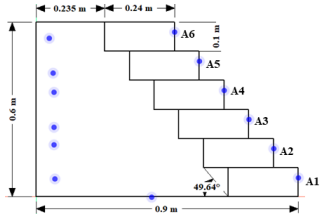

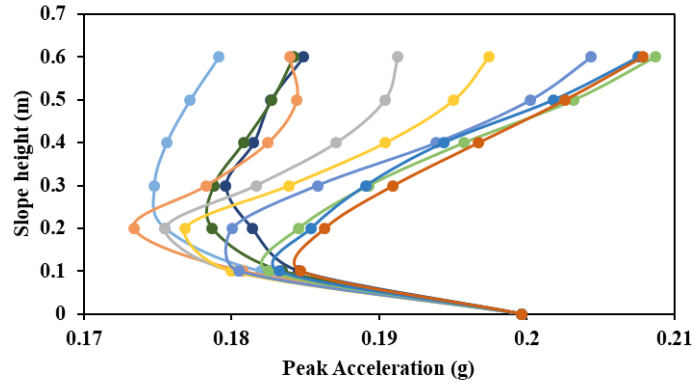

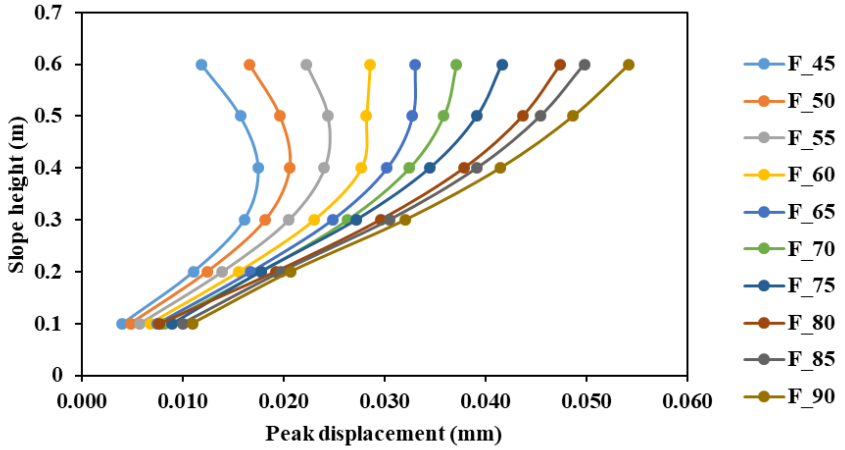

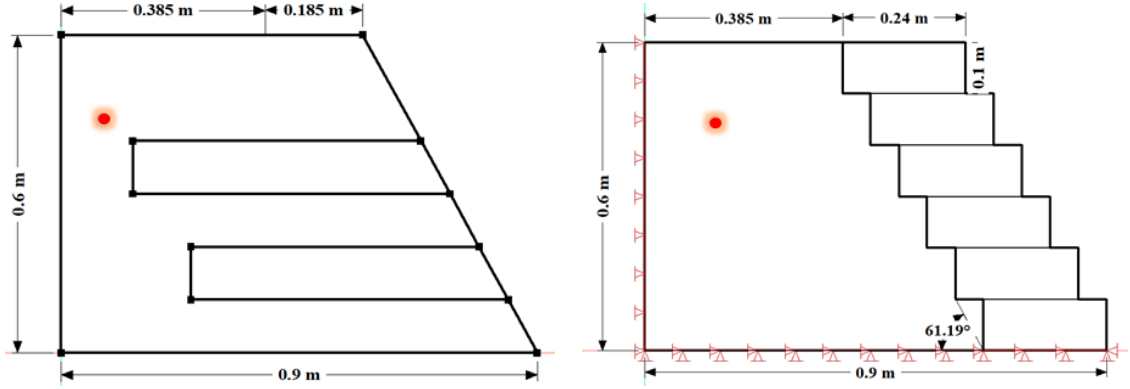

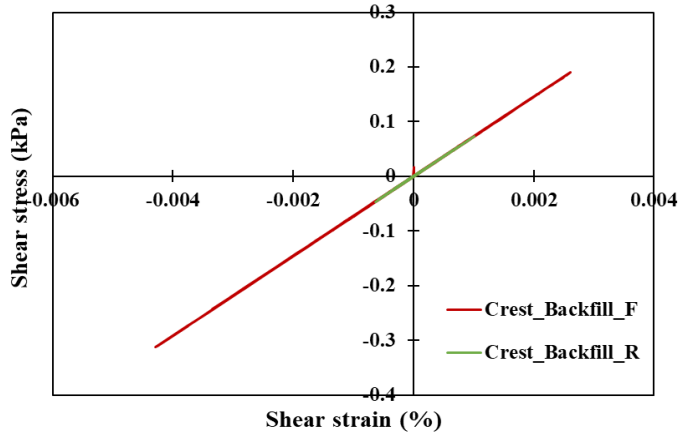

Fig. Hysteresis behaviour

- Peak acceleration at crest increases with slope angle from 60°
- Maximum displacement shifts from mid-slope to the crest with increase in the slope angle.

The configuration type influences the shear capacity of the backfill

Key Contributions from the study

- Systematically establishing the **damping characteristics of geocell-reinforced slopes**, thereby highlighting their energy dissipation capacity under dynamic loading.
- Identifying the **failure mode of geocell-reinforced slopes** subjected to **seismic loading**, thereby providing critical insights into their behavior during earthquake events.
- Determining the **best feasible geocell placement configuration**, which elucidated that the Fascia-Reinforcement arrangement is the most effective one for enhancing slope stability.

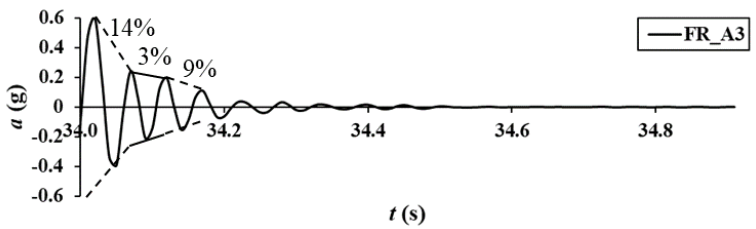

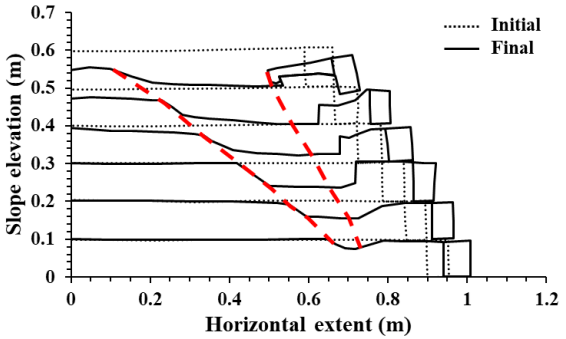

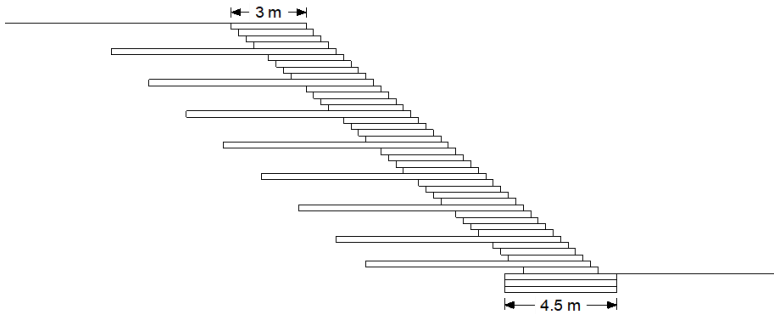

Seismic Response of Large-Height Geocell-Fascia Multi-Tiered Geosynthetic Reinforced Soil (GRS) Wall: A Forensic Investigation of a Hillslope Reclamation Project

Geosynthetic Reinforced Soil (GRS) Wall

Geosynthetic Reinforced Soil (GRS) walls are a type of engineered retaining structure that combine geosynthetic materials with compacted soil to create a mechanically stabilized structure capable of retaining soil, resisting erosion, and accommodating various

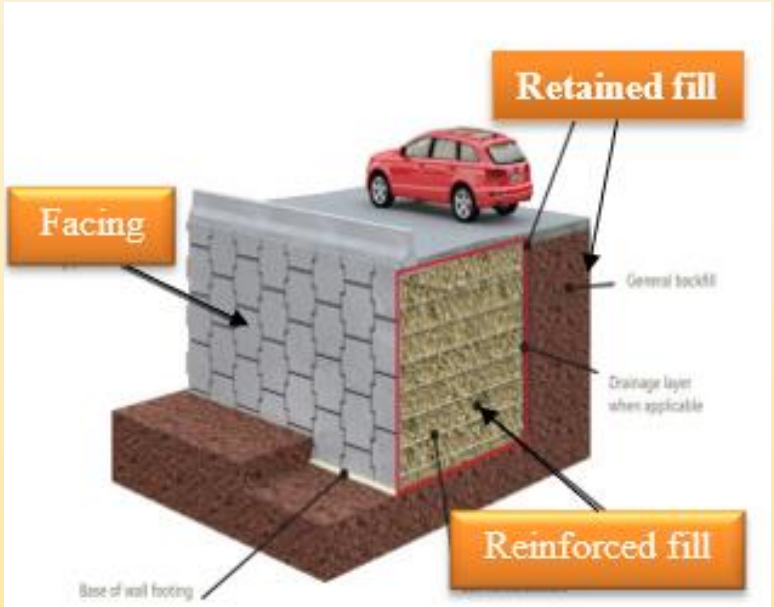

Components of GRS wall

- Reinforcement
- Facing
- Backfill Material

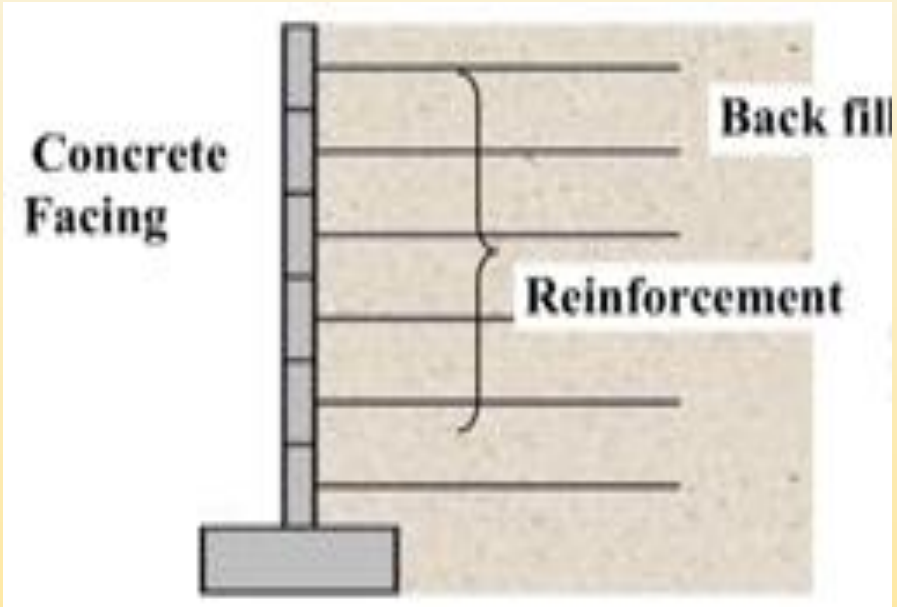

Geosynthetic Reinforced Soil (GRS) Wall

- Preference of geosynthetic-reinforced soil (GRS) walls over conventional rigid retaining walls
  - ✓ Flexibility in design of complex structures
  - ✓ Relatively economical and quick to construct
  - ✓ Reliable long-term sustainability and better aesthetic appeal

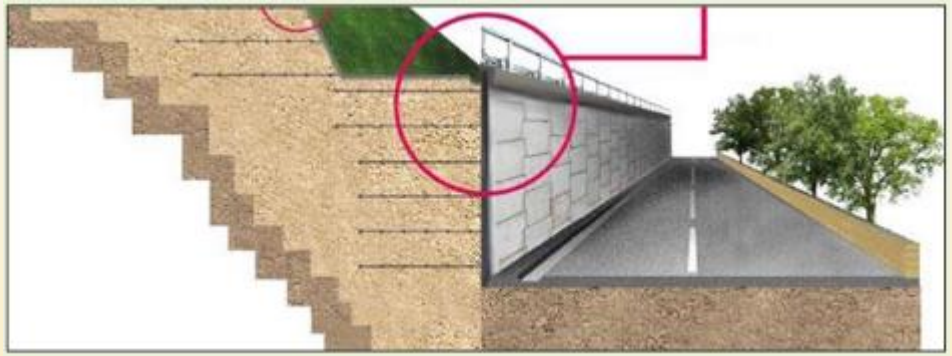

- Performance and overall stability of GRS wall
  - ✓ Combinatorial interaction of **fascia**, **backfill** and **reinforcement**
- GRS walls advocate seismic resilience to earthquake conditions
  - ✓ ~1% exhibiting severe damage out of 1600 structures **(Kuwano et al., 2014)**
- Failures are still reported, even when existing design guidelines are followed **(Kim et al., 2010)**
  - ✓ Necessity of forensic investigations to refine design practices and construction approaches

Types of GRS Walls

- Geosynthetic Reinforced Soil (GRS) walls include a range of different types and configurations, each made to specific project requirements and site conditions.
  - **Modular Block GRS Walls**
  - **Wrapped-face GRS Walls**
  - **Crib GRS walls**
  - **Hybrid GRS Walls**
  - **Green GRS retaining wall**
  - **Gabion GRS retaining walls**

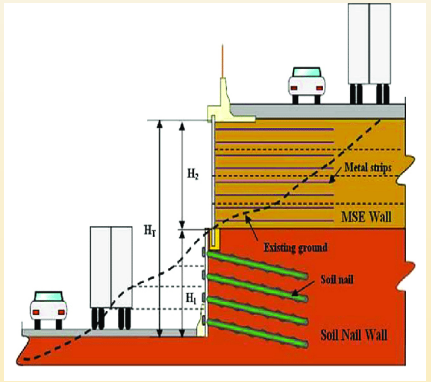

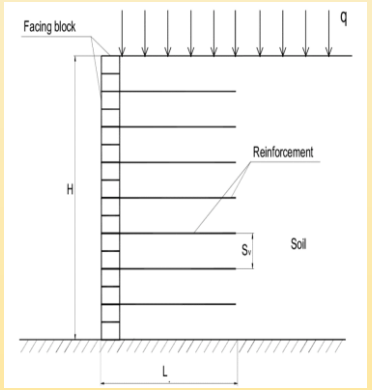

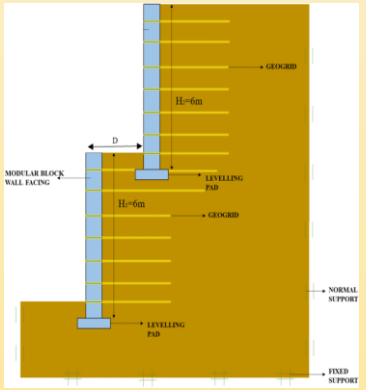

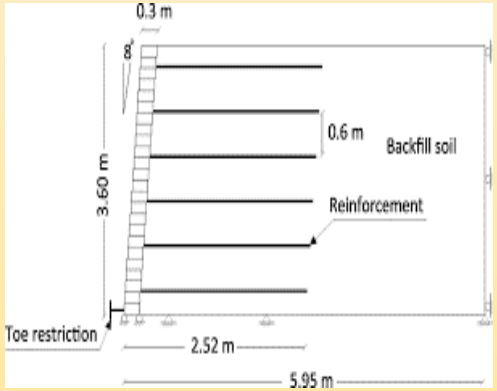

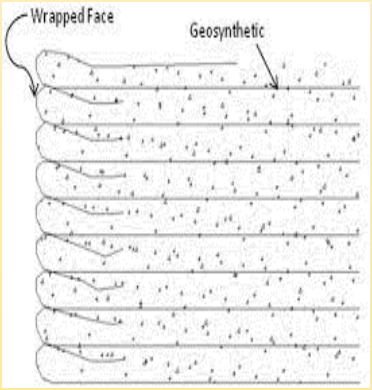

Classification of GRS Walls

- Geosynthetic Reinforced Soil (GRS) walls can be classified based on several criteria, including backfill material, reinforcement type, wall height, and application (Lee and Wu, 2004)

Based on backfill material

- Granular soil GRS walls
- Cohesive soil GRS walls
- Marginal Backfill GRS Walls
- Organic Backfill GRS Walls
- Recycled Material Backfill GRS Walls

Based on reinforcement type

Geogrid Reinforced GRS Walls

- Geotextile Reinforced GRS Walls
- Geocell Reinforced GRS Walls
- Geosynthetic Strip Reinforced GRS Walls
- Natural Fiber Reinforced GRS Walls
- Combination Reinforced GRS Walls

Based on application

- Retaining Walls
- Bridge Abutments
- Embankments
- Noise Barriers
- Landfill Containment
- Slope Stabilization

Failure of GRS Walls

Collin (2001) Geosynthetic-reinforced soil segmental retaining wall → **rainfall induced failure**

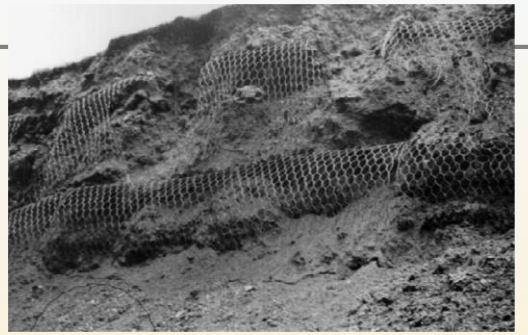

Huang *et al.* (2003) GRS wall face failure triggered by **insufficient connection strength** or **excessive buckling-mode deformation** of the modular block facing

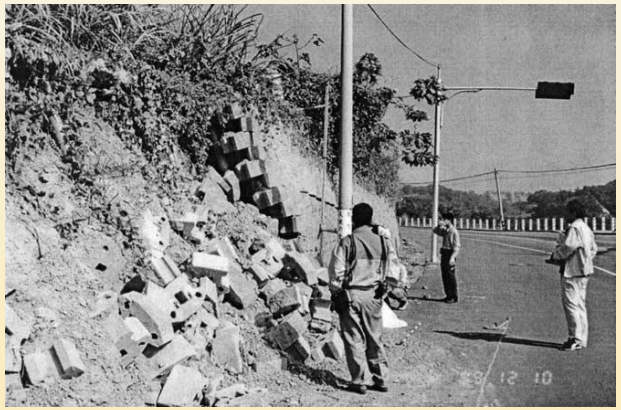

Xiao *et al.* (2021) **Improperly designed connections** and **use of poor-quality or highly plastic fines-rich backfill soil** contribute directly to failure

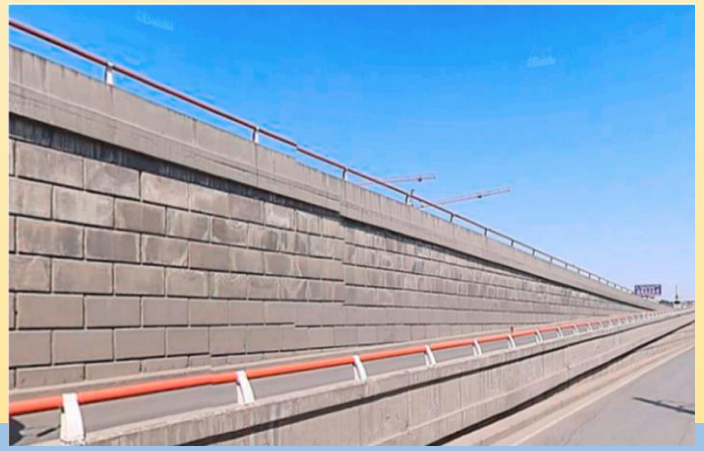

Failure of GRS Walls

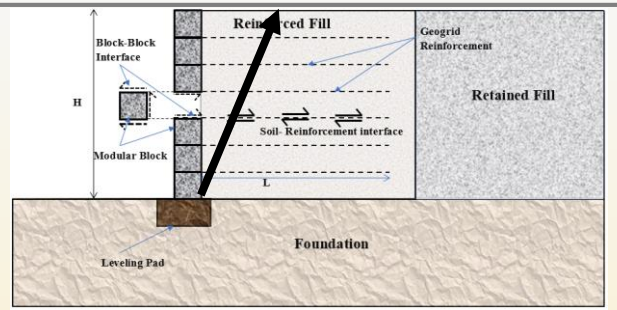

Koerner & Koerner (2018); Yang et al. (2019); Xiao et al. (2021); Guller et al. (2023)

Major Causes of Facing Failure

- ✓ Drainage issues
- ✓ Improper backfill selection and compaction
- ✓ Connection failures
- ✓ Foundation settlement

Types of Facing Failure

- ✓ Outward displacement and bulging
- ✓ Cracking and spalling of facing elements
- ✓ Panel collapse
- ✓ Vertical settlement or tilting

Prevention and Recommendations

- ✓ Effective drainage
- ✓ Engineering of connections
- ✓ Routine inspection
- ✓ High-quality compaction

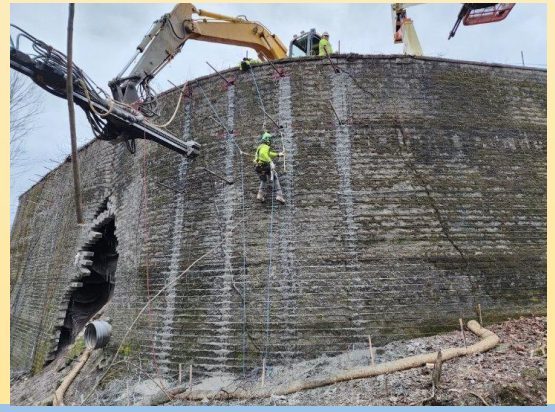

Failure of GRS Walls

Failures in Geosynthetic-Reinforced Soil (GRS) walls can occur due to various factors, ranging from design deficiencies to external conditions **(Xiao et al., 2021, Huang, 2000; Mosallanezhad et al., 2015)**.

Common failure modes are:

- Sliding failure
- Bearing capacity failure
- Global stability failure
- Pull-out failure
- Facing failure
- Tensile rupture
- Seismic failure

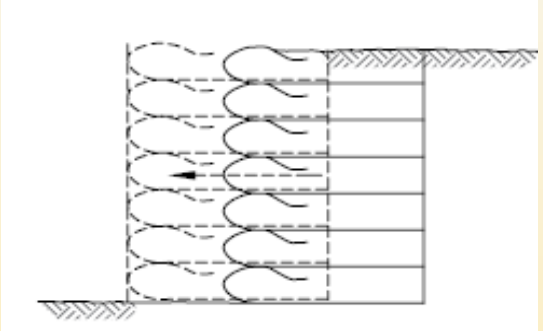

Sliding failure

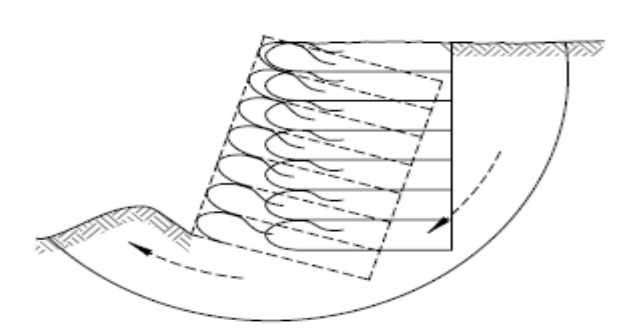

Global Stability Failure

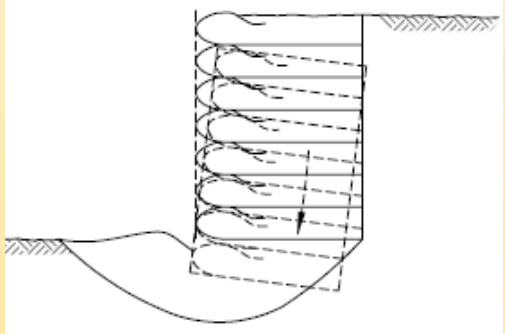

Bearing Capacity Failure

Tensile rupture

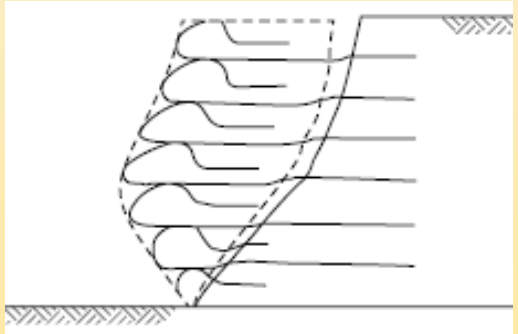

Pullout failure

Case Study: Hillslope Reclamation Project

2020: Landslide-induced partial cliff collapse due to toe erosion by River Teesta in Sikkim

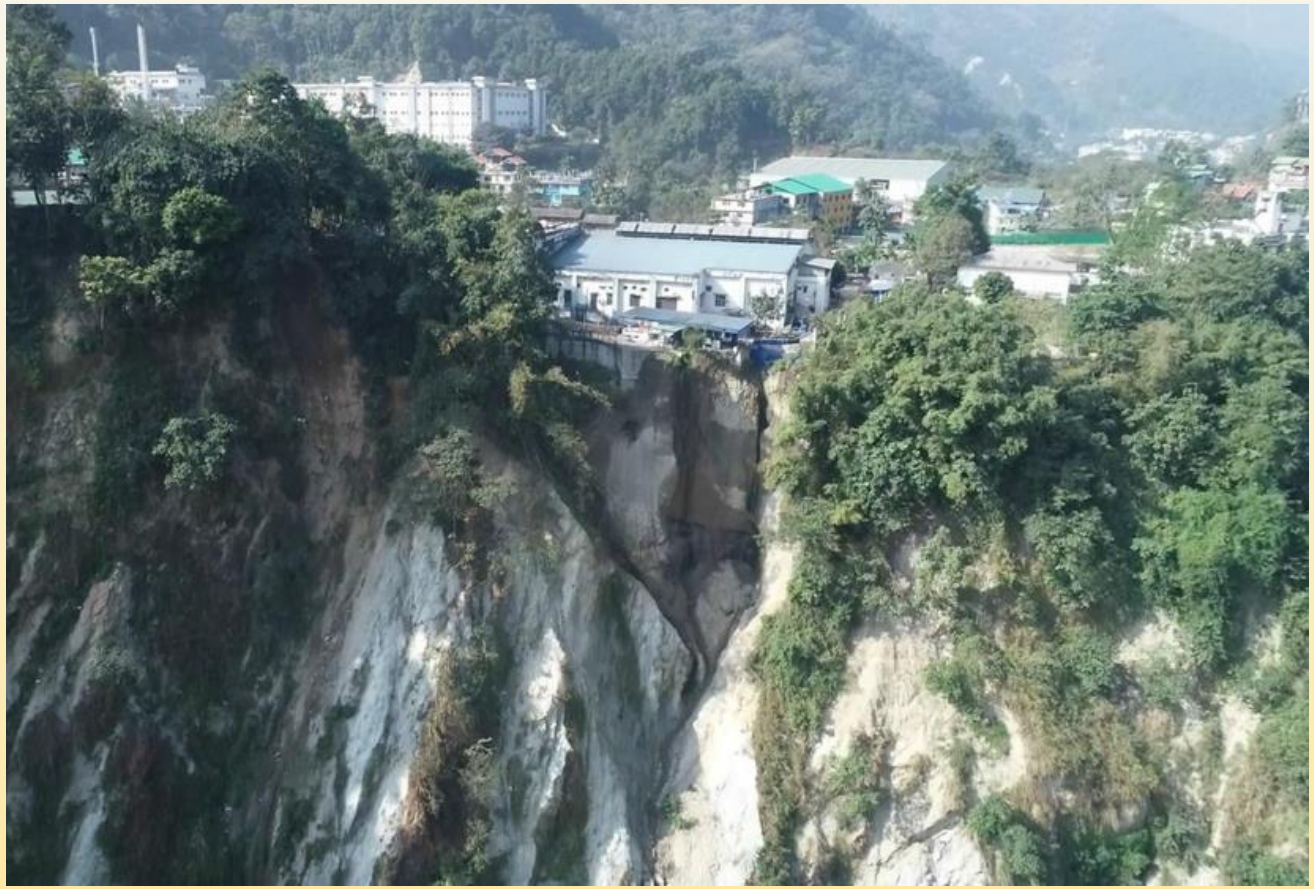

Aerial view of the site

Gabion retention and GRS wall for reclamation

Case Study: Hillslope Reclamation Project

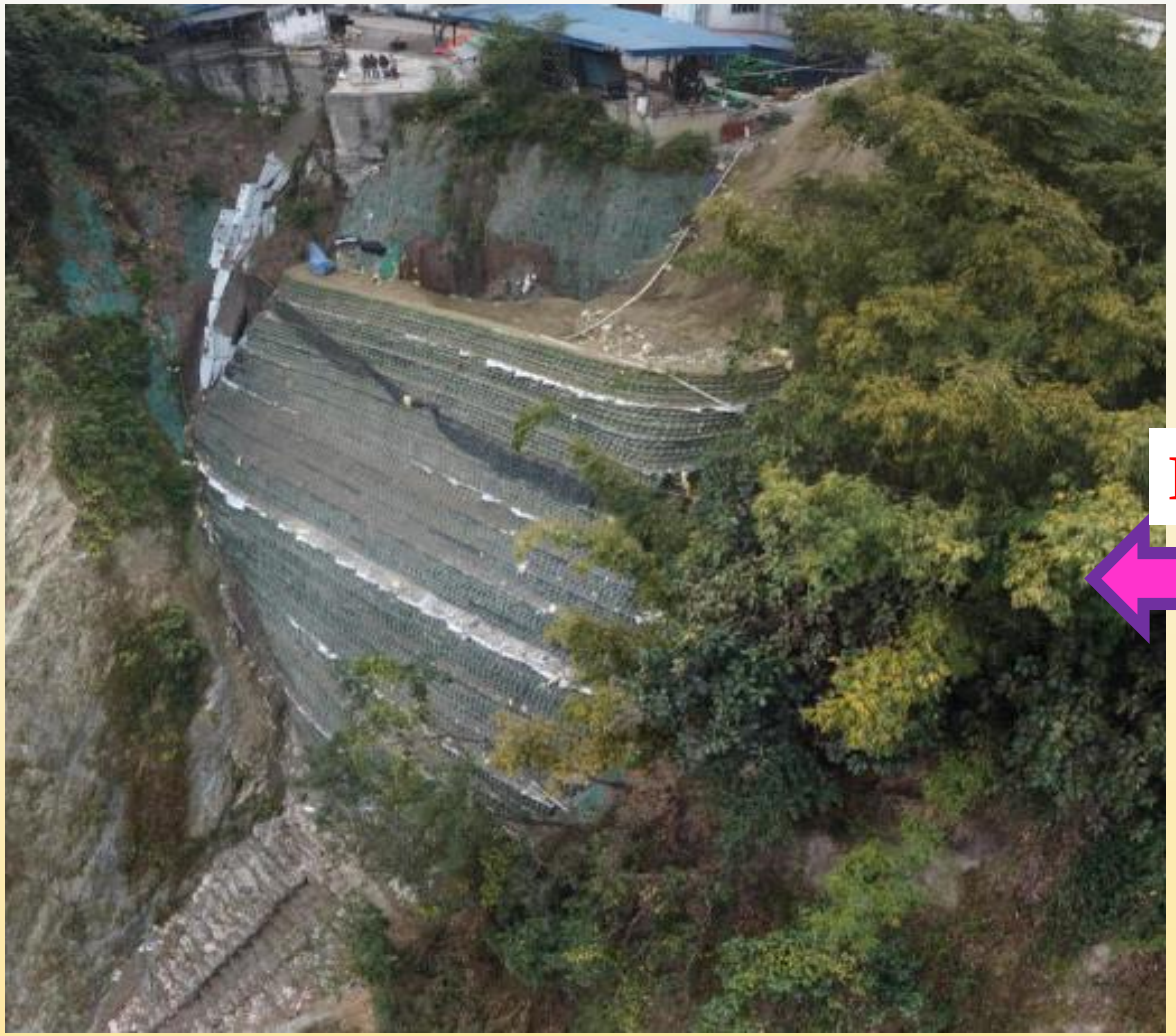

M_w 3.5

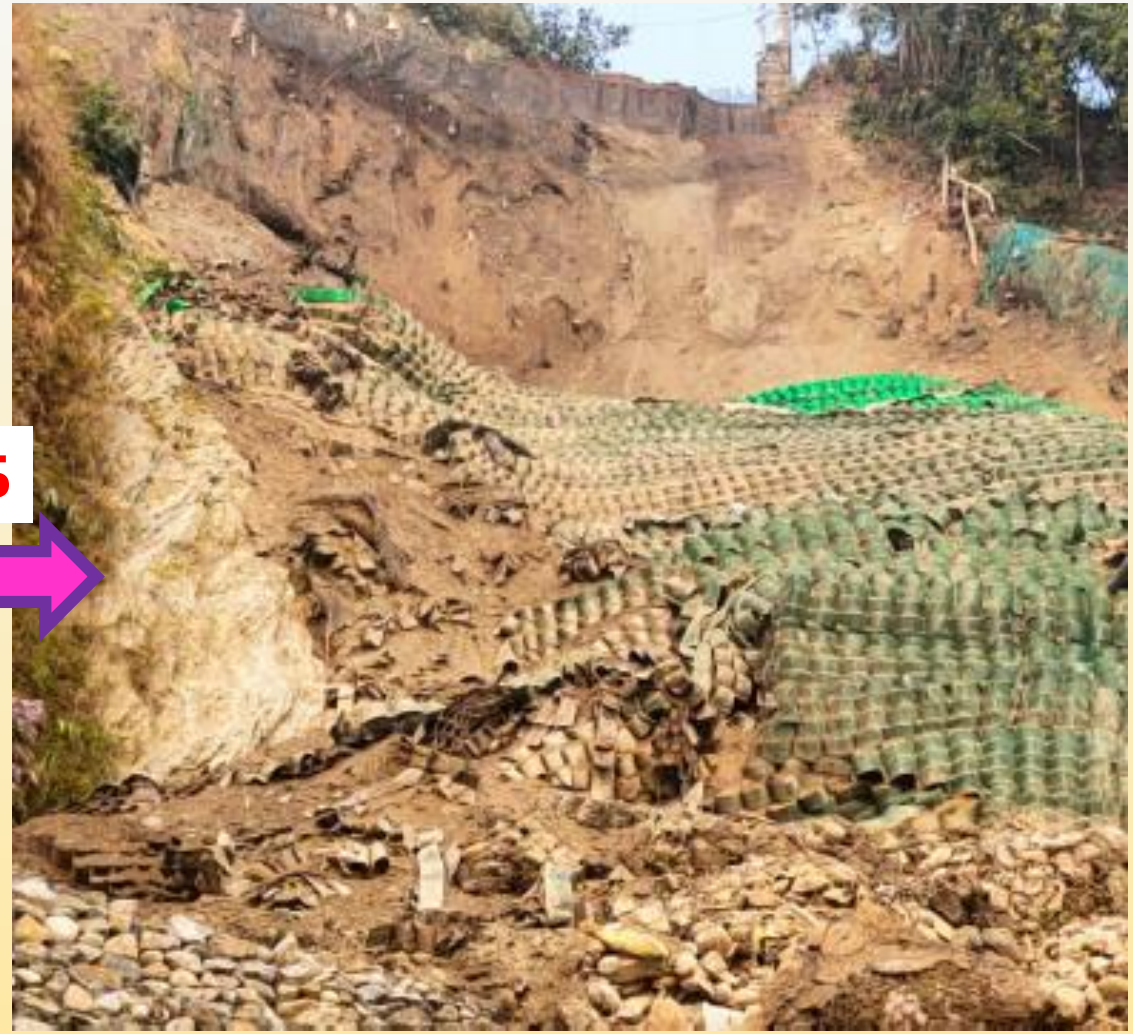

GRS wall: Before collapse (Near completion)

GRS wall: After collapse

Glimpses from Construction Period

Numerical Modelling of Proposed Reclamation

Material Specifications

Material Name	Unit weight (kN/m^3)	Poisson's ratio	Young's Modulus (MPa)	Angle of internal friction (°)	Cohesion (kPa)
Retained fill	19	0.3	192	50	40
Foundation	20	0.2	192	33	100
Concrete Pedestal	24	0.15	$1.58x10^4$	45	750
Reinforced Soil	18	0.3	312	32	0
Geocell Fascia	18	0.3	468	32	33

Reinforcement type	Ultimate tensile strength (kN/m)	Reduction factor	Allowable design strength (kN/m)
GG-TT	100	1.786	56
GG-MT	200	1.961	102
GG-BT	250	1.667	150
EA-BT	200	-	-
EA-Surface	50	-	-

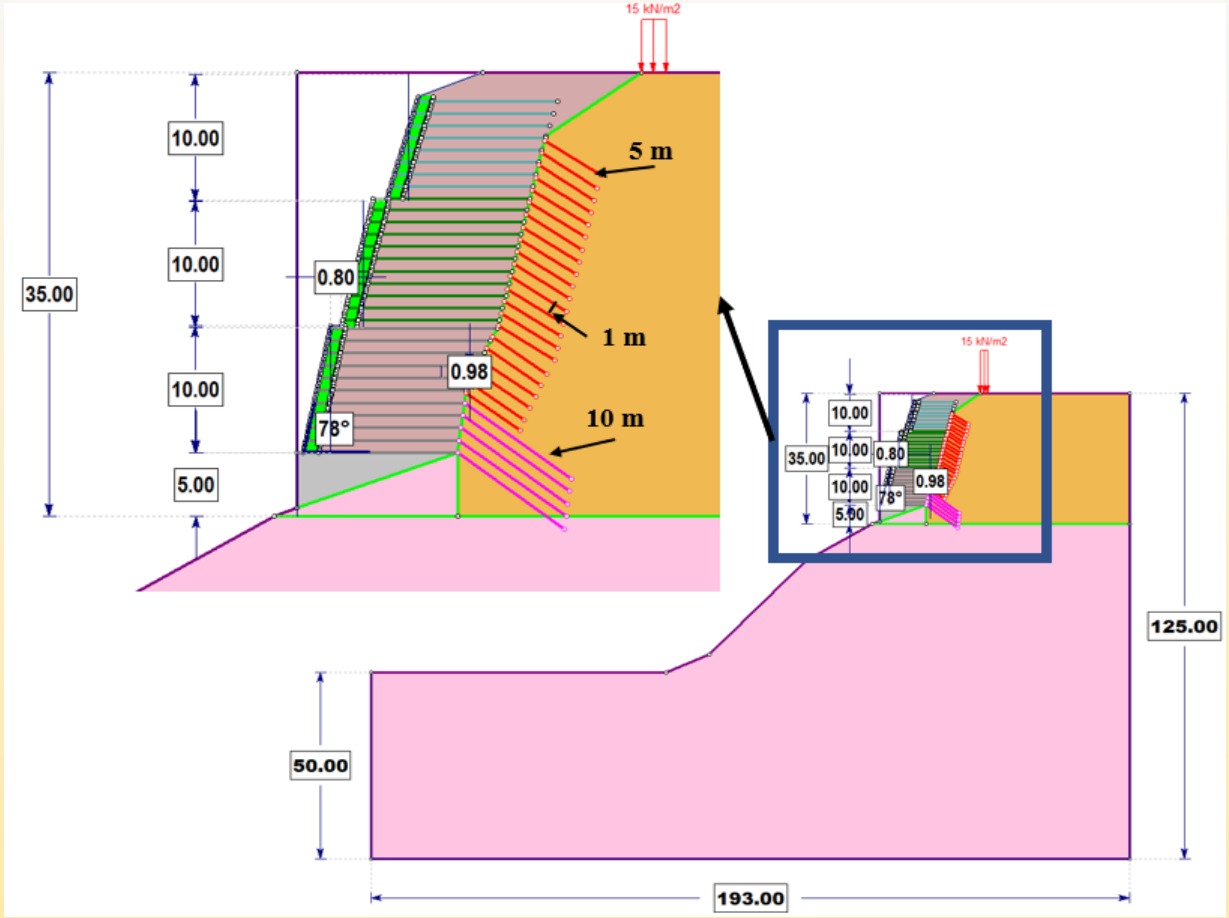

Numerical Model: Rocscience RS2 Platform

Natural Vibration of GRS Structure

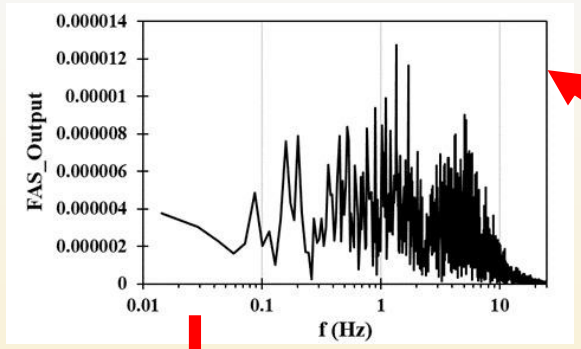

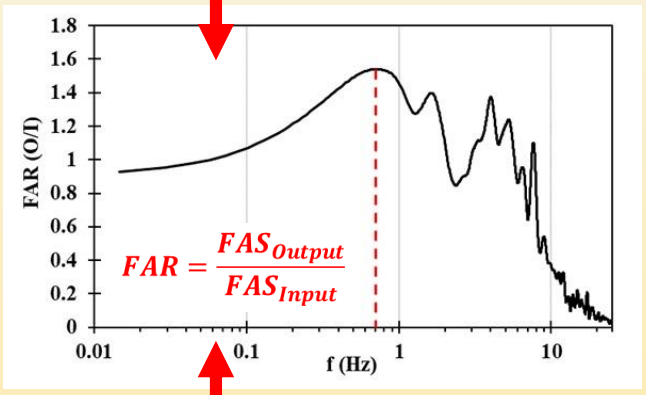

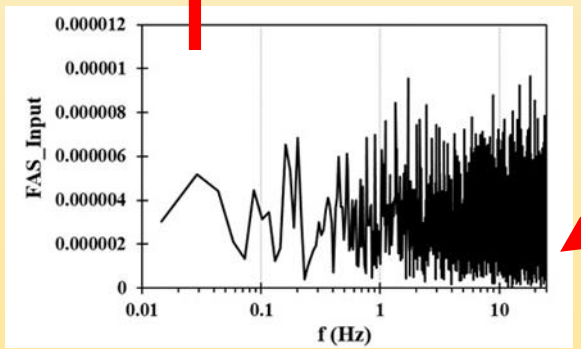

White Noise Analysis

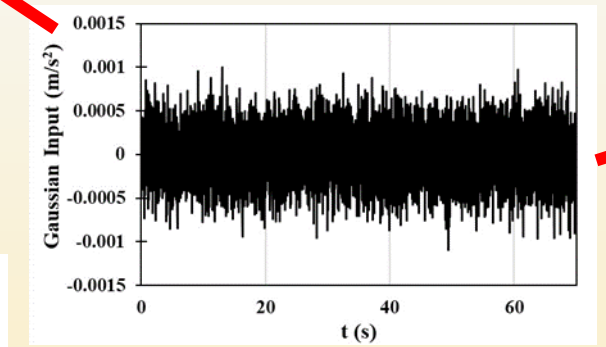

Fundamental frequency (f_n) = 0.7 Hz

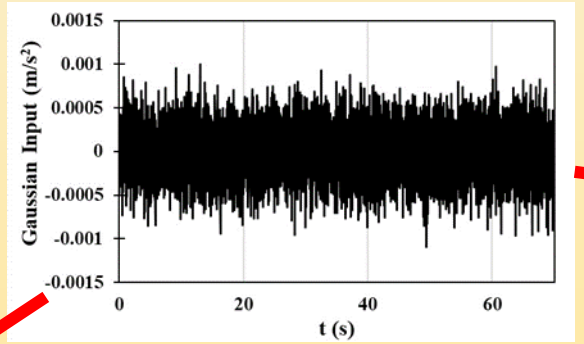

Long-Period Structure

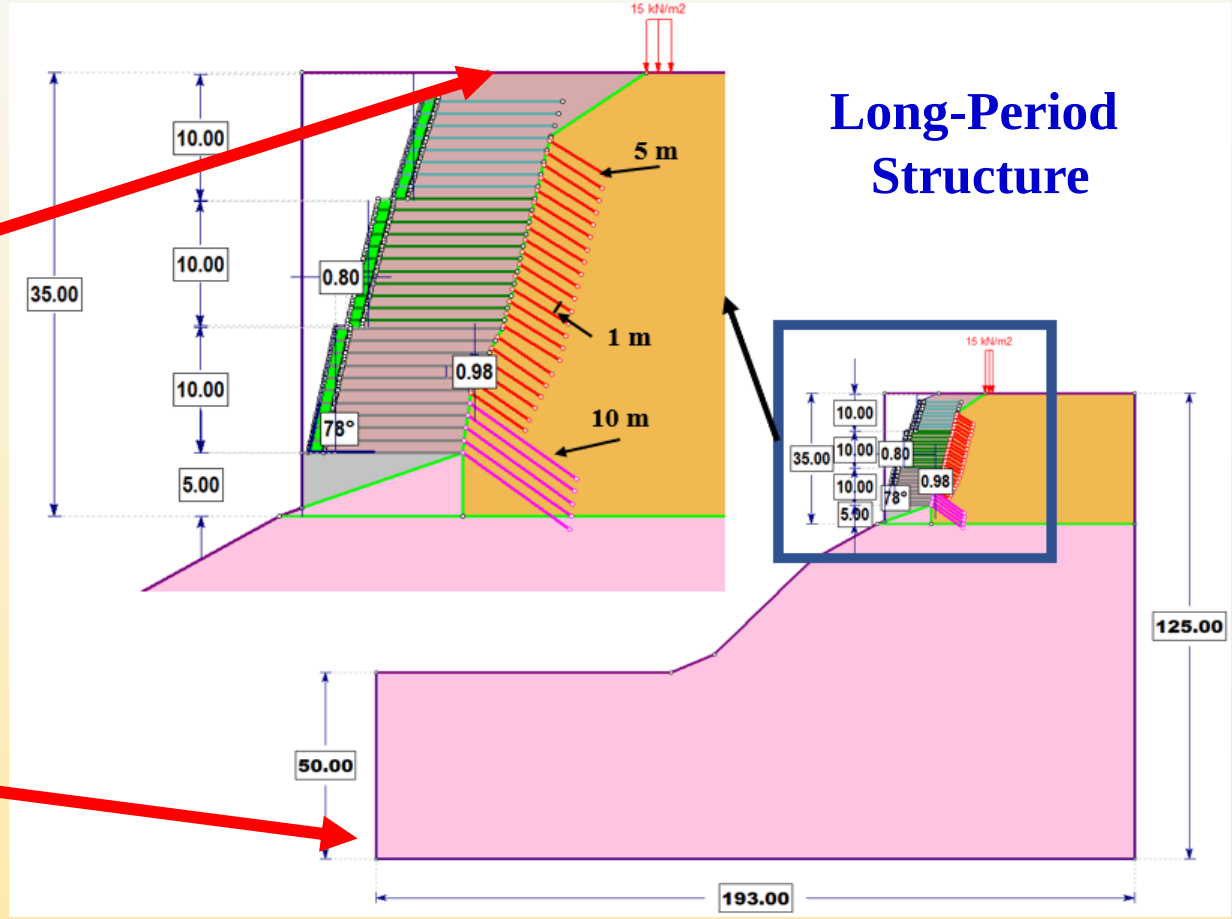

Numerical Model: Rocscience Slide2 & RS2 Platforms

Static Stability Analysis

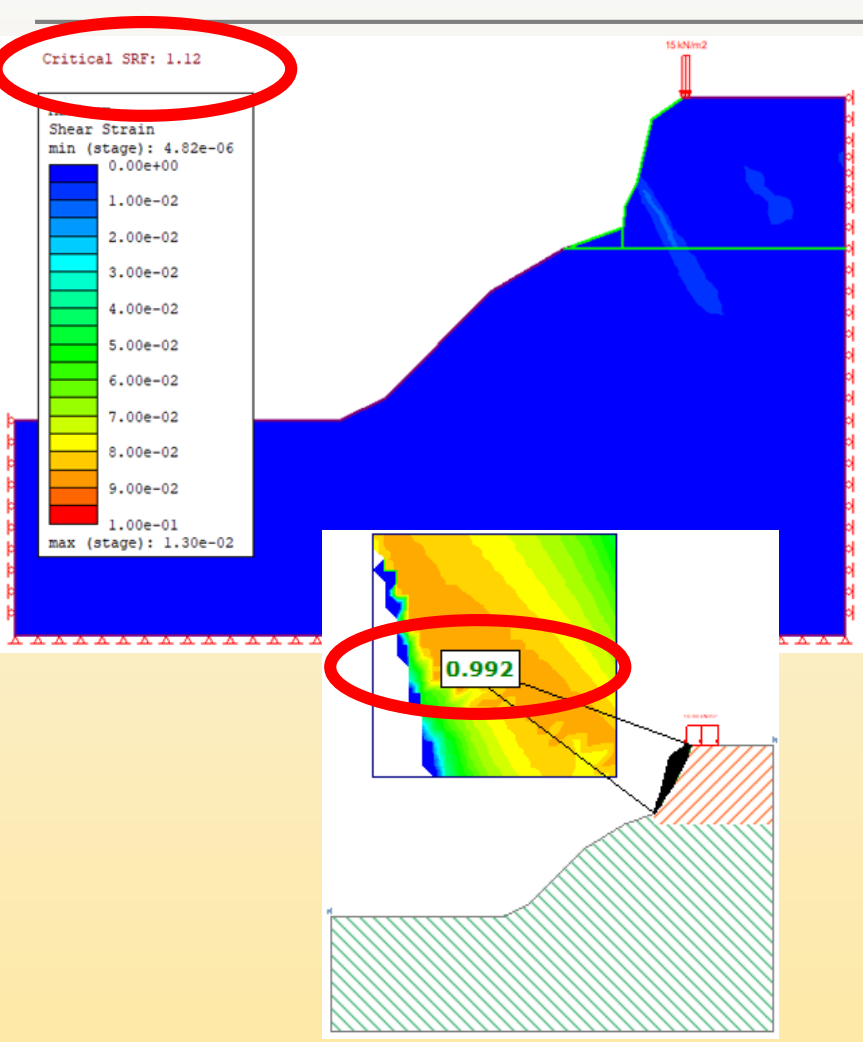

In-situ virgin slope

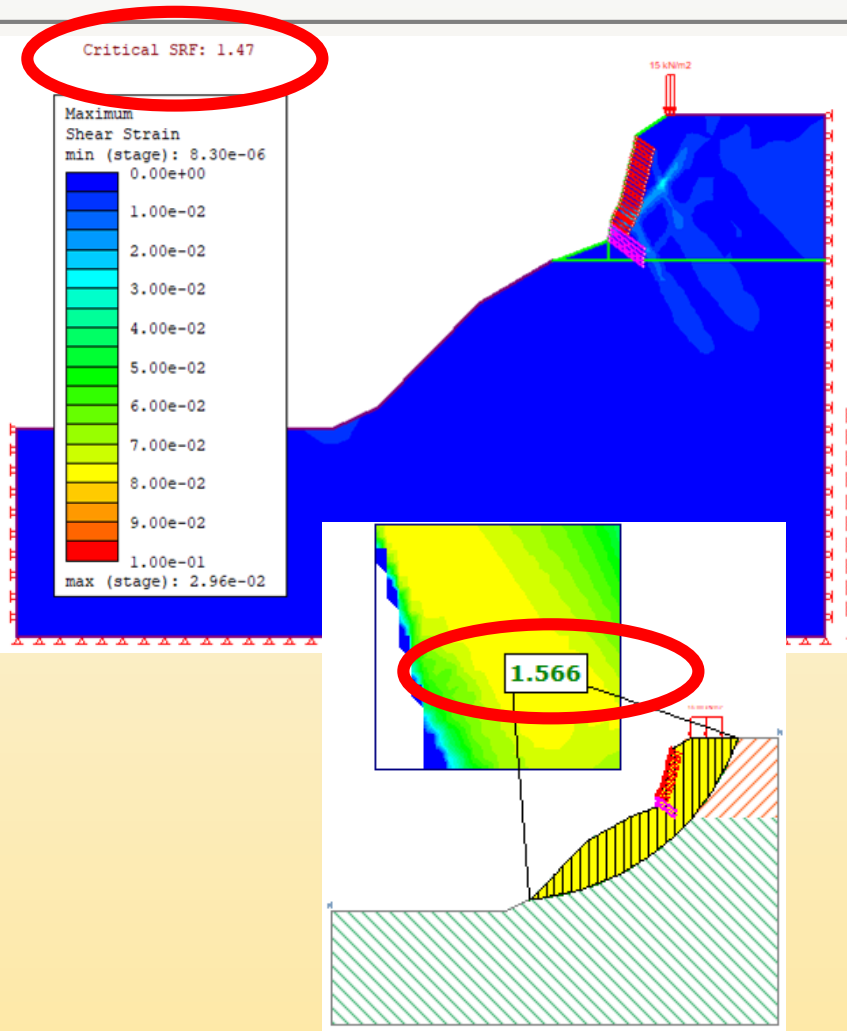

Retained in-situ anchored slope

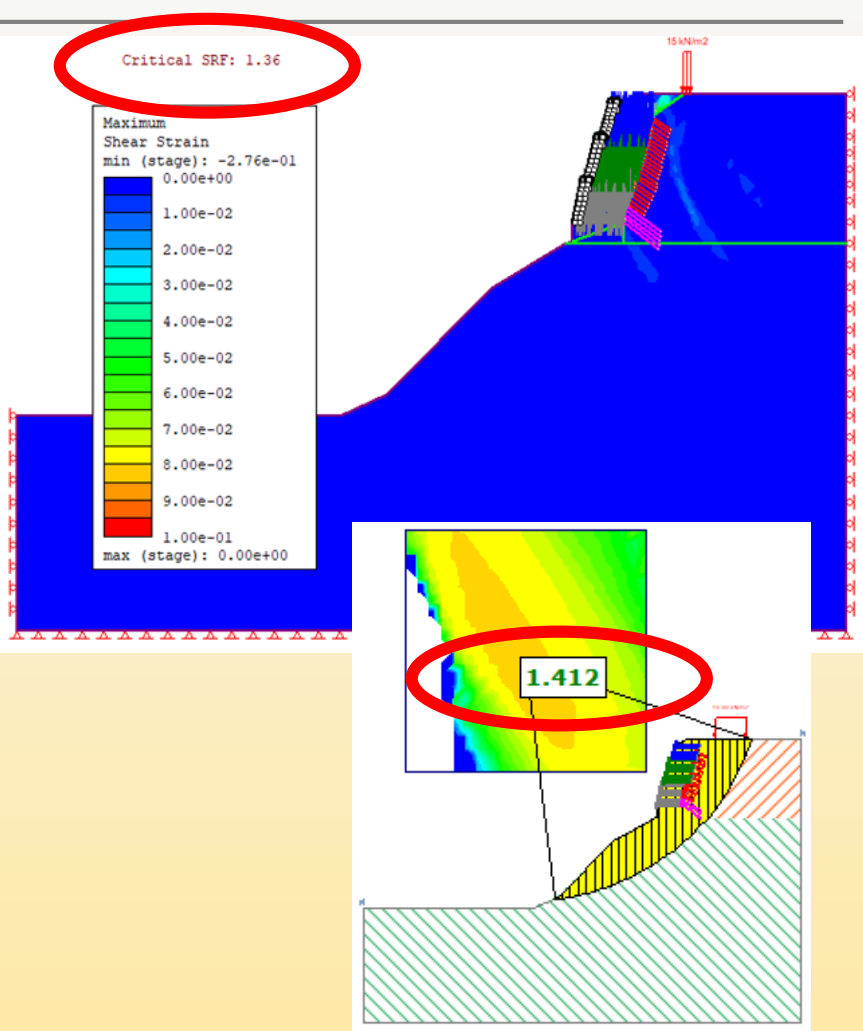

Reclaimed slope with GRS structure

Pseudo-Static Stability Analysis

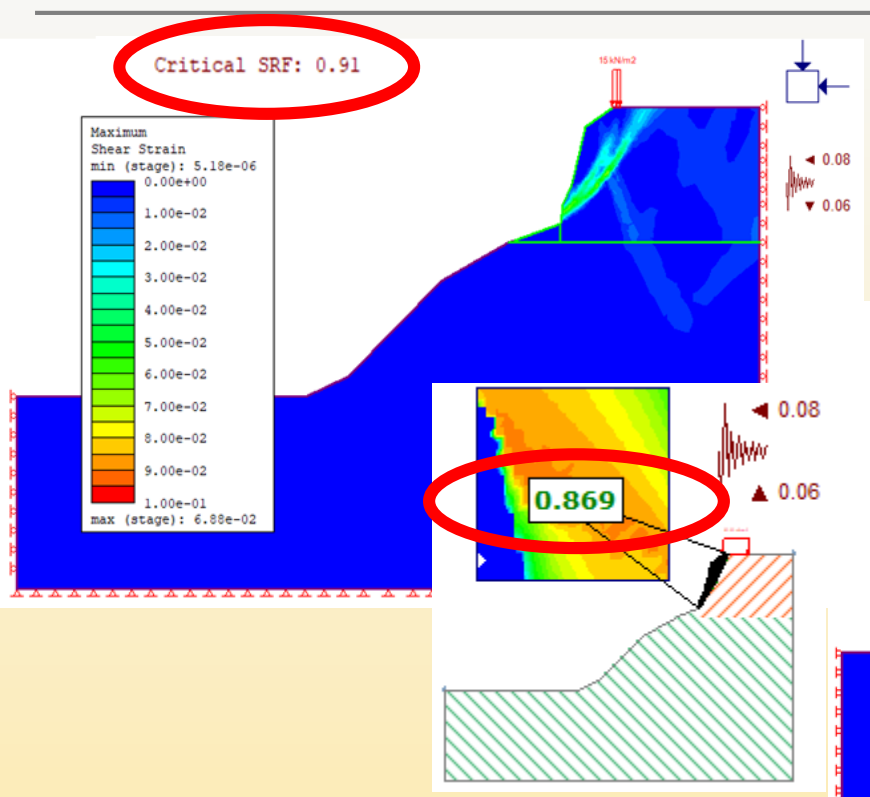

In-situ virgin slope

Meagre Pseudo-Static Forces

$k_h = 0.08, k_v = 0.06$

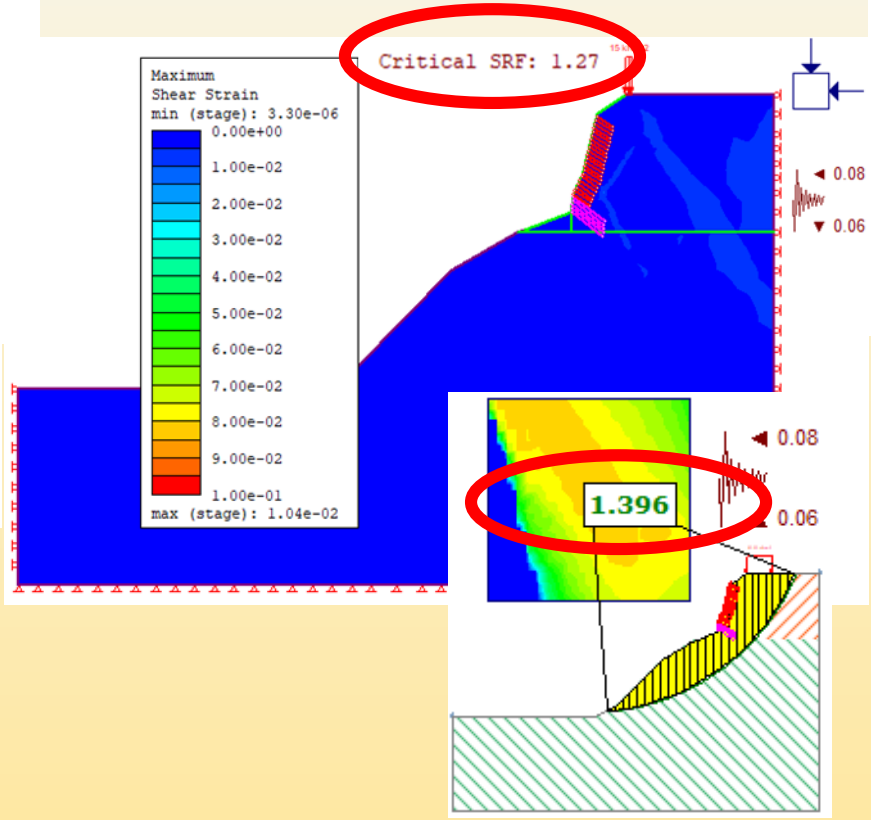

Retained in-situ anchored slope

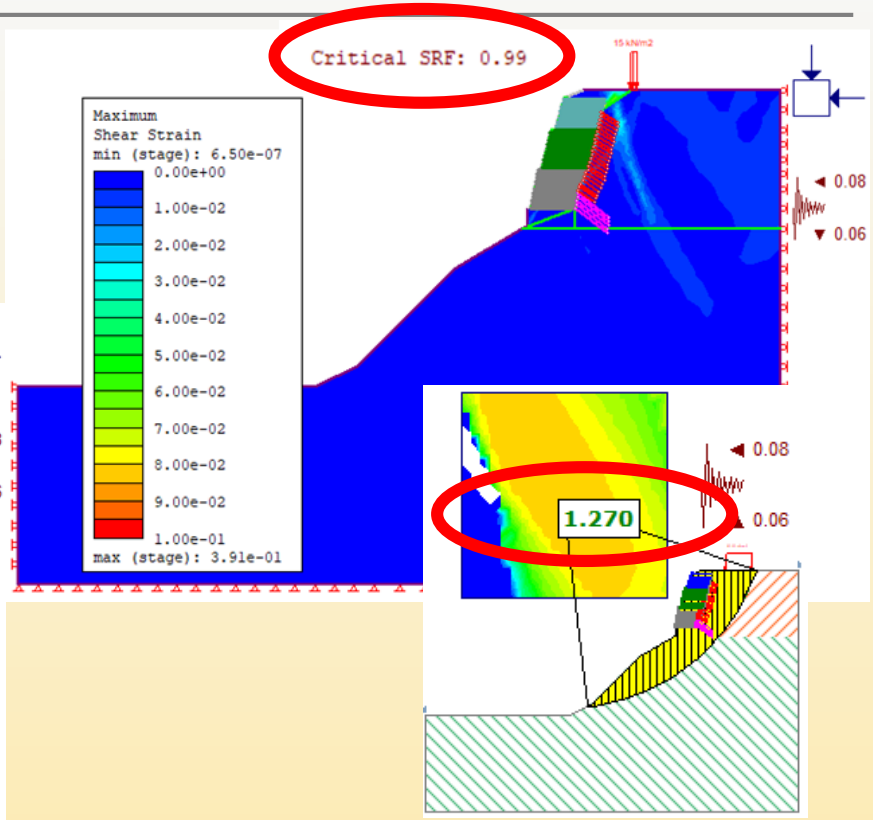

Reclaimed slope with GRS structure

Seismic Analysis: Ground Motions

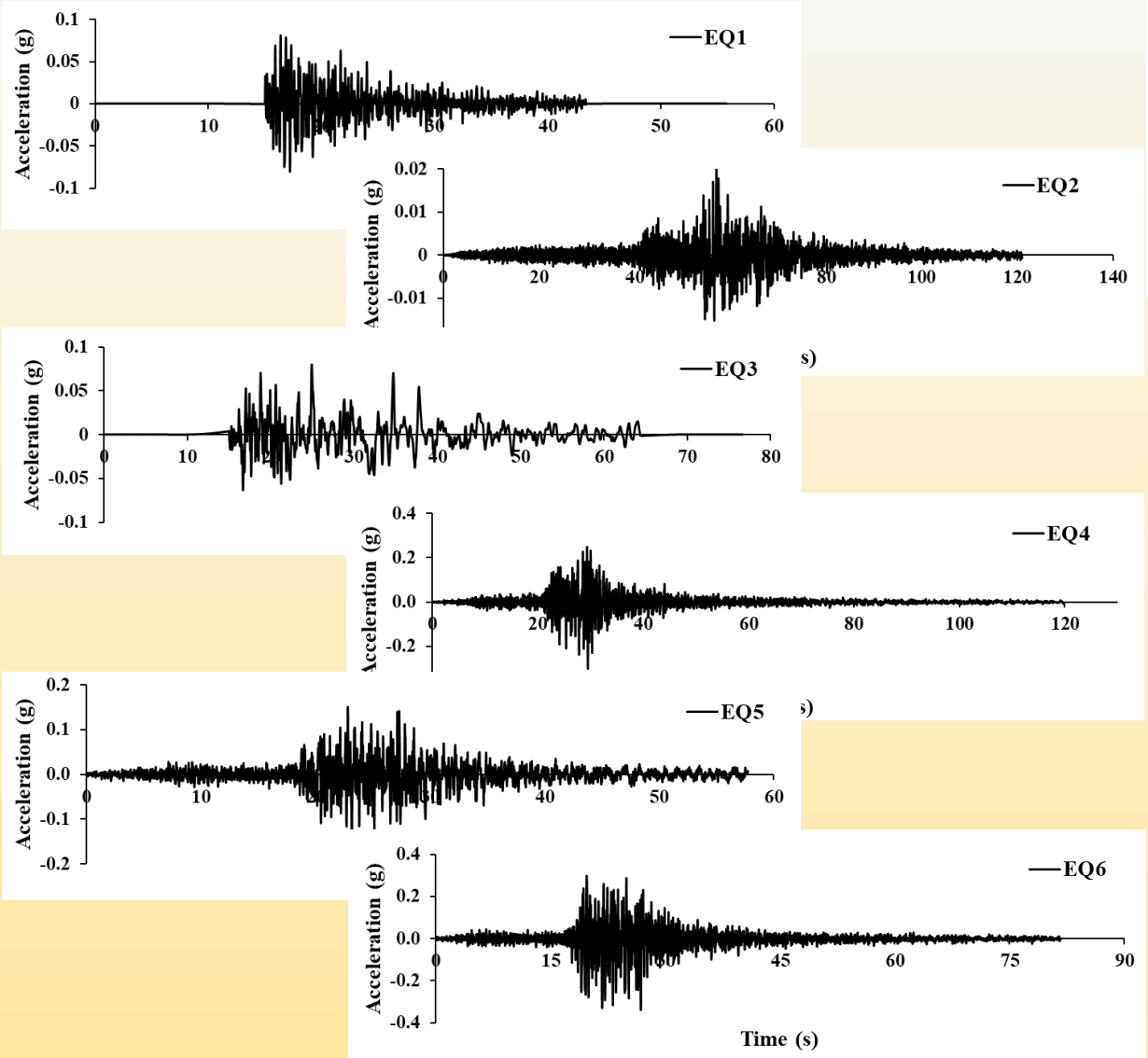

Earthquake Motions

Earthquake	Year	Magnitude	Recording station	Component	Notation
Indo-Burma	1995	M6.4	Berlongfer	S76W	EQ1
Sikkim	2011	M6.9	IIT Guwahati	N90E	EQ2
Imphal	2016	M6.7	-	-	EQ3
Myanmar-India	1988	M7.3	Berlongfer	S76W	EQ4
Myanmar-India	1988	M7.3	Bokajan	N34E	EQ5
Myanmar-India	1988	M7.3	Diphu	S00W	EQ6

Characteristics

Parameters	EQ1	EQ2	EQ3	EQ4	EQ5	EQ6
Peak Ground Acceleration, PGA (g)	0.08	0.02	0.08	0.3	0.15	0.34
RMS Acceleration, RMSA (g)	0.012	0.002	0.013	0.03	0.024	0.048
Arias Intensity, I_a (m/s)	0.12	0.01	0.21	1.67	0.53	2.9
Significant duration (s)	16.96	34.89	32.14	23.82	21.96	17.02
Characteristic Intensity, I_c	0.0095	0.0012	0.0132	0.0571	0.0287	0.095
Predominant period (s)	0.24	0.38	0.4	0.34	0.18	0.44
Fundamental frequency (Hz)	1.9	0.3	0.1, 0.2	1.74	1.37	1.94

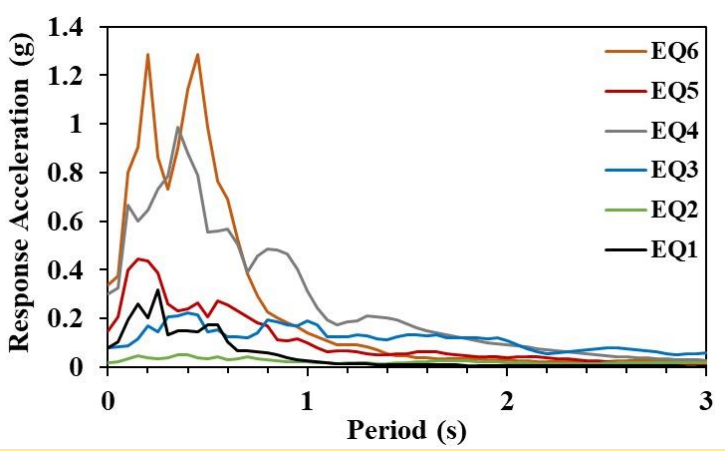

Acceleration spectra

Dynamic Responses

Acceleration Amplification Factor (AAF)

- Seismic wave amplification **higher through the reinforced fill zone**
  - ➢ Amplification responses display **inertial difference between the in-situ and reinforced fill of the reclaimed slope**

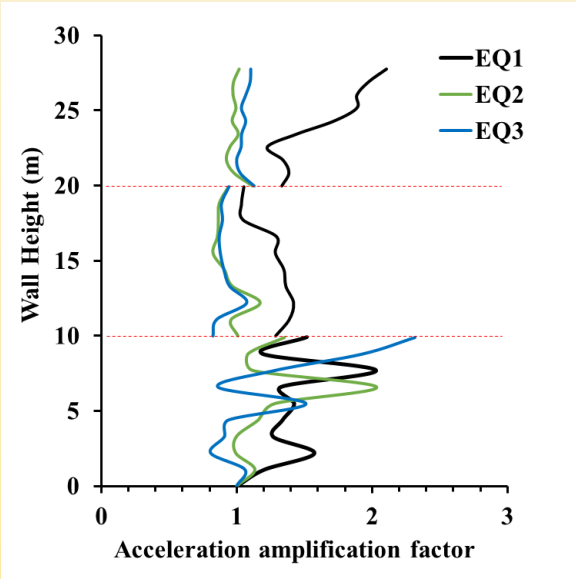

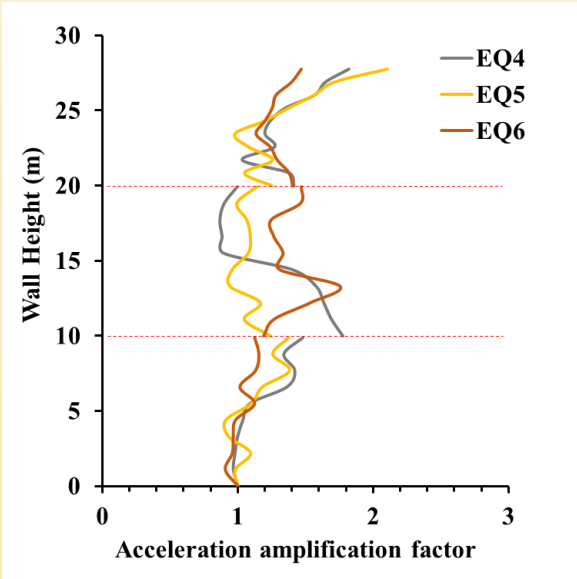

AAF profiles of GRS wall fascia

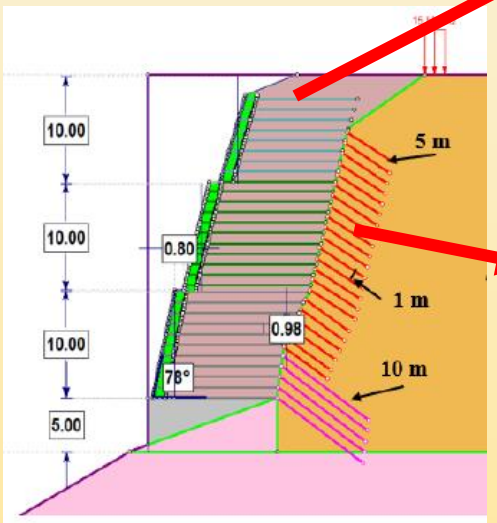

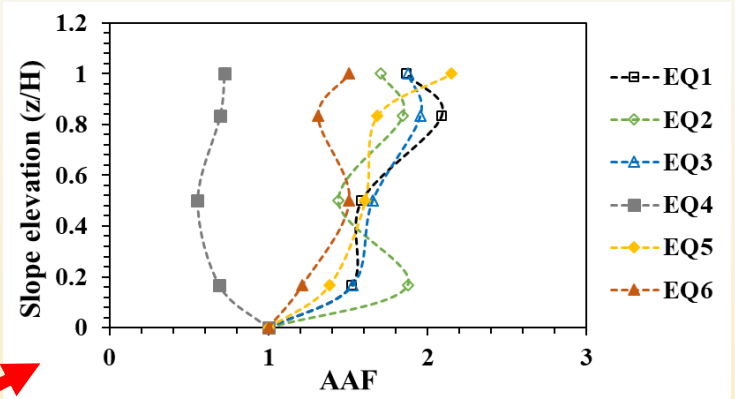

Reinforced fill

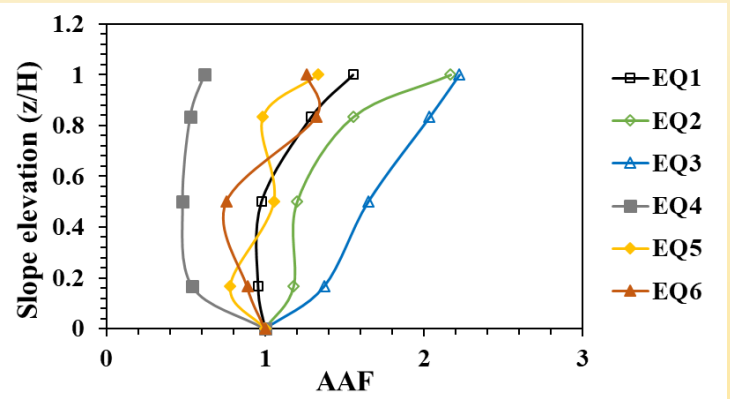

In-situ part of the reclaimed slope

Dynamic Responses

Dynamic Lateral Earth Pressure

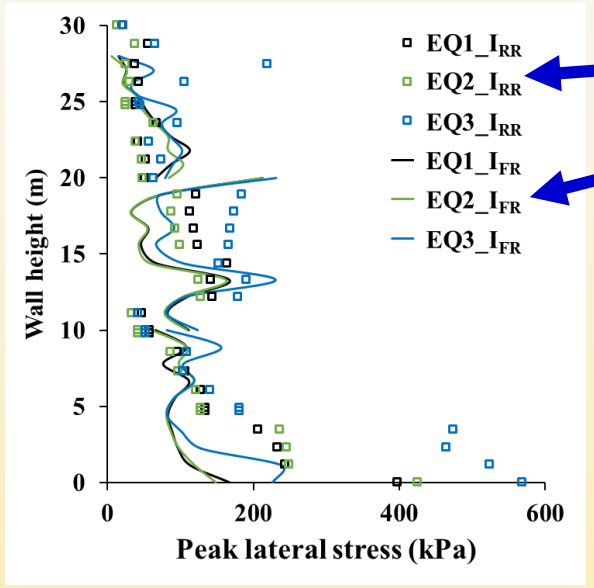

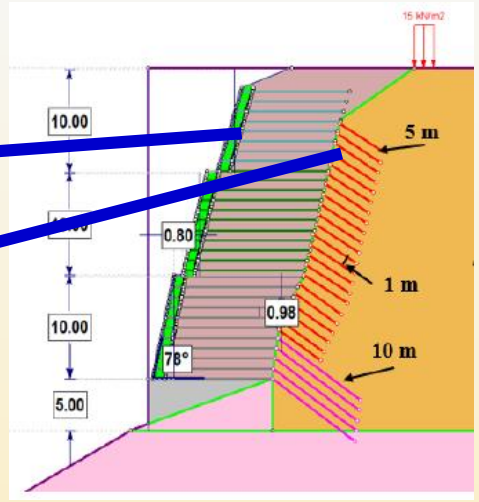

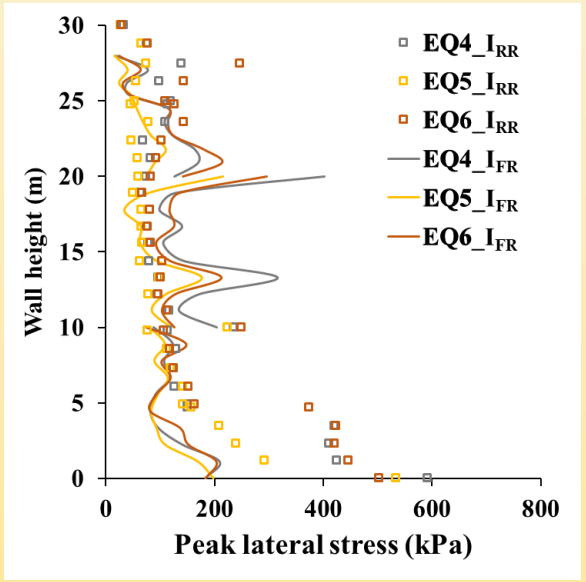

- **Triangular stress distribution in each tier**
- **Stresses: $I_{FR} \approx 0.33\ I_{RR}$**
  - Flexibility of fascia

Peak and Residual Shear Stresses

- **Difference in peak and residual shear stresses**
  - More prominent for strong motions
  - Extremely recognizable for lower tiers

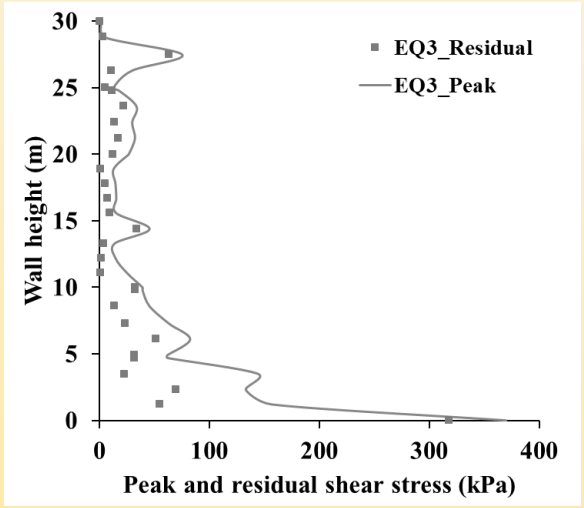

Weak motion

Strong motion

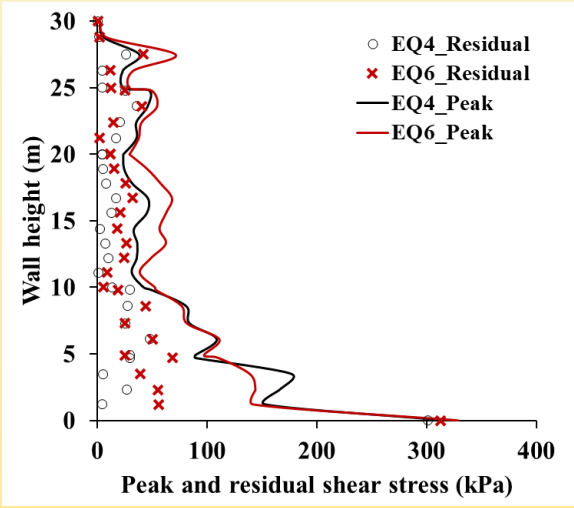

Lateral Displacement of GRS wall

Static analysis

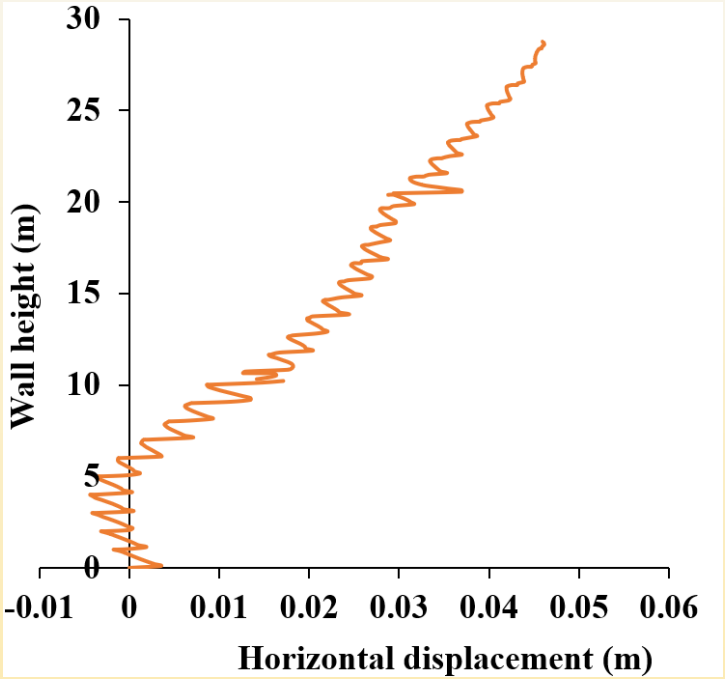

Pseudo-static analysis

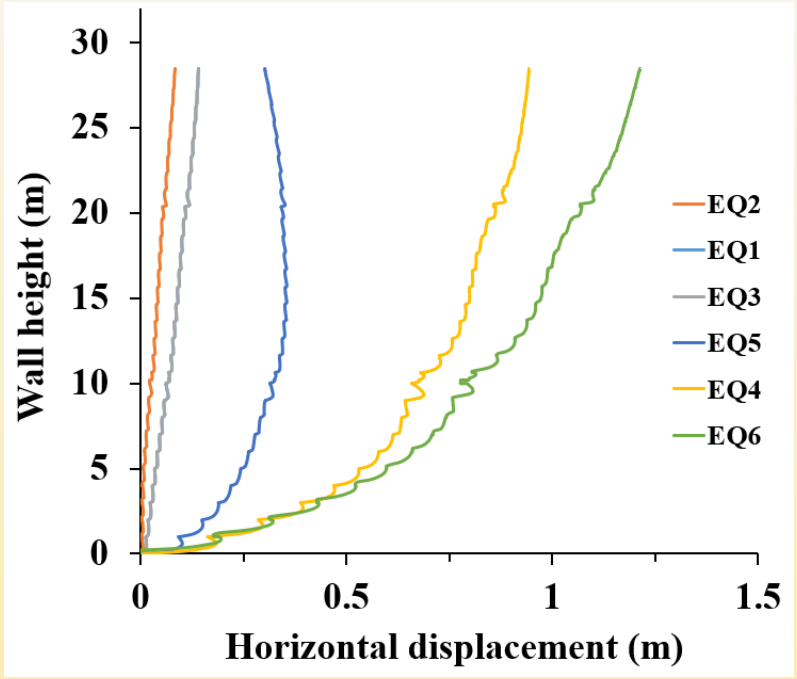

Dynamic analysis

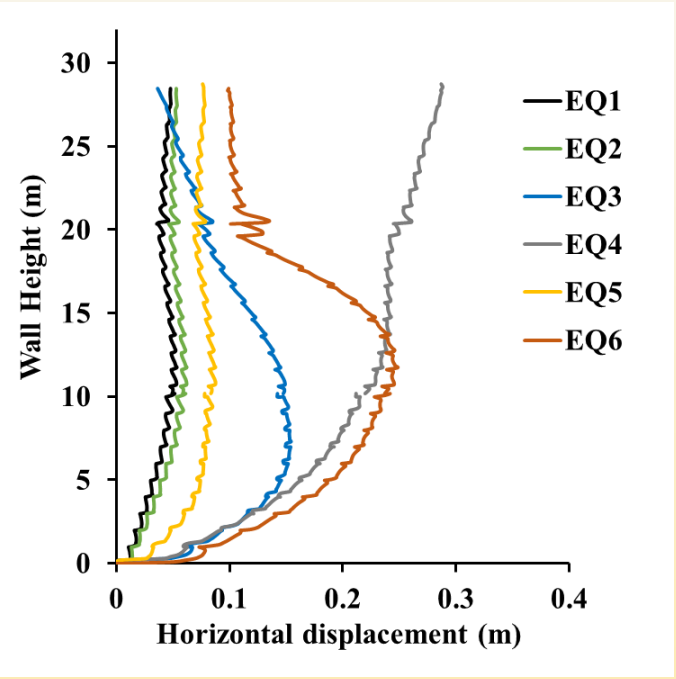

- **Static and Pseudo-static scenarios**
  - Wall deflection increases towards the crest

- **Dynamic scenarios**
  - Wall deflection is more towards the bottom two tiers, exhibiting **bulging**

Reinforcement Load

Static analysis

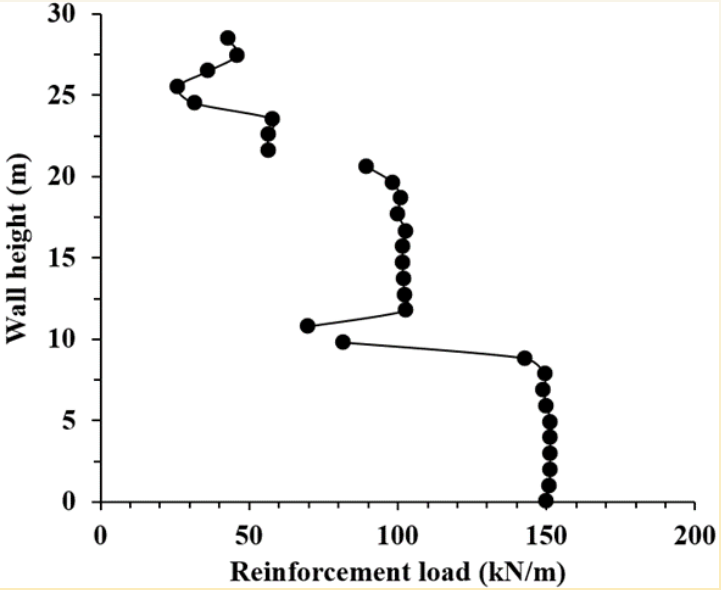

Pseudo-static analysis

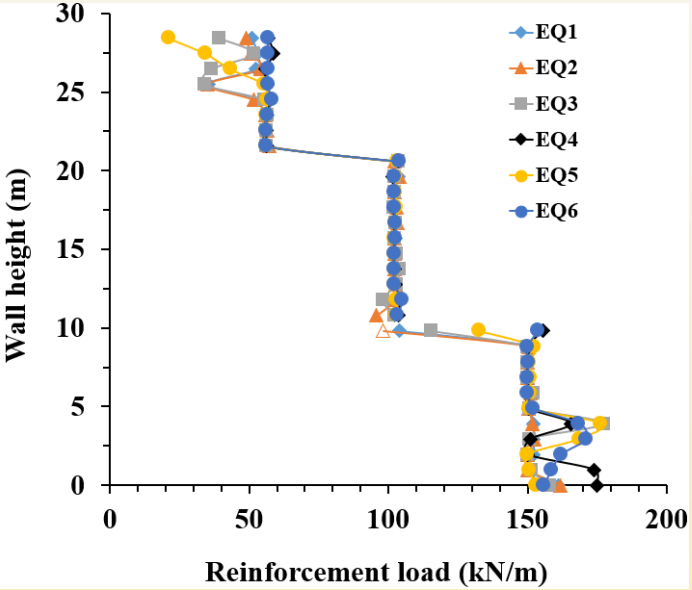

Dynamic analysis

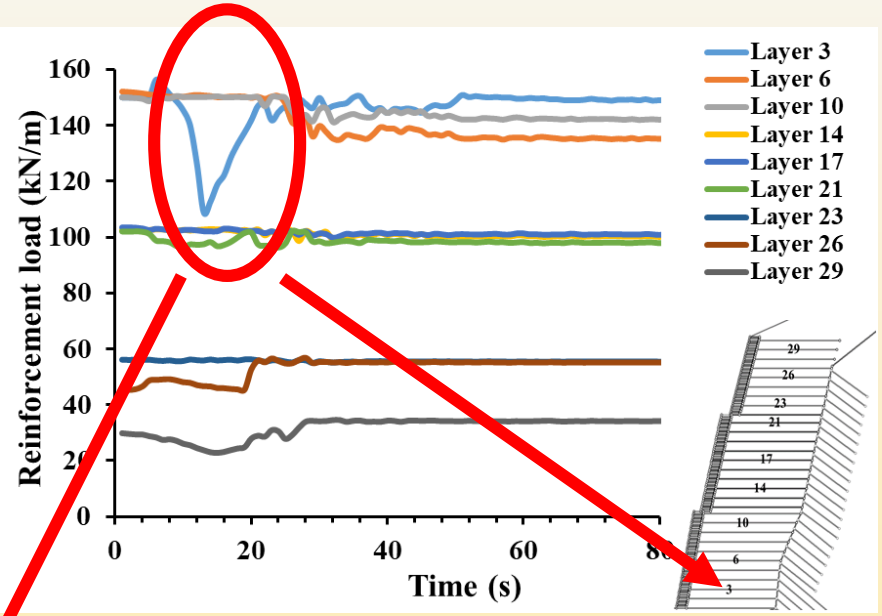

- **Dynamic Scenario: Sudden dip in the reinforcement load**
  - Rapid mobilization of the tensile capacity in reinforcement layers in the lower tier

Connection Load

Dynamic analysis

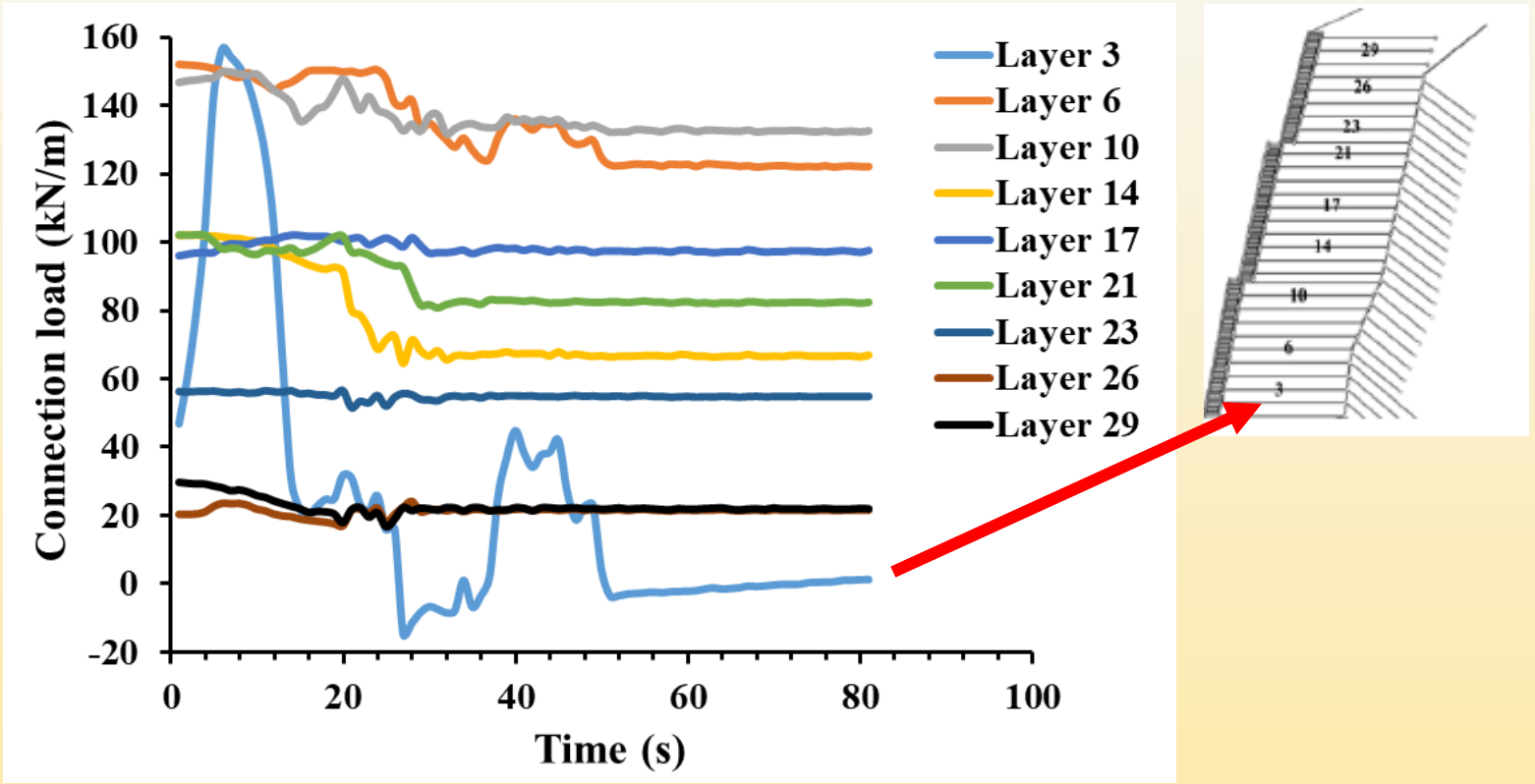

- **Connection load in Layer 3 drops down to zero** during the termination of the seismic event
  - **Failure of the adjacent reinforcements and hence, the collapse of the structure**

Shear Strain Concentrations: Collapse Mechanism

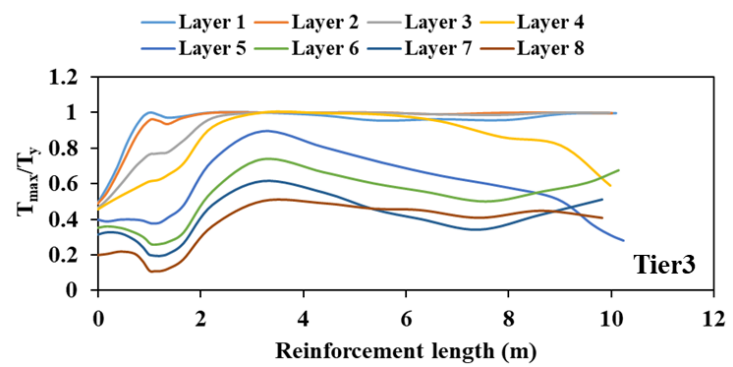

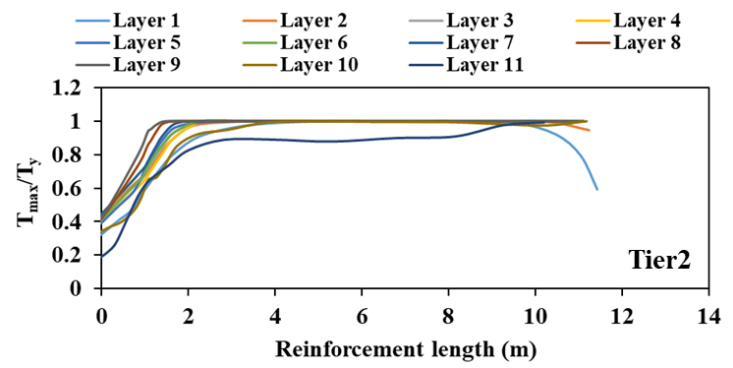

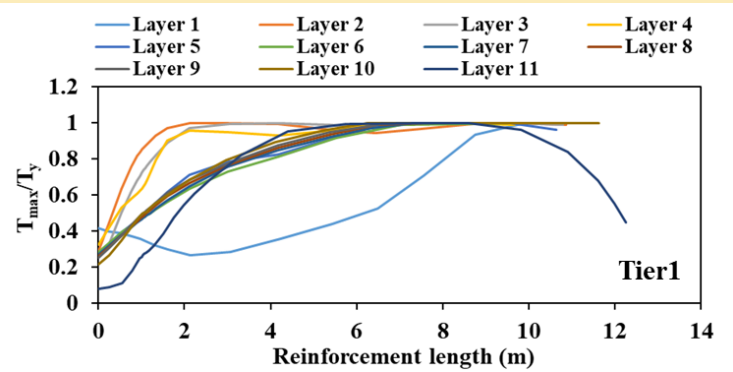

Conjugate failure line passing through several reinforcement layers of bottom two tier

Exceedance of connection capacity

Potential failure of the plum concrete pedestal

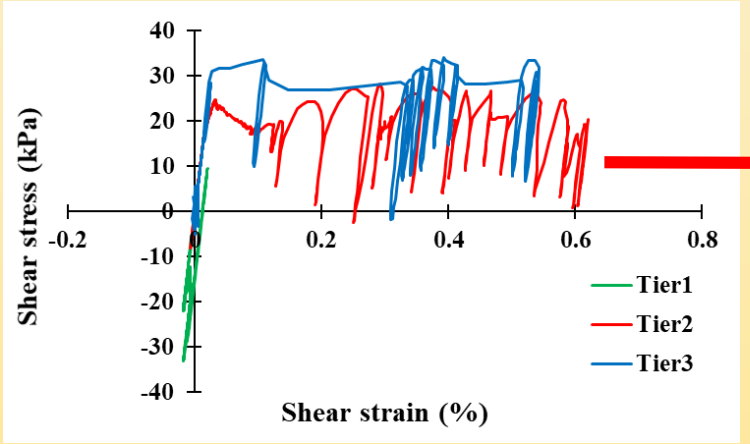

Dynamic analysis

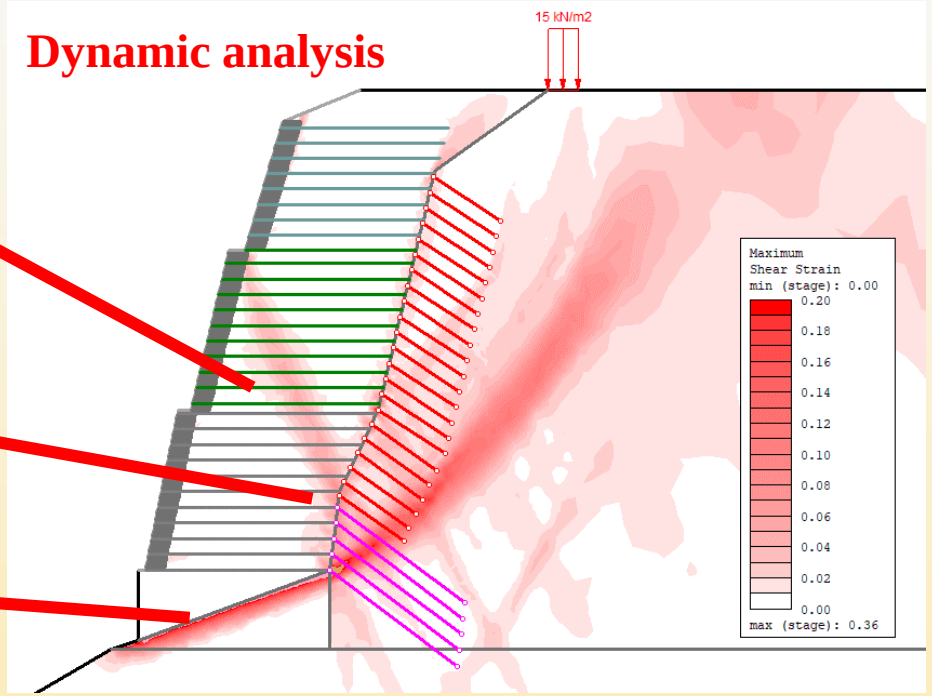

Tiers 2 and 3: Significant strain accumulation without sufficient increase in stress

Cascading collapse of upper tiers due to mobilization in lower tier

Final Remarks

- Large height GRS walls are critical infrastructures
  - Seismic design consideration are very important (especially in a seismicity prone zone)
    - Pseudo-static analysis is to be used only for initial screening
    - FE-based coupled stress-deformation analysis is a must for complete understanding

- Disciplined and ethical construction practices are necessary
  - Thorough geotechnical investigation
  - Proper choice of materials
  - Proper field implementation
  - Scenario-basis deviation from codal guidelines might be required
    - Should be thoroughly scrutinized
    - Supported by in-depth analysis

Acknowledgments

Sureka

Mihretab

Nayan

Deepali

Aman

Further Information

- Webpage

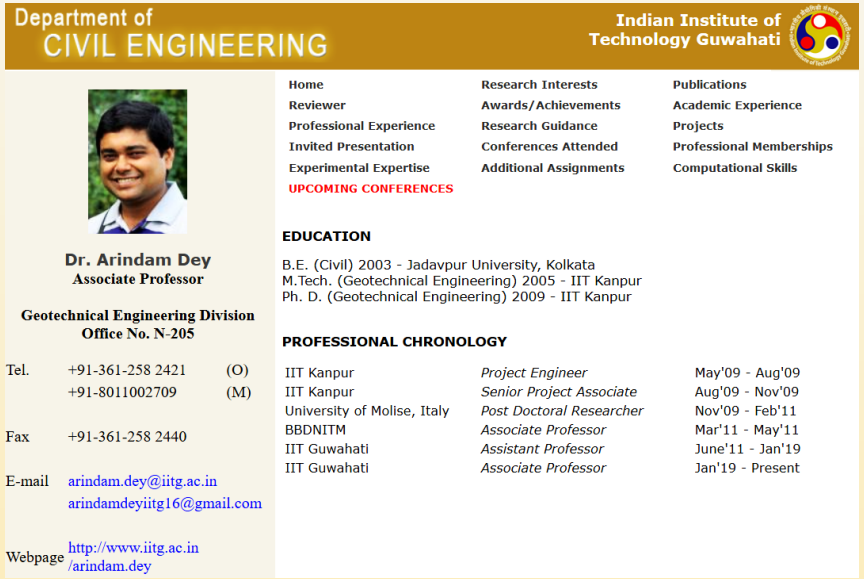
Department of CIVIL ENGINEERING

Indian Institute of Technology Guwahati

Home | Reviewer | Professional Experience | Invited Presentation | Experimental Expertise | UPCOMING CONFERENCES | Research Interests | Awards/Achievements | Research Guidance | Conferences Attended | Additional Assignments | Publications | Academic Experience | Projects | Professional Memberships | Computational Skills

Dr. Arindam Dey
Associate Professor

Geotechnical Engineering Division
Office No. N-205

Tel. +91-361-258 2421 (O)
+91-8011002709 (M)

Fax +91-361-258 2440

E-mail arindam.dey@iitg.ac.in
arindamdeyiitg16@gmail.com

Webpage http://www.iitg.ac.in/arindam.dey

EDUCATION

B.E. (Civil) 2003 - Jadavpur University, Kolkata
M.Tech. (Geotechnical Engineering) 2005 - IIT Kanpur
Ph. D. (Geotechnical Engineering) 2009 - IIT Kanpur

PROFESSIONAL CHRONOLOGY

IIT Kanpur	*Project Engineer*	May'09 - Aug'09
IIT Kanpur	*Senior Project Associate*	Aug'09 - Nov'09
University of Molise, Italy	*Post Doctoral Researcher*	Nov'09 - Feb'11
BBDNITM	*Associate Professor*	Mar'11 - May'11
IIT Guwahati	*Assistant Professor*	June'11 - Jan'19
IIT Guwahati	*Associate Professor*	Jan'19 - Present

- Researchgate

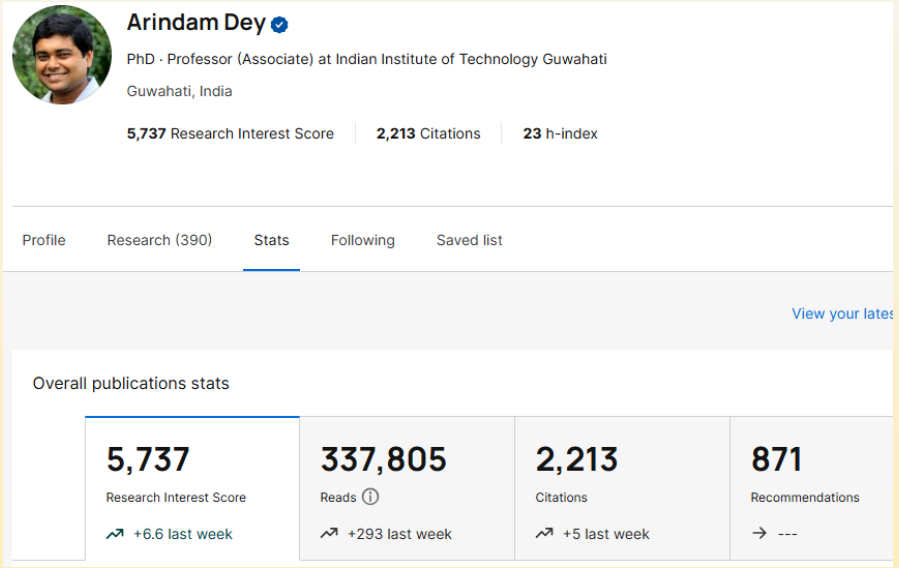
Arindam Dey

PhD · Professor (Associate) at Indian Institute of Technology Guwahati

Guwahati, India

5,737 Research Interest Score | 2,213 Citations | 23 h-index

Profile | Research (390) | Stats | Following | Saved list

View your lates

Overall publications stats

5,737	337,805	2,213	871
Research Interest Score	Reads	Citations	Recommendations
+6.6 last week	+293 last week	+5 last week	---

- Google Scholar


Arindam Dey

FOLLOWING

Associate Professor, IIT Guwahati
Verified email at iitg.ac.in - Homepage

Geotechnical Earthquake E... | Foundation Engineering | Geophysical Investigation | Soil

TITLE	CITED BY	YEAR
Evaluation of dynamic properties of sandy soil at high cyclic strains SS Kumar, A Murali Krishna, A Dey Soil Dynamics and Earthquake Engineering 99, 157-167	224	2017
Hydraulic failures of earthen dams and embankments P Talukdar, A Dey Innovative Infrastructure Solutions 4, Article 34, 1-20	78	2019
Influence of digital elevation models on the simulation of rainfall-induced landslides in the hillslopes of Guwahati, India	71	2020

Cited by VIEW ALL

	All	Since 2021
Citations	2392	1719
h-index	25	21
i10-index	67	43

400 300 200 100 0

2019 2020 2021 2022 2023 2024 2025 2026

Thank You for Patient Hearing